Highly Multiplexed Single Cell In Situ Transcriptomic Analysis

by

Lu Xiao

A Dissertation Presented in Partial Fulfillment
of the Requirements for the Degree
Doctor of Philosophy

Approved November 2019 by the
Graduate Supervisory Committee:

Jia Guo
Xu Wang
Chad Borges

ARIZONA STATE UNIVERSITY

December 2019

ABSTRACT

Spatial resolved detection and quantification of ribonucleic acid (RNA) molecules in single cell is crucial for the understanding of inherent biological issues, like mechanism of gene regulation or the development and maintenance of cell fate. Conventional methods for single cell RNA profiling, like single-cell RNA sequencing (scRNA-seq) or single-molecule fluorescent *in situ* hybridization (smFISH), suffer either from the loss of spatial information or the low detection throughput. In order to advance single-cell analysis, new approaches need to be developed with the ability to perform high-throughput detection while preserving spatial information of the subcellular location of target RNA molecules.

Novel approaches for highly multiplexed single cell *in situ* transcriptomic analysis were developed by our group to enable single-cell comprehensive RNA profiling in their native spatial contexts. Reiterative FISH was demonstrated to be able to detect >100 RNA species in single cell in situ, while more sophisticated approaches, consecutive FISH (C-FISH) and switchable fluorescent oligonucleotide based FISH (SFO-FISH), have the potential for whole transcriptome profiling at the single molecule sensitivity. The introduction of a cleavable fluorescent tyramide even enables sensitive RNA profiling in intact tissues with high throughput. These approaches will have wide applications in studies of systems biology, molecular diagnosis and targeted therapies.

DEDICATION

This thesis dedicated to my parents who love me deeply, to my wife, Wa Gao, who support me unconditionally. Without their love and encouragement, I would not be able to come through all the difficulties.

ACKNOWLEGEMENTS

I would like to express my sincere respect and appreciation to my advisor Dr. Jia Guo for his kindly helped toward career. He shows me how to become a scientist with his patience, passion, and immense knowledge. I would not achieve all my accomplishment without his mentorship.

I also would like to show my gratitude to my committee members, Dr. Xu Wang and Dr. Chad Borges. They have provided valuable suggestions and encouragement to my research.

Additionally, I am grateful to all my colleagues who I have been working with for the last six years. It has been a with great pleasure to work with them.

Finally, I would like to thank all my friends who have supported me during the past six years.

TABLE OF CONTENTS

Page

CHAPTER Page

LIST OF FIGURES

Figure Page

CHAPTER 1

INTRODUCTION

1.1 Single-cell RNA analysis

Complete study of cellular regulatory networks within cells and tissue sections plays an important role in the deep and detailed understanding of complex biological processes like organism development, tissue regeneration and cancer[1,2]. Conventional biomedical and molecular assays, though being extensively used in the study of gene expression patterns, signaling networks, and gene regulatory circuits, usually provide average properties of cell poplulations[3]. It has been demonstrated that the average properties of cell population could not represent biological process in single cells[4,5]. Genetic differences, functional states, and microenvironment will all lead to cell heterogeneity[6]. Moreover, it is reported that the minority cell populations of many biological systems that consists heterogeneous cell types often govern the overall system behavior[2]. In order to fully understand the complex biological systems, it is essential to use single-cell analysis to reveal spatial organizations and biological interactions between diverse cell types in complex natural context.

Copy number and intracellular localization of RNA molecules plays a principal role in cell function and cell identity[7]. Hence, the ability to profile a large number of different transcripts at transcriptomic level in single cell will provide us with inherent biological information, such as mechanism of gene regulation, the heterogeneous behavior of cells and the development and maintenance of cell fate[8].

The development of microarray technologies[9] and high-throughput sequencing[10] has leaded to several sequencing-based approaches for single-cell transcriptomic analysis[11–16].

A typical experiment starts with the dissociation of the tissue into a single-cell suspension via digestive enzymes or mechanical shearing[17,18]. Individual cells are subsequently isolated from each other via different technologies, such as flow cytometry[17], microscopy-assisted micropipeting[19] and microfluid[20]. Quantitative real time PCR (qPCR)[21] or RNA sequencing (RNA-seq)[22–24] is then performed toward isolated cells to obtain transcriptomic information at single-cell resolution. Although the application of conventional qPCR and RNA-seq assays provides us with fundamental 'snapshots' on the whole-cell transcriptome at single-cell level, a cell's spatial environment and precise subcellular locations of target transcripts are lost during the process of cell separation. Both sources of information play an important role in the interpretation of the precise state of a cell.[25]

Single-molecule fluorescence *in situ* hybridization (smFISH) of RNA molecules, on the other hand, has provide powerful tools for quantitative analysis of different transcripts in single cells with spatial information preserved[26,27]. In smFISH, 30 to 50 fluorescent labeled oligonucleotides, with a length of 20 base pairs, collectively hybridize to the same target RNA molecule, enabling visualization of individual transcripts as diffraction-limited spots. An amplified version of smFISH, called RNAscope[28], is also introduced to allow robust detection and quantification of low-abundance transcripts in tissues and thick cleared brain samples. In this approach, a collection of preamplifier probe pairs, containing 20 binding site for amplifiers, is designed to hybridize to a target transcript. Subsequent sequential hybridization of amplifier probes builds up a branched structure, ultimately allowing the recruitment of a large number of short fluorescent labeled oligonucleotides for signal amplification. Technologies based on fluorescent *in situ* hybridization of RNA molecules

provide us with a method to quantitatively analyze transcripts at even sub-cellular resolution with spatial information of cells preserved. However, due to the spectral overlap of small organic fluorophores[29], these technologies could only analyze a small number of different transcripts simultaneously, preventing the study of single cells at transcriptomic level.

In order to get the global map of transcripts with spatial information, new methods for single cell transcriptomic analysis need to be developed. Here I summarize several pioneering technologies that enable high throughput and spatially resolved transcriptomics analysis of single cells. These technologies could be classified into two categories: sequencing-based approaches and imaging-based approaches. I will introduce the concepts of these technologies, together with their advantages and limitations. I will also discuss current applications of single cell transcriptomics and its future perspectives.

1.2 Sequencing-based approaches

Sequencing-based approaches like qPCR and RNA-seq has been long used to study single cell transcriptomics[11–16]. However, in order to preserve spatial information of cell transcriptome during sequencing, especially within a primary tissue or organoid model, new technologies need to be developed.

Satija's group has developed an indirect approach for sequencing-based spatial transcriptomic analysis[30]. In this approach, a computational strategy called Seurat is introduced to construct a spatial reference map from the *in situ* hybridization data of a small set of "landmark" transcripts. By combining RNA-seq profiles of individual cells with its location in this reference map, Seurat is able to obtain spatial transcriptomic information

at single-cell resolution. Satija's group has successfully applied Seurat to s patially map 851 single cells from dissociated zebrafish embryos and generated a transcriptome-wide map of spatial patterning. However, this approach largely relies on the existence of spatial expression of certain "landmarks" genes in the tissue of interest, which limits it application. An alternative approach is "spatial transcriptomics" developed by Lundeberg's group[31]. In this approach, barcoded reversed transcription oligo(dT) primers are immobilized on to glass slides. A barcoded oligo(dT) primer consists of a cleavage site, an amplification handle for RNA-seq, a spatial barcode (ID) for spatial mapping of RNA-seq results, a unique molecule identifier (UMI) for noise reducing and a oligo(dT) region for mRNA capture (Figure 1.5.1A). After tissues are fixed and permeabilized onto the slides, free polyadenylated transcripts within the tissue are captured onto the barcoded oligo(dT) nearby. Next, cDNAs are generated, cleaved from the slide and converted into an RNA-seq library. The ID index in the sequencing data is then used spatially mapped each read on the tissue. However, since the oligo(dT) spots on the array have a diameter of 100 μm, transcripts captured by the oligos are more likely from multiple cells rather than single cells, which leads to a low resolution problem.

Laser capture microdissertion (LCM) is also reported to be applied in single-cell transcriptomic analysis[32–34]. In this approach, RNA molecules are extracted from LCM captured cells and followed by RNA-seq. Data derived from the captured cells could then be annotated with the know original location. However, this approach will damage the target tissue during microdissertion, which limits its application. A more sophisticated noninvasive approach involves the application of transcriptome *in vivo* analysis (TIVA)[35].

In this approach, a photoactivatable mRNA capture molecule (TIVA tag) (Figure 1.5.2) consisting of a trapped poly(U) oligonucleotide is used to collect mRNA molecules in selected cells. After penetrating the cell membrane with the help of a cell-penetrating peptide (CPP), the TIVA tag is selectively photoactivated in desired cells to unblock the poly(U) sequence for the capture of poly(A) tailed cellular mRNAs for RNA-seq analysis. However, photoactivation of individual cells is time consuming, thus leads to a low throughput of the approach.

Although sequencing-based approaches has been widely used for spatial transcriptomic analysis, there are a few drawbacks that limit its potential applications. Firstly, current RNA-seq protocols usually capture cellular RNA molecules via poly-T priming[36], which leads to the readout of only polyadenylated transcripts. Therefore, investigation of non-polyadenylated transcript classes, like microRNAs[37,38] or circular RNAs[39,40], could not be achieved by current methods. Moreover, the low capture efficiency of mRNA (approximately 10%)[41] makes current sequencing based approaches ill suited for the detection of low abundant transcripts[41–43]. Lastly, the amplification steps for construction of RNA-seq libraries also leads to high levels of technical noise, which makes data analysis challenging and may even mask underlying biological variations[36].

1.3 Imaging-based approaches

The sub-cellular location of mRNAs plays an important role in cellular gene expression regulation[44]. An important advantage of imaging-based approaches for transcriptomic analysis is its ability to preserve spatial information about the transcript inside the cell. Yet due to the limited availability of fluorophores with non-overlapping spectra, the number of

transcripts that could be analyzed simultaneously via conventional imaging-based approaches like smFISH[27] has been limited.

By using repetitive hybridization and a spectral barcode to achieve multiplexing RNA analysis, sequential fluorescence *in situ* hybridization (seqFISH) is developed by Cai's group[45] (Figure 1.5.3A). In this approach, each transcript is encoded as a series of fluorescent signal across consecutive rounds of hybridizations. In each round of hybridization, transcripts of interested are detected by probes labeled with specific color, followed by probe removal using DNase I. After several rounds of consecutive hybridization, the identity of a transcript at a given location can then be assigned by the sequence of fluorescent signals at a given spot. Theoretically, the number of distinct transcripts that can be analyzed would be F^N with F different fluorophores and N rounds of hybridizations. A revised version of seqFISH that involves signal amplification via hybridization chain reaction (HCR)[46] is introduced to achieve multiplexing transcripts analysis in tissue sections[47]. However, the use of DNase I to remove probes is time consuming with low efficiency. Moreover, DNase I removes all the probes, including the large oligonucleotides library hybridized to target RNAs. Therefore, the expensive oligonucleotides library has to be rehybridized in every analysis, which leads to the increase of the assay time and cost.

Zhuang's group has developed another barcode approach called multiplexed error-robust FISH (MERFISH)[48] (Figure 1.5.3B). MERFISH uses one single fluorophores for transcripts detection. In each hybridization rounds, only a subset of transcripts will be labeled. After 16 rounds of consecutive hybridization, identity of each transcript is

recognized as a 16-bit binary code with zeros and ones representing the absence or presence of positive signal in each hybridization, respectively. However, this approach relies on the precise recognition of positive and negative signal in each round as well as the robust hybridization of probes. A mistake in 0 or 1 assignment will potentially alter the derived identity of the transcript. To address this problem, a 4 Hamming distance algorithm (HD-4)[48] is introduced to recognize transcripts with less than 4 bits different identical. This, however, will dramatically reduce the potential transcripts amount MERFISH could analyze.

Instead of using hybridization events for transcriptomic analysis, approaches via spatial resolved sequencing of RNA molecules directly in fixed cells are also developed. In one such approach developed by Nilsson's group[49] (Figure 1.5.4A), RNA is first reverse transcribed into cDNA. The result cDNA is then targeted with a padlock probe with specific barcode corresponded to transcript's identity. After the padlock probe is circulated and amplified by rolling circle amplification (RCA), its barcode region is then sequenced via sequencing by ligation to reveal transcript's identity. Another approach called fluorescent in situ sequencing (FISSEQ), which involves direct *in situ* RNA sequencing, is developed by Church's group[50]. In this approach (Figure 1.5.4B), the result cDNA is first crosslinked inside the tissue. Its ends are then ligated to form a circular product and amplified by RCA. The product RCA amplicons are then cross linker with each other and finally sequenced *in situ* using SOLiD sequencing by ligation to identify transcripts. However, both *in situ* sequencing approach suffers from low sensitivity and signal overcrowding issues, which limit its ability to perform high throughput in situ sequencing.

Imaging-based approaches discussed above provide us with new methods to obtain spatial transcriptomic information at sub-cellular resolution. However, due to high technical difficulty and advanced equipment required to perform such approaches, its wide application has been hindered. Moreover, complicated computational tools are also required to analyze the data they produce.

1.4 Summary and perspective

During the past decade, many sophisticated technologies, from profiling of localized transcripts to the visualization of individual RNA molecules, have been developed to achieve the study for spatial single-cell transcriptomics. Each having its own capabilities and limitations. These technologies have combined together to become a powerful platform to address many biological problems which cannot be solved by conventional bulk cell assays.

One of the application for spatial resolved transcriptomic analysis is to dissect heterogeneous cell population and complex tissues. Clustering[51–53] or dimensionality reduction algorithms[20,54] have been used on transcriptomic data to define cell subpopulations based on transcriptomics similarity and detect the underlying population structure in an unsupervised manner. This will help us identifying existing cell types[20,51,55,56] and even leading to the discovery of new cell subtypes[57–59] or new biomarkers for existing cell types[20,59,60]. Single-cell transcriptomics data is also used to infer gene regulatory networks (GRNs)[61–63]. By study the similarity of expression profiles collected by single-cell transcriptomic approaches, co-regulation of different genes could be revealed[51,52,55,64–66]. Moreover, the spatial information these technologies obtained could

potentially help us to study cell to cell interaction which will enable the large scale reconstructions of a tissue's metabolic network[67].

One of the future direction for single-cell transcriptomics is the development of new approaches for the detection of large number of RNA molecules directly *in situ*. Both seqFISH and MERFISH suffer from the lack of signal amplification, thus would have problems when applied inside thick tissues. Hybridization chain reaction (HCR)[46] and other amplified version of smFISH[28] have been applied to improve the signal-to-noise ratio. Alternatively, hydrogel tissue-clearing technique is also reported to reduce noise for tissue section analysis[68]. Moreover, current barcoding FISH or *in situ* sequencing approaches suffer from the signal overcrowding issue when the transcripts amount analyzed is large. To overcome this limitation, expansion FISH (ExFISH)[69] is used to link RNA molecules to a swellable gel for super resolution transcriptomic imaging. Third-generation sequencing technologies, like Oxford Nanopores[70], could also be applied to in situ transcriptomic analysis in future. By applying nanopores technology, in situ RNA sequencing at transcriptome level could easily be achieved with high efficiency and accuracy.

Another future direction involves the development of dynamic single-cell transcriptomic analysis. Molecule behaviors in cells are highly dynamic and constantly changing. It is reported that molecular state of single cells will not only differ from other cells, but also from themselves at different time points[71]. These dynamics differences form a basis for important regulatory mechanism controlling cell identities. Therefore it is important to quantify and analyze dynamic RNA molecule changes in single cells at transcriptome

resolution. However, rather than a static snapshot analysis, non-invasive *in vivo* analysis of transcripts need to be achieved to keep cells alive and unchanged for a long period of time. Moreover, the acquisition and analysis of time-resolved data need much complex and specialized solutions.

Single-cell multi-omics is another important future direction. By combining single-cell genomics, transcriptomics and proteomics, we could accurately map the cell states and therefore have a deeper view of regulatory mechanisms. For example, combining single-cell genomics and transcriptomics in acute lymphoblastic leukemia cells finds out that genetic heterogeneity is not responsible for the diverse response of drug treatment[72]. Future multi-omics ultimately aims to characterize all molecules at sub-cellular resolution in a single cell, since the cellular phenome is defined as the set of all phenotype expressed by a cell.

In conclusion, spatial-resolved single-cell transcriptomic analysis has become a fast growing field with huge potential future applications. It will play an important role to help us understand the fundamental biological problems and nature of human disease. I believe the past few years remarkable growth in this field will keep continuing to develop more sophisticated approaches for a deeper and broader understanding of biological complexity.

1.5 Figures

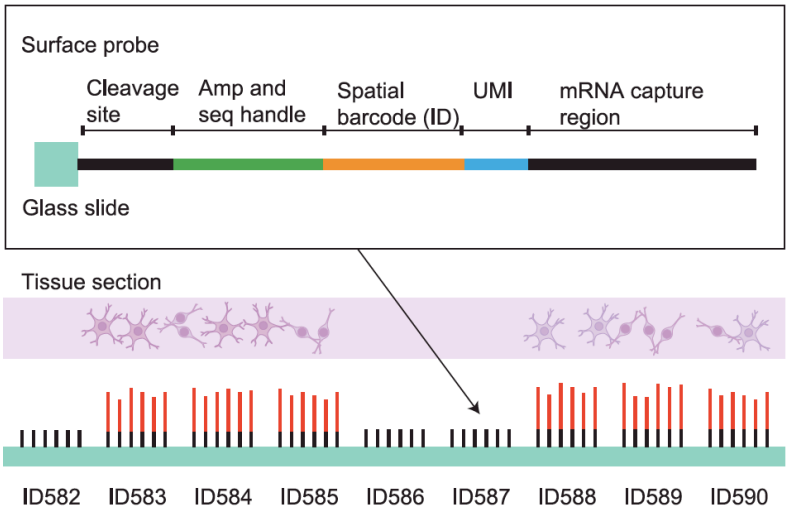

Figure 1.5.1. An illustration of spatial transcriptomics array. Each array features with unique spatial-barcoded probes consist of a cleavage sit, a T7 amplification and sequencing handle, a spatial barcode (ID), a unique molecular identifier (UMI), and an oligo(dT) capture region. cDNA generated from captured mRNA via reverse transcription is shown in red. Reproduced from Ref[31] with permission.

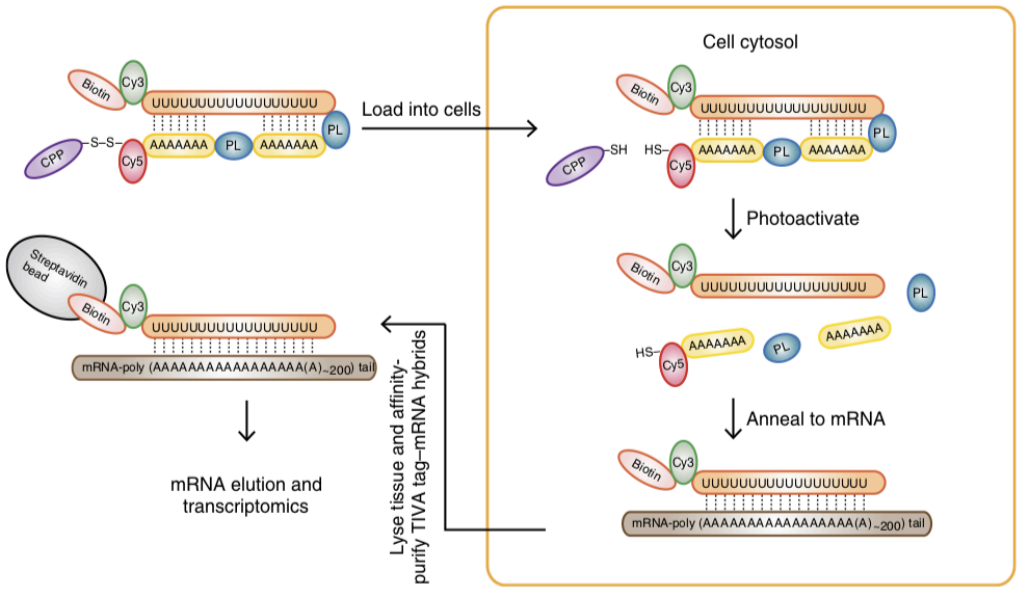

Figure 1.5.2. An illustration of how a TIVA tag works. The TIVA tag is composed of several functional groups: biotin, Cy3, poly(A) tail binding 2′-F RNA poly(U) oligo (orange), photocleavable linker (PL), 2′-OMe RNA poly(A) oligo (yellow), Cy5, disulfide bond (S-S) and CPP. Reproduced from Ref[35] with permission.

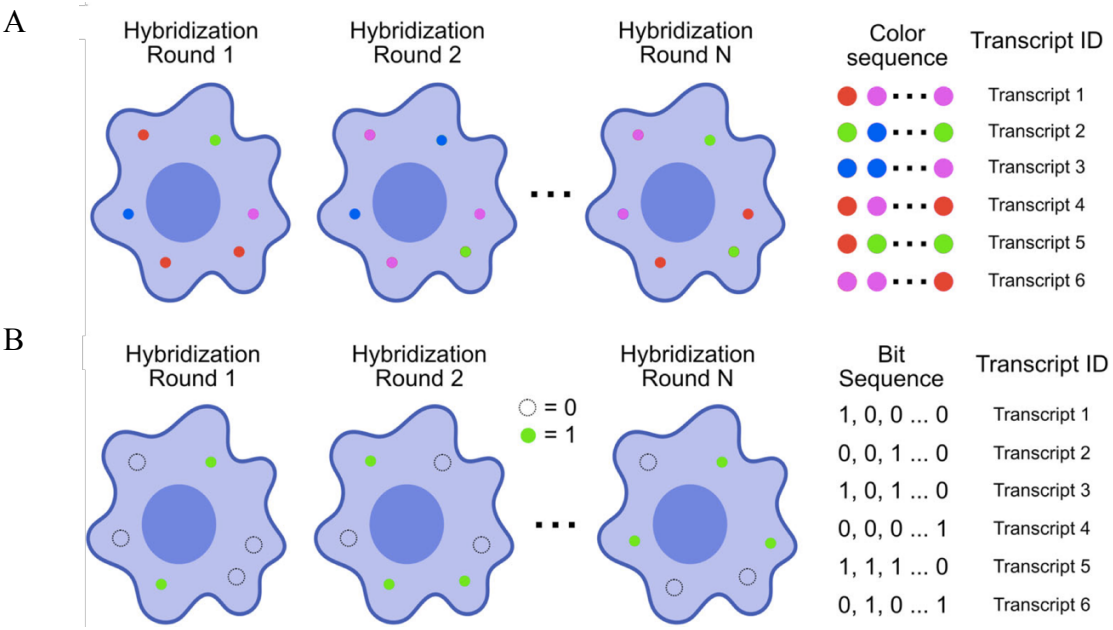

Figure 1.5.3. (A) Illustration of seqFISH. In each hybridization round, each transcript is assigned to a specific color code. When all the hybridization rounds are considered, each transcript can be recognized as a sequence of different colors. (B) Illustration of MERFISH. In each hybridization, only a subset of transcripts is labeled. Therefore, each transcript is assigned to either 1 or 0, representing positive signal or negative signal, respectively. After all the hybridization rounds, each transcript can be recognized as a binary sequence. Reproduced from Ref[73] with permission.

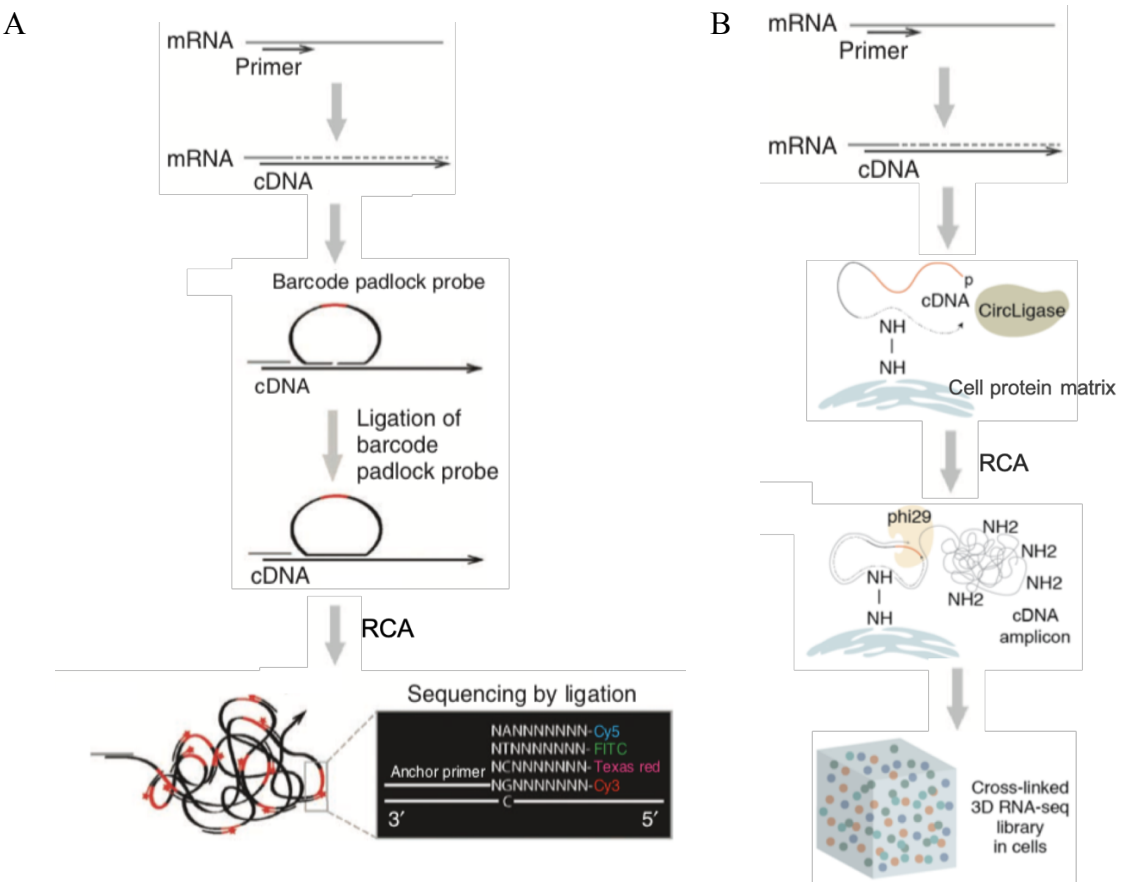

Figure 1.5.4. (A) Illustration of padlock sequencing. Target mRNA is first reverse transcribed to cDNA. A barcode padlock probe is then hybridized onto the product cDNA. After ligation, circled padlock probe is amplified via RCA followed by sequencing by ligation. (B) Illustration of fluorescent *in situ* sequencing (FISSEQ). Target mRNA is first reverse transcribed to cDNA. cDNA is then cross linker and ligated to a circle production. After RCA amplification of circled cDNA, RCA amplicons are cross linked followed by sequencing by ligation.

CHAPTER 2

MULTIPLEXED SINGLE-CELL IN SITU RNA ANALYSIS BY REITERATIVE HYBRIDIZATION

2.1 Abstract

Most current approaches for quantification of RNA species in their natural spatial contexts in single cells are limited by a small number of parallel analyses. Here we report a strategy to grammatically increase the multiplexing capacity for RNA analysis in single cell *in situ*. In this method, transcripts are detected by fluorescence *in situ* hybridization (FISH). After imaging and data storage, the fluorescence signal is efficiently removed by photobleaching. This enables the reinitiation of FISH to detect other RNA species in the same cell. Through reiterative cycles of hybridization, imaging and photobleaching, the identities, positions and copy numbers of a large number of varied RNA species can be quantified in individual cells *in situ*. Using this approach, we analyzed seven different transcripts in single HeLa cells with five reiterative RNA FISH cycles. This approach has the potential to detect over 100 varied RNA species in single cells *in situ*, which will have wide applications in studies of system biology, molecular diagnosis and targeted therapies.

2.2 Introduction

Understanding how cellular regulatory networks function in normal cells and malfunction in diseased cells is an important goal of post genomic research[1]. Microarray technologies[9] and high-throughput sequencing[10,29,74,75] have been widely used to infer the function of genes or to detect altered expression patterns in diseased cells by RNA profiling on a genome-wide scale. However, these approaches carried out with extracted and purified

RNA mask the spatial information of transcripts. Imaging-based methods, such as molecular beacon[76,77] and fluorescence *in situ* hybridization (FISH)[27], enable the RNA analysis in their natural spatial contexts. Nonetheless, due to the spectral overlap of small organic fluorophores, these approaches are limited by the small number of parallel analyses. To integrate the advantage of high-throughput technologies and *in situ* analysis methods, combinatorial labeling[5,78,79], sequential barcoding[45] and *in situ* sequencing[49,80] have been explored recently. Although these approaches significantly advanced our ability to study gene expression *in situ*, some non-ideal factors still exist. For example, the multiplexing capacities of combinatorial labeling and sequential barcoding need to be further enhanced to allow the transcriptome-wide analysis; the current *in situ* sequencing technologies may miss transcripts with lower copy numbers.

We report here an alternative multiplexed single-cell *in sit*u RNA analysis approach by reiterative hybridization. In this method, fluorescently labeled oligonucleotides are hybridized with their target RNA. Under a fluorescence microscope, each RNA molecule is visualized as a single spot. By counting the number of spots in single cells, we can quantify the abundances of the target RNA species in their natural spatial contexts. After fluorescence imaging and data storage, the fluorescence signals are efficiently removed by photobleaching. In the next cycle, different oligonucleotides labeled with the same set of fluorophores as the ones used in the first cycle are added to the sample to quantify their target RNA. Upon reiterative cycles of target hybridization, fluorescence imaging and photobleaching, a comprehensive in situ RNA profiling can be achieved in single cells (Figure 2.4.1). Using this multicolor and multicycle approach, we successfully detected

seven different RNA species in single HeLa cells *in situ* with five reiterative RNA FISH cycles.

2.3 Results and discussion

2.3.1 Design and synthesis of RNA FISH probes

To assess the feasibility of this reiterative hybridization approach, a panel of seven libraries of fluorescently labeled probes was designed and synthesized. These probes target mRNA breast cancer 2 (BRCA2), topoisomerase I (TOP1), breast cancer 1 (BRCA1), polymerase II polypeptide A (POLR2A), PR domain containing 4 (PRDM4), glyceraldehyde-3-phosphate dehydrogenase (GAPDH) and actin beta (ACTB), which are expressed at different levels in HeLa cells, ranging from 10 to 1000 copies per cell. Each library of probes is composed of about 48 20mer oligonucleotides complementary to the coding sequences of their target mRNA. These amino-modified oligo-nucleotides belonging to one library were combined and coupled to succinimidyl ester functionalized fluorophore Quasar 570 or Cy5. After coupling, the fluorescently labeled probes were purified by high-performance liquid chromatography (HPLC) (Figure 2.4.2). The peaks appearing in both the 260 nm and the fluorophore absorbance channels correspond to the coupling products. These results indicate that the fluorophores were successfully coupled to the libraries of oligonucleotides, which can be applied as RNA FISH probes.

2.3.2 Fluorescence signal removal efficiency

One requirement critical for this reiterative hybridization approach is to efficiently remove fluorescence signals at the end of each RNAFISH cycles. Consequently, the fluorescence leftover in previous cycles will not lead to false positive signals in the subsequent cycles.

Due to its high signal removal efficiency, photobleaching has been explored for multiplexed immunofluorescence[81]. To test the possibility of applying photobleaching for reiterative RNA FISH, we stained mRNA BRCA1 and TOP1 with Quasar 570 and CY5 labeled probes, respectively. Upon hybridization, individual transcripts were visualized under a fluorescence microscope as diffraction-limited spots (Figure 2.4.3a and b). To minimize the photobleaching effects during imaging acquisition, the cells were imaged in an antifade buffer containing glucose and glucose oxidase; while to maximize the photobleaching efficiency, the samples were photobleached in 1× phosphate buffered saline (PBS). After photobleaching, almost all the fluorescence signals were removed (Figure 2.4.3c and d). We quantified the photobleaching efficiencyby analyzing the fluorescence intensities of 30 spots before and after photobleaching. The ON/OFF ratios for Quasar 570 and Cy5 labeled probes are over 12 : 1 (Figure 2.4.3e) ($P < 0.001$). We also counted the number of fluorescent spots in 30 cells before and after photobleaching, almost no spots were observed (Figure 2.4.3f) ($P < 0.0001$). These results indicate that the fluorescence signals generated by hybridization of RNA FISH probes can be efficiently erased by photobleaching, and the minimum leftover signal will not interfere with the subsequent cycles.

2.3.3 Effects of photobleaching on subsequent cycles

Another requirement for this reiterative hybridization approach is to maintain the integrity of the specimen exposed to extensive photobleaching. To achieve that, we washed the sample every three minutes during photobleaching to remove the radicals generated from degradation of the fluorophores. We assessed the effects of photobleaching on subsequent

cycles by comparing the mRNA expression levels and patterns with and without photobleaching before hybridization of RNA FISH probes. After photobleaching with the Quasar 570 filter for 2 h, the expression pattern (Figure 2.4.4a) closely resembles the one without photobleaching (Figure 2.4.4b). Under both conditions, the copy numbers of BRCA1 transcripts per cell are similar (Figure 2.4.4e). For cells exposed to photobleaching with the Cy5 filter for two hours, the TOP1 expression patterns (Figure 2.4.4c) and levels (Figure 2.4.4e) also closely resemble those without photobleaching (Figure 2.4.4d). These results suggest that the photobleaching process does not compromise the accuracy of the RNA FISH analysis in subsequent cycles.

2.3.4 Multiplexed single-cell *in situ* RNA analysis

To evaluate the feasibility of our reiterative hybridization approach for multicolor and multicycle RNA detection, we profiled seven different transcripts in single HeLa cells. In the first RNA FISH cycle, BRCA2 (Figure 2.4.5a) and TOP1 (Figure 2.4.5b) transcripts were hybridized with oligonucleotide probes labeled with Quasar 570 and Cy5, respectively. Following fluorescence imaging and data storage, the two fluorophores were efficiently photobleached. This enables the initiation of the second cycle, in which BRCA1 (Figure 2.4.5c) and POLR2A (Figure 2.4.5d) mRNA were stained with Quasar 570 and Cy5 labeled probes. To demonstrate the multicycle potential of this approach, in the subsequent cycles we quantified one transcript per cycle using only Cy5 labeled probes. Upon continuous cycles of target hybridization, fluorescence imaging, and photobleaching, PRDM4 (Figure 2.4.5e), GAPDH (Figure 2.4.5f), and ACTB (Figure 2.4.5g) were unambiguously detected. The distribution patterns of transcripts obtained by this reiterative

hybridization approach are similar to those in conventional one-cycle RNA FISH (Figure 2.4.5h-n). To assess the accuracy of our approach, we compared the mean copy numbers of transcripts per cell measured by reiterative hybridization and conventional RNA FISH. For the seven mRNA species with average copy numbers ranging from 10 to 1000 copies per cell, the results obtained using the two methods are consistent with those in the literature[82] and closely resemble each other (Figure 2.4.6a), with an R^2 value of 0.98 (Figure 2.4.6b). These results indicate this reiterative hybridization approach enables accurate multiplexed RNA profiling *in situ* by multicolor and multicycle staining.

2.3.5 Expression heterogeneity and correlation

Many experiments show that genetically identical cells can exhibit significant cell-to-cell variations in gene expression[83–90]. By enabling comprehensive RNA profiling in single cells, our reiterative hybridization approach can be applied to investigate gene expression heterogeneity. As shown in Figure 2.4.7a, the copy number of transcripts per cell are distributed in a wide range. This significant variation in gene expression leads to the relatively large error bars in Figure 2.4.3f, Figure 2.4.4e, Figure 2.4.6a and b. For all the seven mRNA species, the square of the expression standard deviation is much higher than the mean copy numbers. These results indicate that these mRNA species are synthesized by transcriptional bursts rather than at a constant rate[88]. With the single-cell resolution, our approach also allows the investigation of whether the transcriptional bursts of different genes are coordinated. By correlating RNA expression levels pairwise, we found correlation coefficients ranging from -0.51 to 0.62 (Figure 2.4.7b), suggesting the heterogeneous coordination of transcriptional bursts.

2.3.6 Summary

In summary, we have demonstrated that our reiterative hybridization approach can be applied for multiplexed single-cell *in situ* RNA analysis at the optical resolution. Compared with existing RNA profiling methods, our approach has the following advantages. By directly imaging transcripts *in situ*, this technique preserves the spatial information of RNA in different cells in a structured tissue. This makes our approach a powerful tool to study cell-cell communications in heterogeneous biological systems. Additionally, this method avoids the intrinsic bias generated during cDNA synthesis or target sequence amplification, which enhances the accuracy to quantify transcripts with low copy numbers. Finally, using oligonucleotide probes labeled with the same fluorophore rather that multiple different fluorophores to stain each RNA molecule, our approach allows the detection of short transcripts.

The number of different RNA species that can be quantified in individual cells depends on two factors: the number of RNA FISH cycles and the number of RNA species detected in each cycle. To remove fluorescence signals efficiently, it takes about 6 and 1.5 minutes to photobleach Quasar 570 and Cy5, respectively. And we have shown that after photobleaching for 2 hours, transcripts can still be accurately quantified in subsequent RNA FISH cycles. This suggests that we can further increase the number of RNA FISH cycles significantly. Moreover, by integration with combinational labeling[5,78,79] or multispectral fluorophores[91–93], a much larger number of different RNA species can be quantified in each RNA FISH cycle. Therefore, we envision that this reiterative hybridization approach has the potential to detect more than 100 varied RNA species in

single cell *in situ*. That will bring new insights into systems biology, signaling pathway studies, molecular diagnosis and targeted therapies.

2.4 Figures

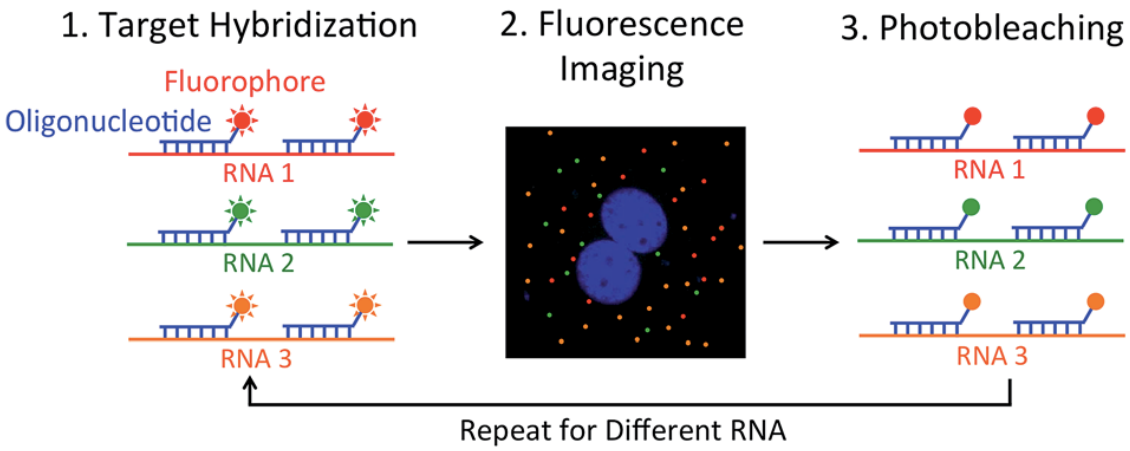

Figure 2.4.1. Multiplexed single-cell *in situ* RNA analysis by reiterative hybridization. RNA in fixed cells is hybridized with fluorescently labeled oligonucleotides. After imaging, the fluorophores are photobleached. Through cycles of target hybridization, fluorescence imaging and photobleaching, a large number of different RNA species can be analyzed in individual cells *in situ*.

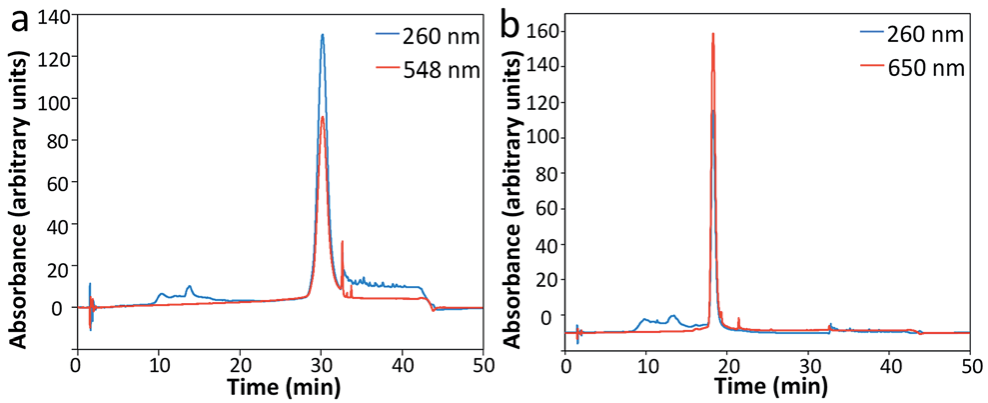

Figure 2.4.2. Sample HPLC chromatographs of (a) Quasar 570 and (b) Cy5 coupled oligonucleotides as RNA FISH probes.

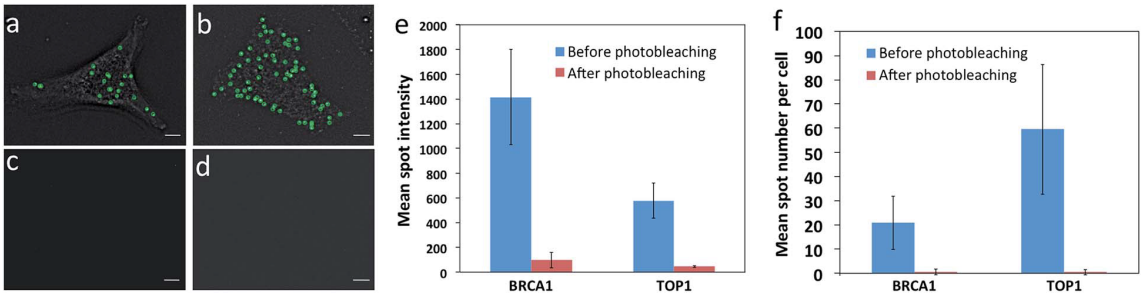

Figure 2.4.3. Photobleaching efficiency. (a) BRCA1 and (b) TOP1 transcripts are hybridized with Quasar 570 and Cy5 labeled probes, respectively. Fluorescent spots are identified computationally and displayed as green cycles. (c) The Quasar 570 fluorescence signal and (d) the Cy5 fluorescence signal are removed by photobleaching. (e) The mean spot intensity (n = 30 spots) before and after photobleaching. (f) The mean spot number per cell (n = 30 cells) before and after photobleaching. Scale bars, 5 μm.

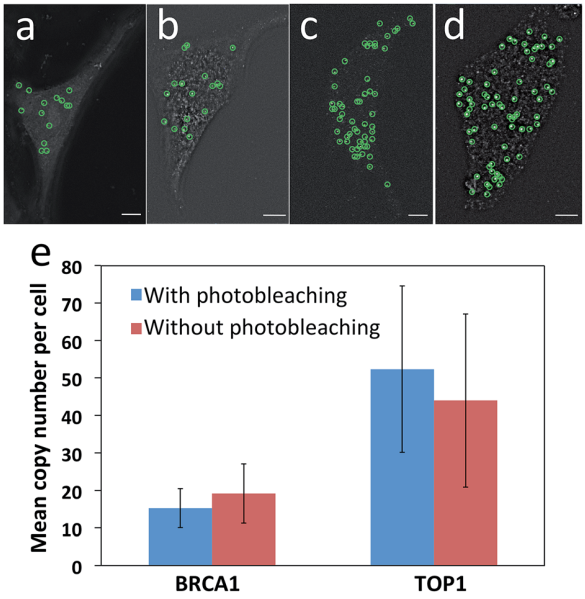

Figure 2.4.4. Effects of photobleaching on subsequent cycles. (a) With and (b) without photobleaching with Quasar 570 filter for two hours in advance, BRCA1 transcripts are hybridized with Quasar 570 labeled probes. (c) With and (d) without photobleaching with the Cy5 filter for two hours in advance, TOP1 transcripts are hybridized with Cy5 labeled probes. Fluorescent spots are identified computationally and displayed as green circles. (e) The mean copy number of BRCA1 and TOP1 transcripts per cell (n = 30 cells) with and without photobleaching before hybridization. Scale bars, 5 μm.

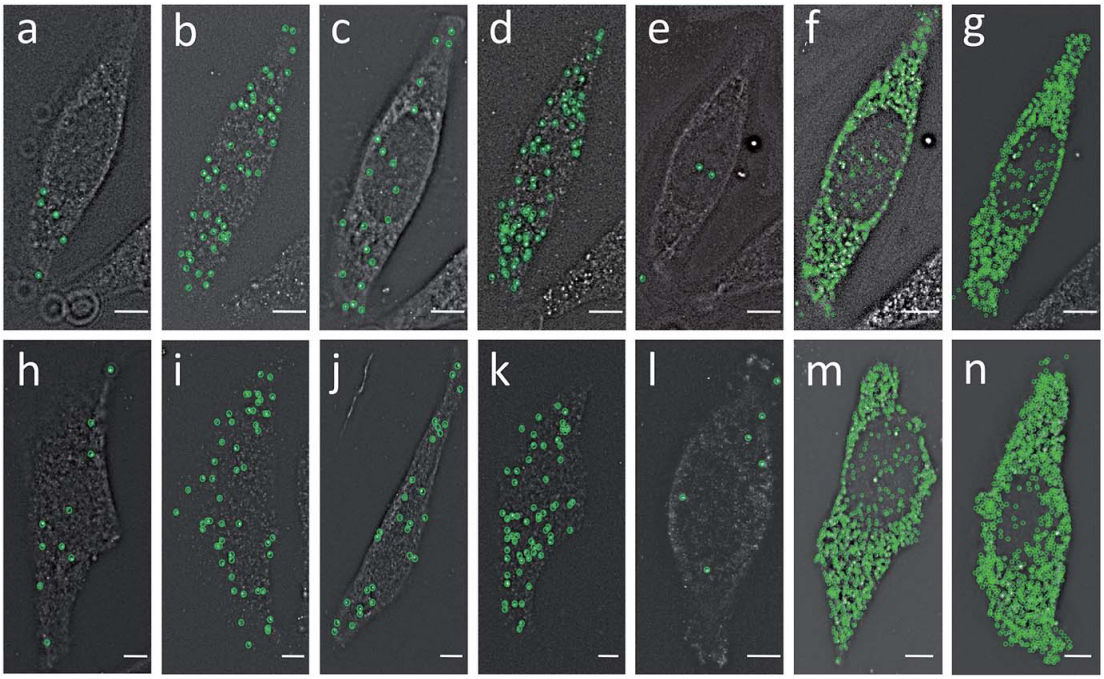

Figure 2.4.5. (a) BRCA2, (b) TOP1, (c) BRCA1, (d) POLR2A, (e) PRDM4, (f) GAPDH and (g) ACTB transcripts are detected in the same cell by our reiterative hybridization approach. (h) BRCA2, (i) TOP1, (j) BRCA1, (k) POLR2A, (l) PRDM4, (m) GAPDH and (n) ACTB transcripts are detected in different cells by conventional RNA FISH. Fluorescent spots are identified computationally and displayed as green cycles. Scale bars, 5 μm.

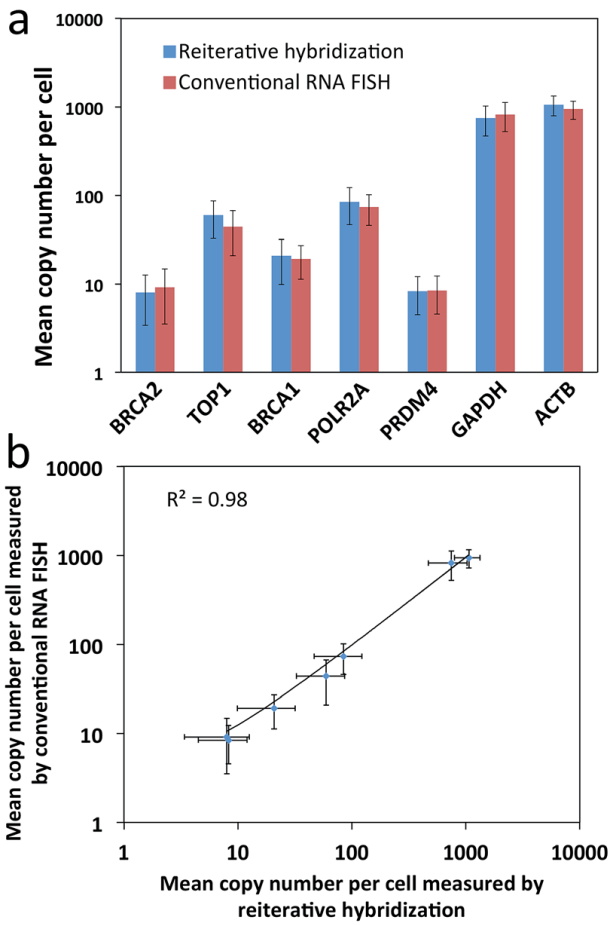

Figure 2.4.6. Validation of the reiterative hybridization approach. (a) Mean copy number per cell (n = 30 cells) of seven transcripts measured by reiterative hybridization and conventional RNA FISH. (b) Comparison of the results obtained by reiterative hybridization and conventional RNA FISH yields R^2 = 0.98 with a slope of 0.96. The axes in both (a) and (b) are on a logarithmic scale.

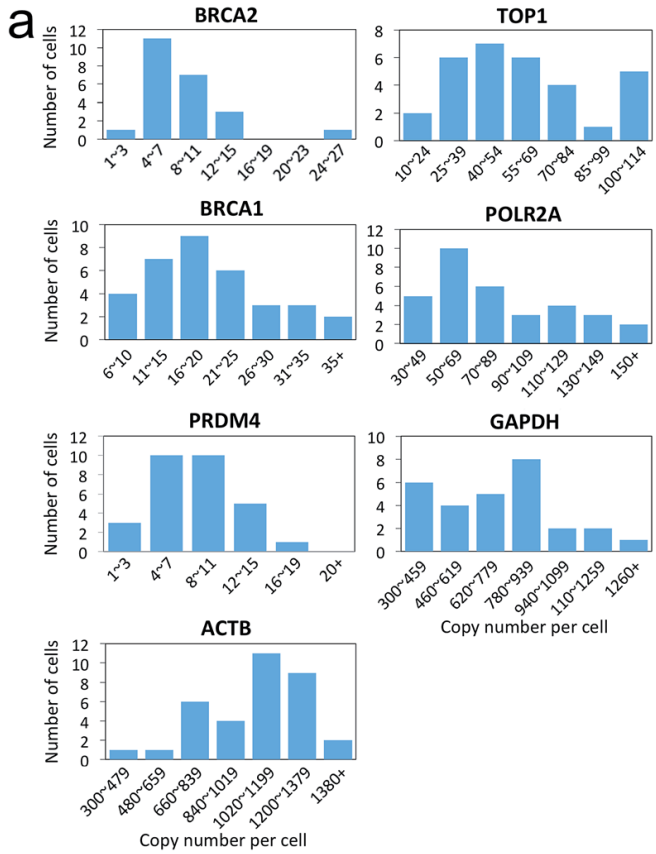

b

BRCA2	-0.095	-0.187	-0.272	-0.155	-0.495	-0.509
	TOP1	0.279	0.539	0.055	0.493	0.293
		BRCA1	0.387	0.285	0.202	0
			POLR2A	0.261	0.524	0.268
				PRDM4	0.497	0.167
					GAPDH	0.62
						ACTB

Figure 2.4.7. Gene expression heterogeneity and correlation. (a) Histograms of the copy number distribution of the seven mRNA species. (b) Expression correlation coefficient of each gene pair, with the darkness corresponding to the correlation coeffiecient.

2.5 Methods

2.5.1 Chemicals and bioreagents

Chemicals and solvents were purchased from Sigma-Aldrich or Ambion and were used directly without further purification, unless otherwise noted. Bioreagents were purchased from Invitrogen, unless otherwise indicated.

2.5.2 Preparation of fluorescently labeled oligonucleotide probes

Oligonucleotides belonging to one library (BioSearch), each at a scale of 25 pmol, was dissolved in 1 μL of nuclease-free water. To this solution was added sodium bicarbonate aqueous solution (1 M, 3 μL) and Quasar 570 (BioSearch) or Cy5 (AAT Bioquest) in DMF (20mM, 5 μL). The mixture was then diluted to a volume of 10 μL with nuclease-free water and incubated at room temperature for 2 h. Subsequently, the fluorescently labeled oligonucleotides were purified by using a nucleotide removal kit (Qiagen) and dried in a Savant SpeedVac Concentrator (Thermo Scientific).

The dried fluorophore conjugated oligonucleotides were then further purified via an HPLC (Agilent) equipped with a C18 column (Agilent) and a dual wavelength detector set to detect DNA absorption (260 nm) as well as the absorption of the coupled fluorophore (5480 nm for Quasar 570, 650 nm for Cy5). For the gradient, triethyl ammonium acetate (Buffer A) (0.1 M, pH 6.5) and acetonitrile (Buffer B) (pH 6.5) were used, ranging from 7% to 30% Buffer B over the course of 30 min, then at 70% Buffer B for 10 min followed by 7% Buffer B for another 10 min, all a flow rate of 1 mL min^{-1}. The collected fraction was subsequently dried in a Savant SpeedVac Concentrator and stored as the stock probe

solution at 4 °C in 200 μL nuclease-free water to which 1 × Tris EDTA (TE) (2 μL, pH 8.0) was added.

2.5.3 Cell culture

HeLa CCL-2 cells (ATCC) were maintained in Dulbecco's modified Eagle's Medium (DMEM) supplemented with 10% fetal bovine serum, 10 U mL^{-1} penicillin and 100 g mL^{-1} streptomycin in a humidified atmosphere at 37 °C with 5% CO_2. Cells were plated on chambered cover glass (Thermo Scientific) and allowed to reach 60% confluency in 1-2 days.

2.5.4 Cell fixation

Cultured HeLa CCL-2 cells were washed with 1 × PBS at room temperature for 5 min, fixed with fixation solution (4% formaldehyde (Polysciences) in 1 × PBS) at room temperature for 10 min, and subsequently washed another 2 times with 1 × PBS at room temperature, each for 5 min. The fixed cells were then permeabilized with 70% (v/v) EtOH at 4 °C at least overnight.

2.5.5 Fluorescence signal removal efficiency

To 100 μL of hybridization buffer (100 mg mL^{-1} dextran sulfate, 1 mg mL^{-1} *Escherichia coli* tRNA, 2 mM vanadyl ribonucleotide complex, 20 μg mL^{-1} bovine serum albumin and 10% formamide in 2 × SSC) was added 2 μL of the Quasar 570 labeled BRCA1 or Cy5 labeled TOP1 stock probe solution. Then the mixture was vortexed and centrifuged to obtain the hybridization solution.

Fixed HeLa CCL-2 cells were first washed once with wash buffer (10% formamide in 2 × SSC) for 5 min, the incubated with the hybridization solution at 37 °C overnight, and

subsequently washed 3 times with wash buffer, each for 30 min, at 37 °C. After incubating with GLOX buffer (0.4% glucose and 10 mM Tris HCl in 2 × SSC) for 1-2 min, the stained cells were imaged in GLOX solution (0.37 mg mL^{-1} glucose oxidase and 1% catalase in GLOX buffer). After imaging, each target cell in 1 × PBS was photobleached individually with the Quasar 570 filter for 20 s or the Cy5 filter for 5 s at each z step. 1 × PBS was changed every 3 min during photobleaching to remove the radicals. Following photobleaching, the HeLa cells were imaged again in GLOX solution.

2.5.6 Effects of photobleaching on subsequent cycles

Fixed HeLa CCL-2 cells in 1 × PBS were first photobleached with the Quasar 570 filter for 2 h, with changing 1 × PBS solution every 3 min. Subsequently, after washing with wash buffer for 5 min, the cells were incubated with the BRCA1 or TOP1 hybridization solution at 37 °C for overnight, and subsequently washed 3 times with wash buffer, each for 30 min, at 37 °C. After incubating with GLOX buffer for 1-2 min, the stained cells were imaged in GLOX solution. Control experiments were carried out using the same protocol without photobleaching steps before the hybridization of BRCA1 or TOP1 probes.

2.5.7 Reiterative RNA FISH

Fixed HeLa CCL-2 cells were first washed once with wash buffer for 5 min, then incubated with the hybridization solution at 37 °C overnight, and subsequently washed 3 times with wash buffer, each for 30 min, at 37 °C. After incubating with GLOX buffer for 1-2 min, the stained cells were imaged in GLOX solution. After imaging, each cell in 1 × PBS was photobleached individually with the Quasar 570 filter for 20 s or the Cy5 filter for 5 s at

each z step, followed by the next cycle of RNA FISH. 1 × PBS was changed every 3 min during photobleaching to remove the radicals.

2.5.8 Imaging and data analysis

Stained cells were imaged under a Nikon Ti-E epifluorescence microscope equipped with a 100× objective, using a 5 μm z range and 0.3 μm z spacing. Imaging were captured using a CoolSNAP HQ2 camera and NIS-Elements Imaging software. Chroma filter 49004 and 49009 were used for Quasar 570 and Cy5, respectively. Fluorescent spots were identified computationally using an imaging processing program[27].

CHAPTER 3

HIGHLY MULTIPLEXED SINGLE-CELL IN SITU RNA ANALYSIS BY CONSECUTIVE HYBRIDIZATION

3.1 Abstract

Limitations on the number of RNA species and genomic loci that can be quantified in single cells in situ impede advances in our deep understanding of normal cell physiology and disease pathogenesis. Here we present a method for highly multiplexed single cell in situ RNA and DNA analysis by consecutive fluorescence in situ hybridization (C-FISH). In this method, individual transcripts or genomic loci are visualized as fluorescent spots with fixed locations in individual cells. In each cycle of C-FISH, fluorescently labeled probes hybridize to the probe used in the previous cycle, and also introduce multiple binding sites for the probe of the following cycle. Through consecutive cycles of probe hybridization, fluorescence imaging and photobleaching, different RNA species or genomic loci can be identified as fluorescent spots with unique color sequences. Applying this approach, we demonstrate that with 2 fluorophores and 16 cycles of C-FISH, different transcripts loci is unambiguously identified in individual cells with close to "0" raw data error rate. These results suggest all the varied color sequences (2^{16} = 65,536 or 3^{10} = 59,049) can be applied to identify distinct RNA species or genomic loci, which allows the transcriptome- or genome-wide single cell in situ analysis. This highly multiplexed single cell in situ RNA and DNA analysis technology will have wide applications in signaling network analysis, 3D genome architecture studies, molecular diagnosis and cellular targeted therapies.

3.2 Introduction

The ability to profile transcriptome and genome comprehensively in single cells in situ is crucial for our understanding of cancer, neurobiology and stem cell biology[94]. Microarray technologies[95] and next-generation sequencing[96,97] have been widely applied to study RNA or DNA on a transcriptome- or genome-wide scale. However, since nucleic acids are extracted, purified, and then quantified in these assays, the location information of the nucleic acids are lost during analysis. Fluorescent hybridization probes[98–101] enable RNA and DNA to be profiled in their native spatial contexts in individual cells. Nevertheless, due to the spectral overlap of fluorophores, these imaging-based approaches are limited by their low multiplexing capacity.

To enable highly multiplexed single-cell in situ RNA and DNA analysis, a number of methods have been explored. Such approaches include reiterative hybridization[99,102–104], combinatorial labeling[105–107], in situ sequencing[108,109], sequential hybridization[110], and multiplexed error-robust fluorescence in situ hybridization (MER-FISH)[111]. Although these technologies significantly advance our ability to profile RNA and DNA in situ, some non-ideal factors still exist. For example, the multiplexing capabilities of reiterative hybridization and combinatorial labeling need to be further improved to allow transcriptome- or genome-wide analysis. Due to the limited efficiency of reverse transcription, in situ sequencing has limited detection sensitivity and can miss transcripts with low-expression levels. In sequential hybridization, the probes are degraded by DNase, which has limited signal removal efficiency and also hinders its application for DNA analysis. Additionally, DNase degrades all the probes simultaneously, including the large

oligonucleotides library that directly hybridize to the RNA targets. As a result, this expensive library has to be rehybridized in each analysis cycle, which make this approach less cost-effective and more time-consuming. Without signal amplification, the current version of MER-FISH applies a large number of oligonucleotide probes to hybridize to different regions of each transcript, which limits its application to study short mRNA molecules or partially degraded transcripts in tissue samples. Furthermore, artificial threshold need to be applied for signal recognition, which potentially increases the error rate. A mistake in 0 or 1 assignment may alter the derived identity of the transcript. A Hamming distance algorithm (HD-4)[111] is applied to address the issue, but this will dramatically reduce the potential transcripts amount MERFISH could analyze.

Here we report a highly multiplexed single cell in situ RNA and DNA analysis approach by consecutive fluorescence in situ hybridization (C-FISH). In this method, individual transcripts or genomic loci are visualized as single fluorescent spots, which remain in place during consecutive hybridization. In each cycle of C-FISH, fluorescently labeled probes hybridize to the probe used in the previous cycle, and also introduce multiple binding sites for the probe of the following cycle. Through consecutive cycles of probe hybridization, fluorescence imaging and photobleaching, different RNA species or genomic loci can be identified as fluorescent spots with unique color sequences. The number of varied color sequences increases exponentially with the number of hybridization cycles, which enables comprehensive RNA or DNA analysis in single cells in situ. To demonstrate the feasibility of this approach, we show that with 2 fluorophores and 16 cycles of C-FISH, different transcripts or genomic loci in individual cells are unambiguously identified at the single-

molecule sensitivity with close to "0" raw data error rate. And all the varied color sequences (2^{16} = 65,536 or 3^{10} = 59,049) can be applied to identify distinct RNA species or genomic loci, which allows the transcriptome- or genome-wide single cell in situ analysis.

3.3 Results and discussion

3.3.1 Platform design

In C-FISH, each transcript or genomic locus is first hybridized with a set of pre-decoding probes (Fig. 3.4.1A). These probes have varied targeting sequences to bind to the different regions on their target and the shared decoding sequence to bind to decoding probes. Subsequently, the fluorescent decoding probe is applied to hybridize to the pre-decoding probes. Consequently, individual transcript or genomic locus is visualized as a single spot under the fluorescence microscope (Fig. 1B). A major source of error in sequential hybridization[110] and MER-FISH[111] is the loss of signal as the cycle number increases. To address this issue by amplifying the signal intensities through the hybridization cycles, we design each decoding probe with one binding site to hybridize to the probe in the previous cycle and two binding sites to hybridize to the probe in the following cycle. After fluorescence imaging and data storage, the fluorophores are photobleached to enable the initiation of the next C-FISH cycle. As cells or tissue samples are fixed, transcripts or genomic loci remain in place during the whole C-FISH process. Through consecutive cycles of probe hybridization, fluorescence imaging, and photobleaching, each transcript or genomic locus is identified as a fluorescent spot with a unique color sequence (Fig. 1C). The number of varied fluorophore sequences increases exponentially with the number of hybridization cycles, which enables the transcriptome- or genome-wide analysis. For

example, with M fluorophores applied in each cycle and N cycle of C-FISH, an overall M^N RNA species or genomic loci can be profiled in the same specimen in situ.

3.3.2 2-Cycle C-FISH for RNA analysis

To assess the feasibility of our approaches, we performed a two-cycle C-FISH against mRNA GAPDH with Cy5 labeled decoding probes (Figure 3.4.2A).

A critical requirement for the success of this approach is to efficiently remove the fluorescence signals at the end of each C-FISH cycle. As a result, the signal generated in the previous cycle will not interfere with the signal determination in the following cycle. Additionally, this signal removal process should not lead to loss of RNA or DNA integrity. Only in this way, individual transcript or genomic locus can be visualized in every C-FISH cycle in the same location. Our laboratory has demonstrated these signal removal requirements can be achieved by photobleaching[102]. Therefore, here we applied photobleaching to erase the signals generated by hybridization. By performing this experiment, we observed a signal remove efficiency of >95% (Figure 3.4.2B). Moreover, we noticed 82.8% ± 4.0% of the spots appeared in the first cycle co-localized with the spots in the second cycle (Figure 3.4.2C). This corresponded with the theoretical hybridization efficiency of ~75%[106]. These results suggest that photobleaching in C-FISH can efficiently remove remaining signal while still preserving target RNA integrity.

3.3.3 16-cycle 2-color RNA restaining

One of the keys for C-FISH to achieve high throughput multiplexed RNA analysis is to perform multi-cycle decoding hybridizations. To demonstrate C-FISH's multi-cycle ability, we stained mRNA GAPDH (Figure 3.4.3) and mRNA Ki67 (Figure 3.4.5) in 16

consecutive hybridization cycles using C-FISH. For GAPDH staining, Quasar 570 labeled decoding probes were used in odd decoding cycles and Cy5 labeled decoding probes were used in even decoding cycles. For Ki 67 staining, Cy5 labeled decoding probes were used in odd decoding cycles and Quasar 570 labeled probes were used in even decoding cycles. Over 95% of the spots co-localized in the first two cycles were successfully reappear in the following cycles (Figure 3.4.4B and Figure 3.4.6B). This indicate C-FISH does not damage the RNA integrity, and the branched oligonucleotide structure consisted of both pre-decoding probes and decoding probes from previous cycles remain stable and hybridized to their RNA targets throughout the assay.

We consider the number of spots appears in all 16 cycles per cell the result of transcripts copy number per cell obtained by C-FISH. In order to validate the copy number derived from our C-FISH, we performed conventional smFISH against GAPDH and Ki67. For both GAPDH and Ki67, the average copy number and distribution of the copy number were statistically consistent between C-FISH and smFISH. The match between the two approaches suggests that C-FISH has a reliable detection against mRNA molecules with low error rate.

By reviewing box plots of the FISH spots signal intensity of GAPDH (Figure 3.4.4A) and Ki67 (Figure 3.4.6A) in both Quasar 570 and Cy5 channels, we observed a high staining specificity that all the FISH spots were unambiguously detected in the correct fluorescence channels. This would eliminate the possible detection error caused by misidentification of barcode. Furthermore, we observed steady signal intensity increases throughout 16 C-FISH cycles (Figure 3.4.4A and Figure 3.4.6A). This would prevent the possible signal loss after

cycles. And the signal amplification would also grant C-FISH the potential to detect short RNA molecules.

3.3.4 16-cycle 2-color C-FISH for multiplexed RNA analysis

To further demonstrate the multi-cycle potential of our approach, we co-stained mRNA GAPDH and mRNA Ki67 in the same set of cells in 16 consecutive C-FISH hybridization (Figure 3.4.7). In each odd decoding cycle, decoding probes labeled with Quasar 570 were hybridized against GAPDH and decoding probes labeled with Cy5 were hybridized against Ki67. On the contrary, in each even decoding cycle, decoding probes labeled with Cy5 were hybridized against GAPDH and decoding probes labeled with Quasar were hybridized against Ki67.

Box plots of the FISH spots signal intensity of both GAPDH and Ki67 were shown in Figure 3.4.8A and 3.4.8B, respectively. It is important that there is no mis-hybridization of decoding probes between different transcripts in each cycle. The box plots demonstrated a high staining specificity for C-FISH. In odd cycles, spots corresponded to mRNA GAPDH had significant higher intensity in Quasar 570 channel and spots corresponded to mRNA Ki67 had significant higher intensity in Cy5 channel, while in even cycles, spots corresponded to mRNA GAPDH had significant higher intensity in Cy5 channel and spots corresponded to mRNA Ki67 had significant higher intensity in Quasar 570 channel. This suggested there was no signal crosstalk during C-FISH decoding hybridization. Furthermore, the specific staining allows C-FISH to unambiguously assign each barcode to the correct fluorescence channel. In MERFISH[111], artificial threshold is applied to determine if the barcode in a certain cycle is positive 1 or negative 0. As a result, this can

lead to false negative signals if the stained transcripts have low signal intensity, or false positive signals if the un-stained transcripts have high fluorescence intensity. Instead of using artificial threshold, C-FISH compares the signal intensities of the same spot in different fluorescence channels to determine which channel the barcode should be assigned to. Moreover, unambiguous identification for both strong spots (Figure 3.4.9A and C) and weak spots (Figure 3.4.9B and D) was demonstrated to be easily achieved in each cycle during the 2-color 16-cyle C-FISH.

Furthermore, the barcode survival rate (Figure 3.4.8C and E) and comparison with conventional smFISH results (Figure 3.4.8 D and F) are both in consistency with results of the 16 cycles C-FISH against single transcript GAPDH. These results further validated the copy numbers derived from C-FISH and demonstrated C-FISH's the accurate detection of multi RNAs *in situ*.

3.3.5 Discussion

We have developed a C-FISH technology and demonstrated that our approach could be applied for *in situ* RNA profiling. Comparing with existing RNA profiling methods, our approach has the following advantages. Firstly, by directly imaging transcripts in situ, our approach can analyze absolute transcript expression levels at the single-molecule sensitivity with spatial information of RNA molecules preserved. Secondly, instead of degrading probe libraries via DNase I in seqFISH[110], C-FISH keeps the pre-decoding probe libraries hybridized to their targets throughout the assay. This would dramatically decrease the assay time and cost, since the pre-decoding library is usually composed of thousands of oligonucleotides its hybridization could take overnight to 36 h. Thirdly, C-FISH

unambiguously assigns each barcode to the correct fluorescence channel simply by comparing the signal intensities of the same spot in different channels. This would avoid any false positive and negative signals generated by the artificial threshold, which MERFISH[111] used. Moreover, with signal amplified during the assays, C-FISH could prevent the signal loss after cycles and has the potential to detect shorter RNA molecules. The number of RNA species C-FISH could quantify depends on two factors: the number of decoding hybridization cycles and the number of different fluorophores used in each cycle. We have demonstrated that C-FISH could be carried out for at least 16 cycles with high analysis accuracy. And it has been reported that hundreds of thousands of oligonucleotides could be prepared cost-effectively by massively parallel synthesis on a microarray slide[112]. Therefore, by applying four fluorophores in each cycle, C-FISH could potentially enable the whole transcriptome profiling with in 8 cycles using the 65536 (4^8) distinct fluorophore sequences. Furthermore, by combining C-FISH approach with multiplexed in situ protein analysis technologies, the technology will enable the comprehensive and integrated RNA and protein profiling in single cell *in situ*. This will bring new insights into systems biology, signaling pathway studies, molecular diagnosis and targeted therapies.

3.4 Figures

A

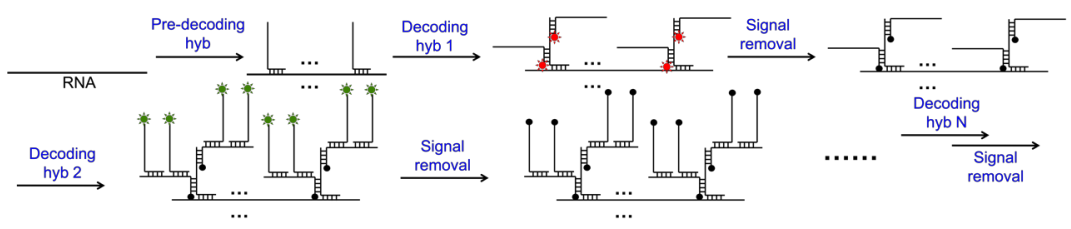

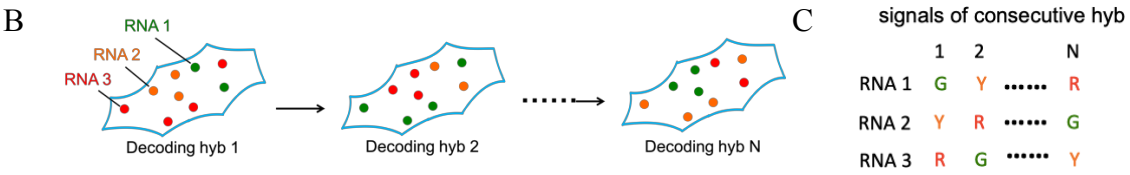

Figure 3.4.1. Highly multiplexed single-cell in situ RNA analysis by C-FISH. (A) Each transcript is first hybridized with a set of pre-decoding probes with varied targeting sequences to bind to the different regions on their target and the shared decoding sequence to bind to decoding probes. After applying fluorescent labeled decoding probes and doing imaging, the fluorophores are photobleached to enable the initiation of the next C-FISH cycle. Through reiterative cycles of decoding hybridization, fluorescence imaging and photobleaching, the target RNA is sequentially stained by a set of decoding probes with varied fluorophores. (B) Schematic diagram of the N cycles of hybridization images. In each cycle, individual transcript in visualized as a single spot with a specific color. (C) As RNA molecules remain in place during different hybridization cycles, different RNA species can be identified by the unique color sequences.

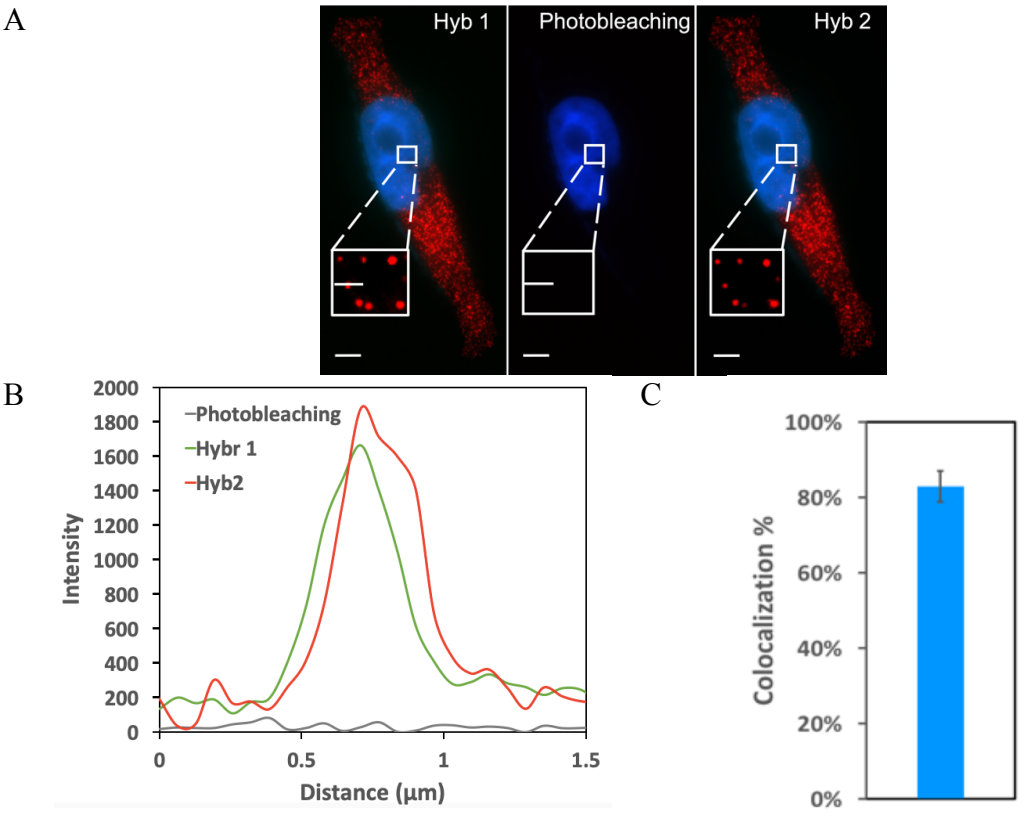

Figure 3.4.2. (A) Fluorescent images of two rounds consecutive FISH against GAPDH transcript in HeLa cell. (B) Signal intensity of spot marked in the zooming area. **(C)** Fraction of GAPDH spots identified from first round of hybridization that reappeared in the second round of hybridization per cell (n = 30 cells). Scale bars, 5 μm.

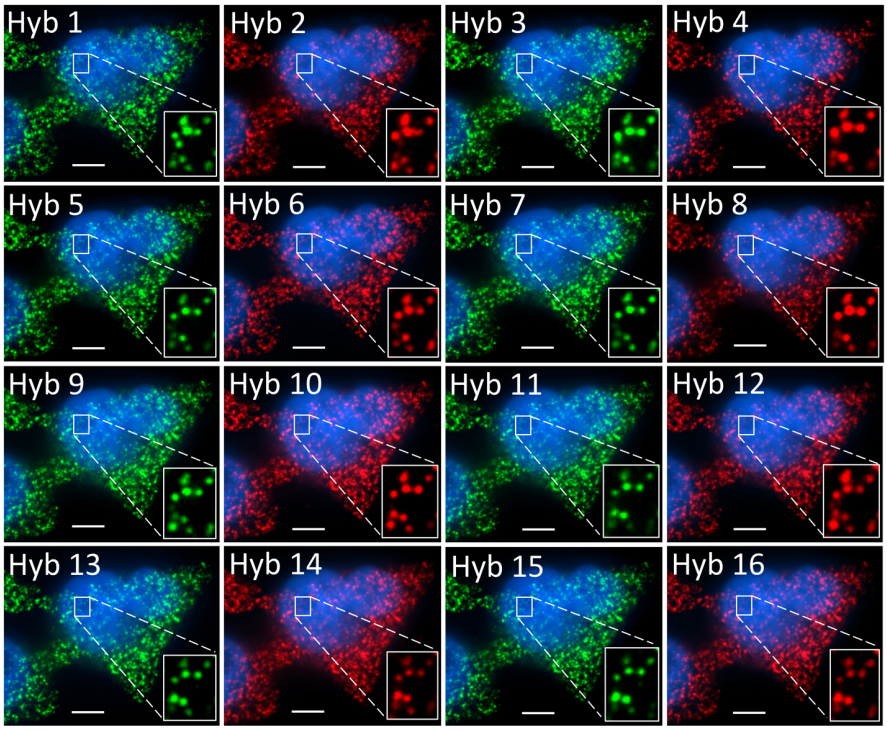

Figure 3.4.3. Fluorescent images of sixteen rounds consecutive FISH against GAPDH transcripts in HeLa cell. Quasar 570 (showed in green) labeled probes were used in odd hybridization rounds. Cy5 (showed in red) labeled probes were used in odd hybridization rounds. Scale bars, 5 μm.

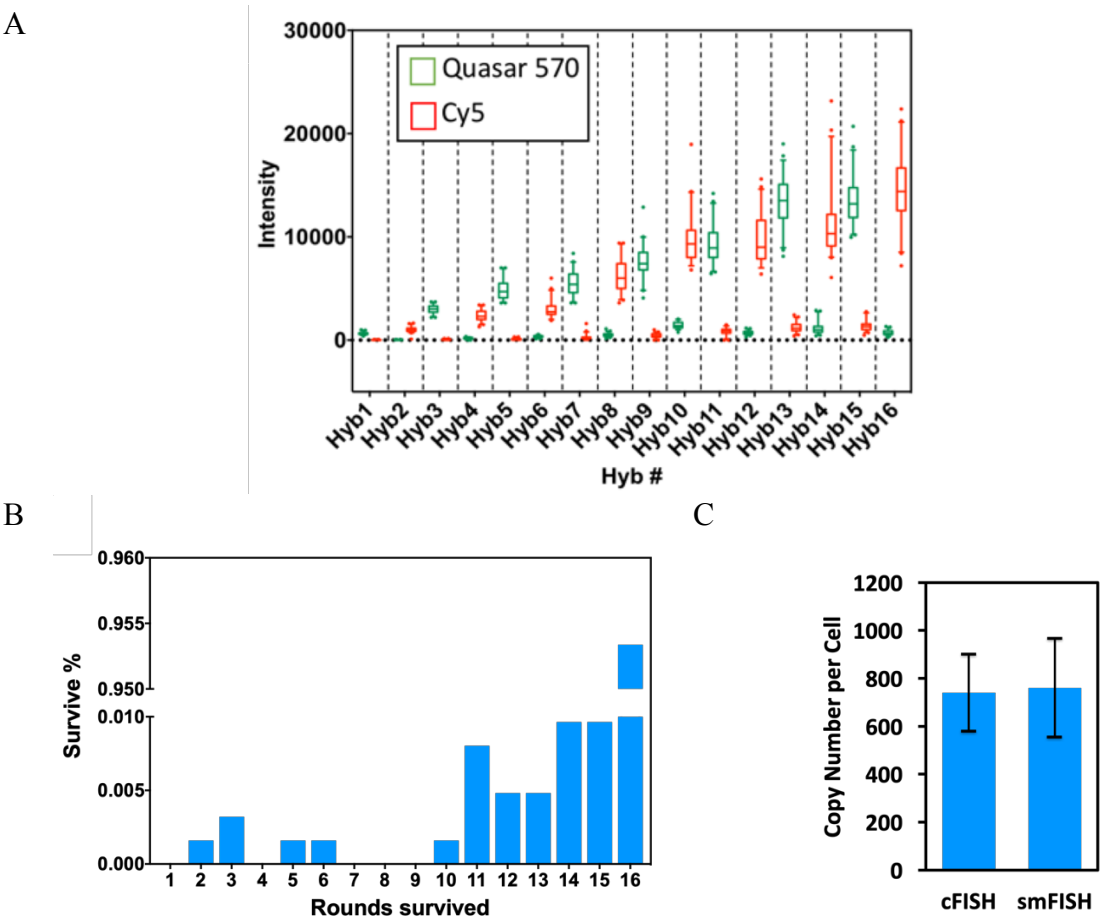

Figure 3.4.4. (A) Intensity distribution (n = 45 spots) in Quasar 570 and Cy5 channels at the position of FISH spots corresponding to GAPDH transcript over sixteen rounds of consecutive FISH. (B) Fraction of GAPDH barcodes spots (1000 spots) identified from first two rounds of hybridization that survived for different rounds of hybridization. (C) Comparison of the mean copy number per cell (n = 30 cells) of GAPDH measured by C-FSIH and conventional smFISH (P = 0.997). Barcodes were identified by colocalization through the first two rounds of hybridizations.

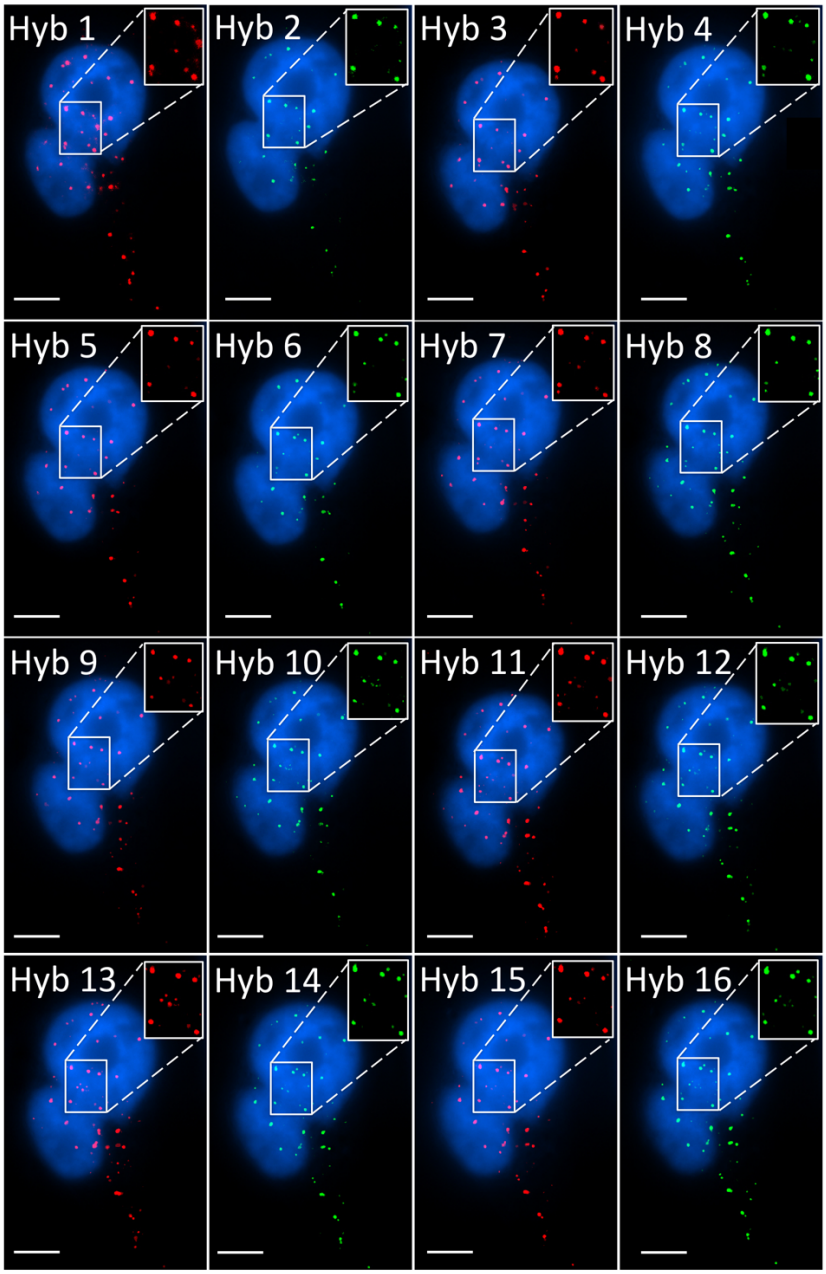

Figure 3.4.5. Fluorescent images of sixteen rounds consecutive FISH against Ki67 transcripts in HeLa cell. Quasar 570 (showed in green) labeled probes were used in odd hybridization rounds. Cy5 (showed in red) labeled probes were used in odd hybridization rounds against. Scale bars, 5 μm.

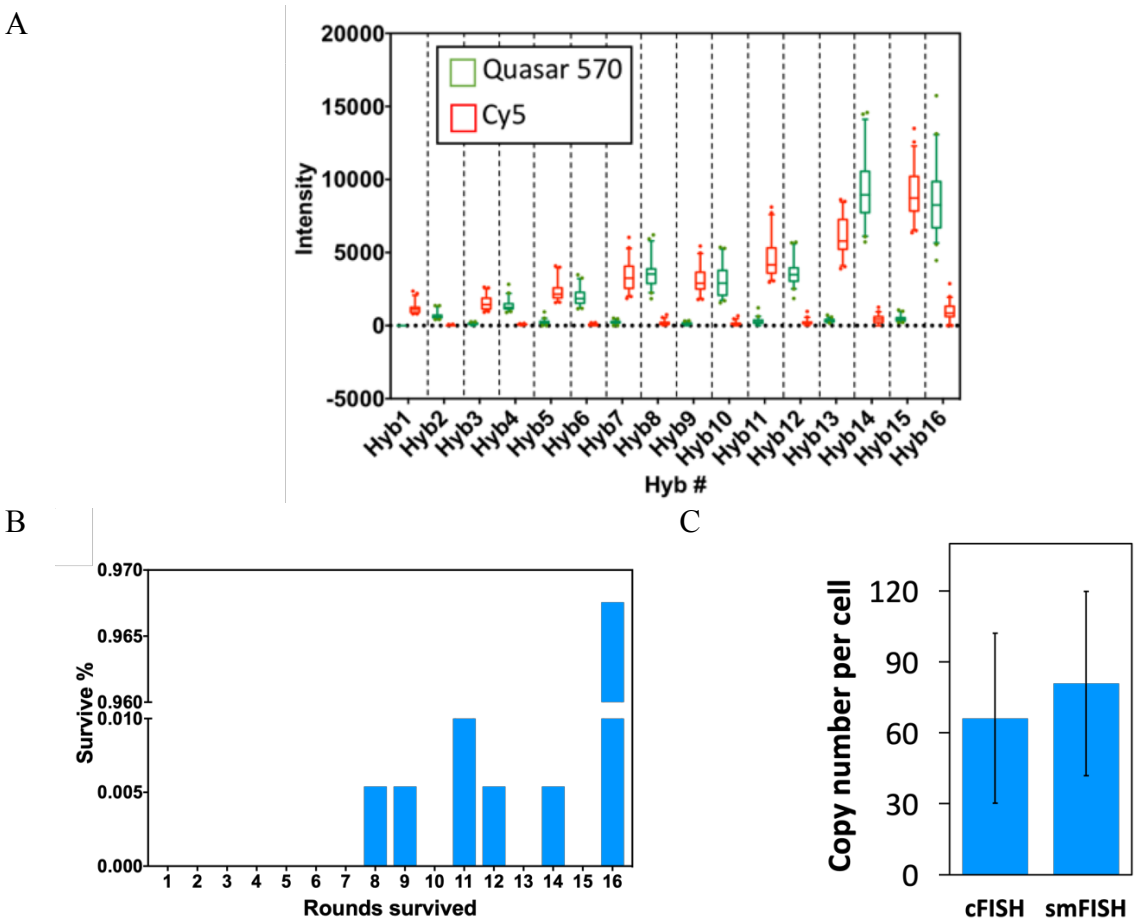

Figure 3.4.6. (A) Intensity distribution (n = 45 spots) in Quasar 570 and Cy5 channels at the position of FISH spots corresponding to Ki67 transcript over sixteen rounds of consecutive FISH. (B) Fraction of Ki67 barcodes spots (1000 spots) identified from first two rounds of hybridization that survived for different rounds of hybridization. (C) Comparison of the mean copy number per cell (n = 30 cells) of Ki67 measured by C-FSIH and conventional smFISH. Barcodes were identified by colocalization through the first two rounds of hybridizations.

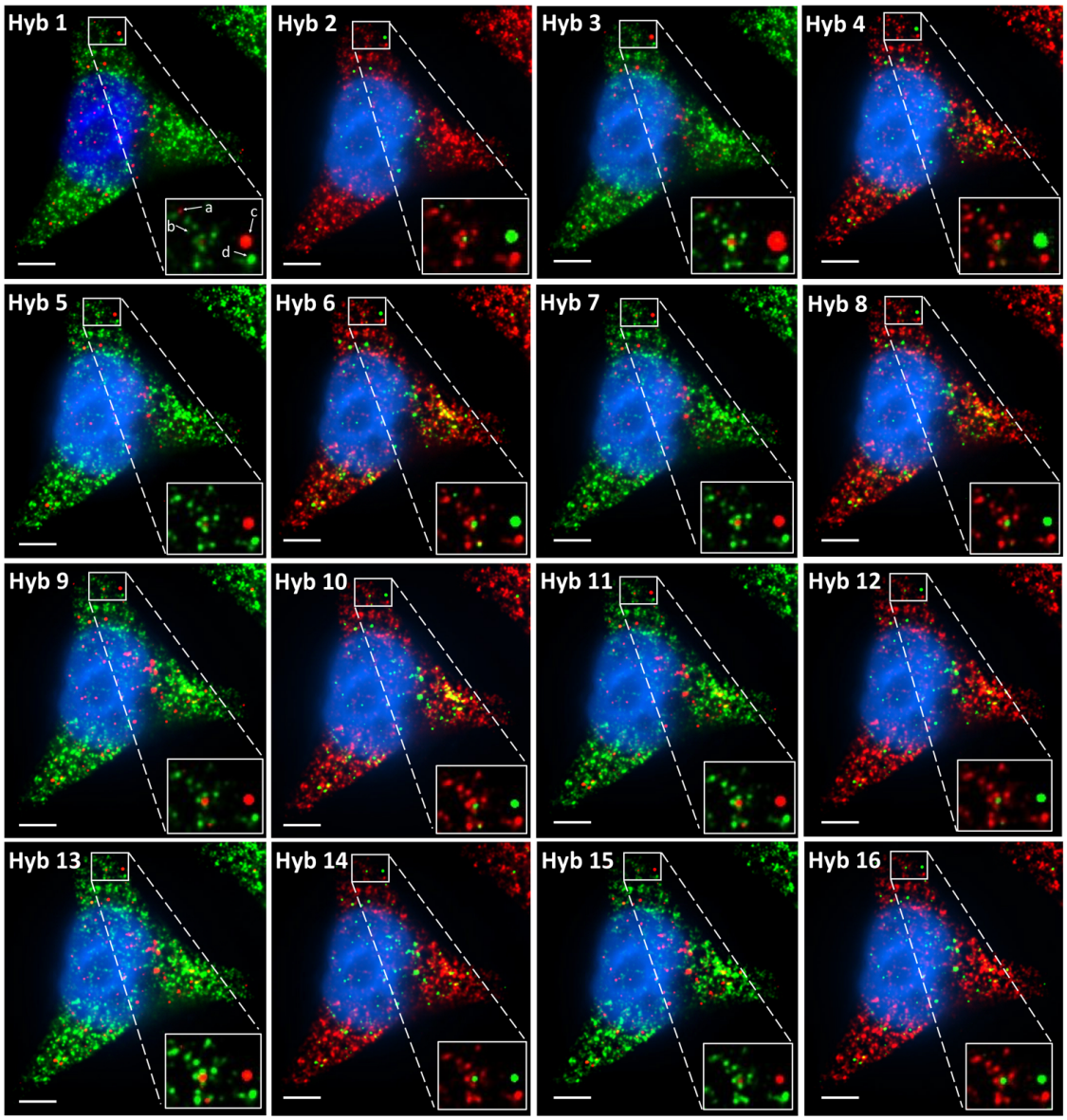

Figure 3.4.7. Fluorescent images of sixteen rounds consecutive FISH against GAPDH and Ki67 transcripts in HeLa cell. Quasar 570 (showed in green) labeled probes were used in odd hybridization rounds against GAPDH and even hybridization rounds against Ki67. Cy5 (showed in red) labeled probes were used in odd hybridization rounds against Ki67 and even hybridization rounds against GAPDH. Scale bars, 5 μm.

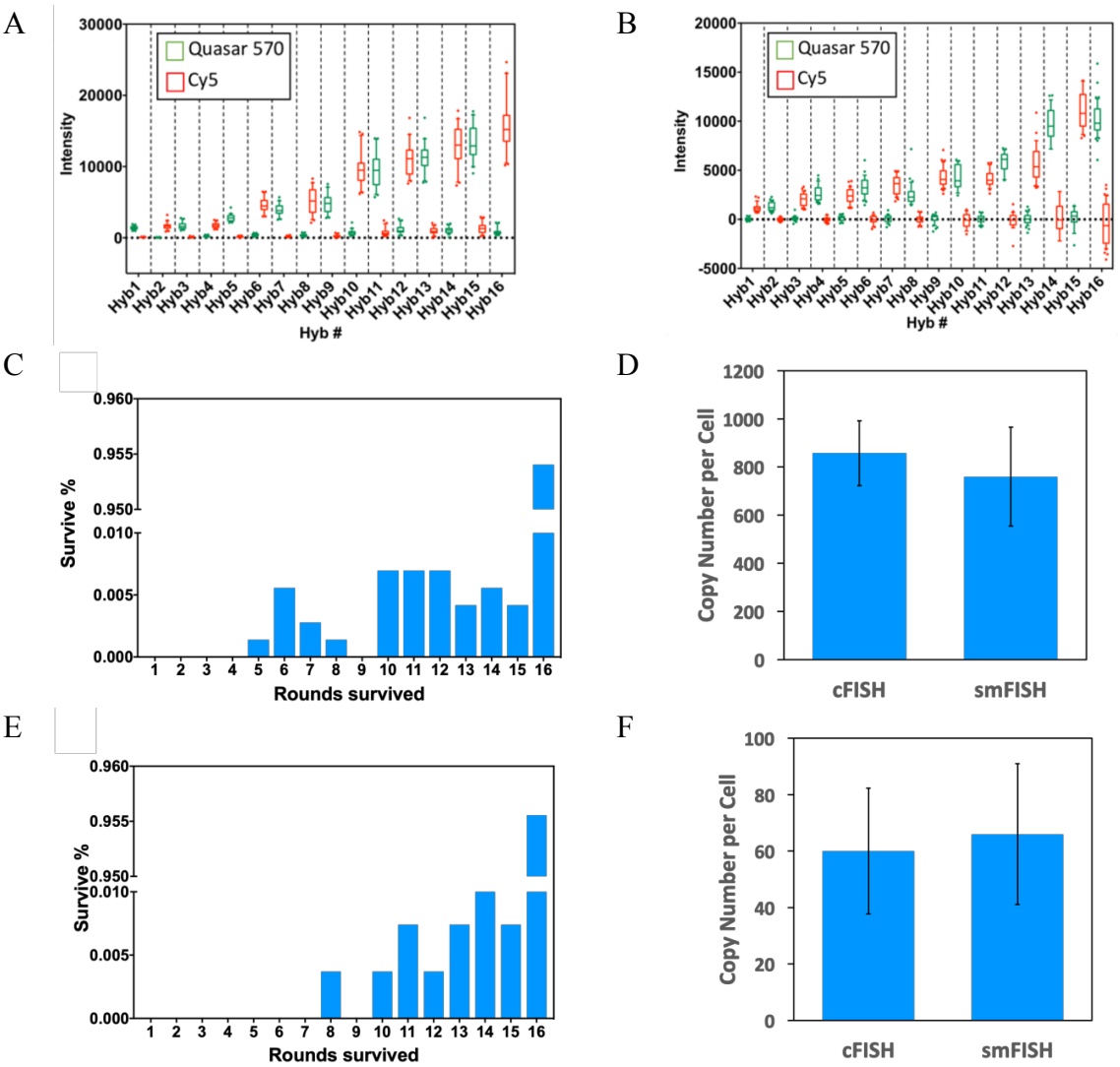

Figure 3.4.8. (A) Intensity distribution (n = 45 spots) in Quasar 570 and Cy5 channels at the position of FISH spots corresponding to GAPDH transcript over sixteen rounds of consecutive FISH. (B) Intensity distribution (n = 45 spots) in Quasar 570 and Cy5 channels at the position of FISH spots corresponding to Ki67 transcript over sixteen rounds of consecutive FISH. (C) Fraction of GAPDH barcodes spots (1000 spots) identified from first two rounds of hybridization that survived for different rounds of hybridization. (D) Comparison of the mean copy number per cell (n = 30 cells) of GAPDH measured by cFSIH and conventional smFISH. (E) Fraction of Ki67 barcodes spots (1000 spots) identified from first two rounds of hybridization that survived for different rounds of hybridization. (F) Comparison of the mean copy number per cell (n = 30 cells) of Ki67 measured by cFSIH and conventional smFISH. Barcodes were identified by colocalization through the first two rounds of hybridizations.

A

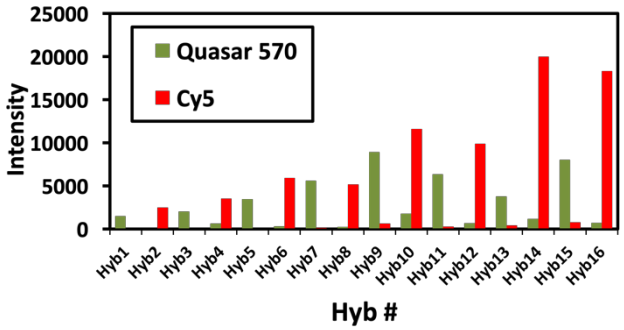

B

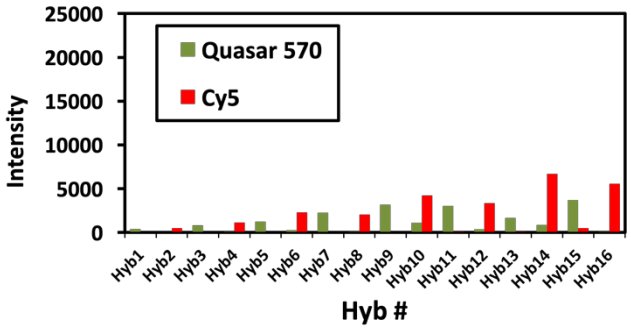

C

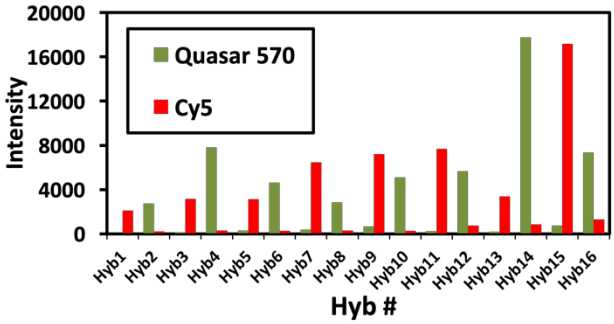

D

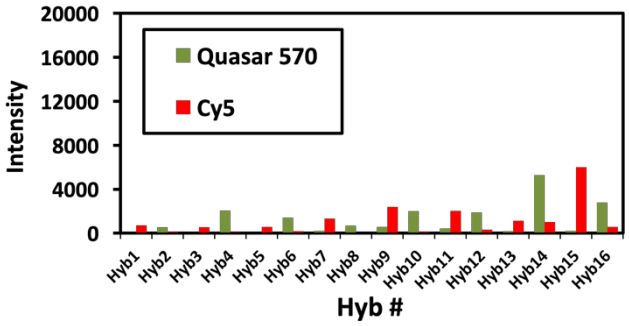

Figure 3.4.9. (A) Intensity at both Quasar 570 and Cy5 channels of a single strong spot against GAPDH transcript. (B) Intensity at both Quasar 570 and Cy5 channels of a single weak spot against GAPDH transcript. (A) Intensity at both Quasar 570 and Cy5 channels of a single strong spot against Ki67 transcript. (A) Intensity at both Quasar 570 and Cy5 channels of a single weak spot against Ki67 transcript.

3.5 Methods

3.5.1 General information

Chemicals and solvents were purchased from Sigma-Aldrich or Ambion and were used without further purification, unless otherwise noted. Biogreagents were purchased from Invitrogen, unless otherwise indicated. All solutions were prepared at RNase-free.

3.5.2 Cell culture

HeLa CCL-2 cells (ATCC) were maintained in Dulbecco's modified Eagle's Medium supplemented with 10% fetal bovine serum, 10 U mL^{-1} penicillin and 100 g mL^{-1} streptomycin in a humidified atmosphere at 37 ℃ with 5% CO_2. Cells were plated on chambered coverglass (Thermo Scientific) and allowed to reach 60% confluency in 1-2 days.

3.5.3 Cell fixation

Cultured HeLa CCL-2 cells were first washed with 1 X PBS at room temperature for 5 min, fixed with fixation solution (4% formaldehyde (Polusciences) in 1 X PBS) at room temperature for 10 min, and subsequently washed another 2 times with 1 X PBS at room temperature, each for 5 min. The fixed cells were then permeabilized with 70% (v/v) EtOH at 4 ℃ at least overnight.

3.5.4 Probe design

The pre-decoding probe contained three 20 nt sequences: (i) a target sequence for in situ hybridization to the target RNA, and (ii) two repeated readout sequences for the first round decoding hybridization. The three sequences were separated from each other by a flanking

5T spacer. The target sequences for both GAPDH and Ki67 transcripts were designed by the online Stellaris Probe Designer provided by Biosearch Technology. The readout sequences of the pre-decoding probe were complimentary to the the binding sequences of first round decoding probes.

The decoding probe also contained three 20 nt sequences: (i) a binding sequence for hybridization to the readout sequence from the last round hybridization, and (ii) two repeated readout sequences for the next round hybridization. The three sequences were separated from each other by a flanking 5T spacer.

The 20 nt sequences from decoding probes corresponding to GAPDH and Ki67 transcript were generated from a set of orthogonal 25 nt sequences[113]. These sequences were trimmed to 20 nt and selected for a GC content of 45% to 55%.

To further ensure the specificity, all the sequences were subsequently screened against the human transcriptome by using Basic Local Alignment Search Tool (BLAST)[114] to ensure there were no more than 10 nt of homology. Sequence alignment test were also performed by BLAST within these sequences to ensure there were no more than 8 nt of homology.

All the decoding probes were C6 amino modified at 5' end for fluorophore labeling.

3.5.5 Probe preparation

Pre-decoding oligonucleotides belonging to one library (IDT) were mixed and then stored as pre-decoding probe stock solution (0.01 M in 1% 1X Tris EDTA, pH 8.0) at 4 ℃.

Each decoding oligonucleotide, at a scale of 1 nmol, was dissolved in 3 μL of nuclease-free water. To this solution was added sodium bicarbonate aqueous solution (1M, 3 μL) and Quasar 570 (Biosearch) or Cy5 (AAT Bioquest) in DMF (20 mM, 5 μL). The mixture

was incubated at room temperature for 2 h and then purified by using a nucleotide removal kit (Qiagen). The fluorophore conjugated oligonucleotides were subsequently purified via an HPLC (Agilent) equipped with a C18 column (Aligent) and a dual wavelength detector set to detect DNA absorption (260 nm) and the fluorophore absorbtion (548 nm for Quasar 570, 650 nm for Cy5). For the gradient, triethyl ammonium acetate (Buffer A) (0.1 M, pH 6.5) and acetonitrile (Buffer B) (pH 6.5) were used, ranging from 7% to 30% Buffer B over the course of 30 in, the at 70% Buffer B for 10 min followed by 7% Buffer B for another 10 min, all at a flow rate of 1 mL min^{-1}. The collected fraction was then dried in a Savant SpeedVac Concentrator and stored as decoding probe stock solution at 4 ℃ in 100 μL 1% 1X Tris EDTA (pH 8.0).

3.5.6 Pre-decoding hybridization

To 100 μL of pre-decoding hybridization buffer (100 mg mL^{-1} dextran sulfate, 1 mg mL^{-1} Escherichia coli tRNA, 2 mM vanadyl ribonucleoside complex, 20 μg mL^{-1} bovine serum albumin and 10% formamide in 2 X SSC) was added 1 μL of the pre-decoding probe stock solution. Then the mixture was vortexed and centrifuged to obtain the pre-decoding hybridization solution.

HeLa CCL-2 cells after fixation and permeabilization were first incubated with wash buffer (2 mM vanadyl ribonucleoside complex and 10% formamide in 2 X SSC) for 5 min at room temperature, then incubated with 100 μL of pre-decoding hybridization solution at 37 ℃ overnight. Cells were then washed 3 times with wash buffer, each for 30 min, at 37 ℃.

3.5.7 Consecutive RNA FISH

To 100 μL of decoding hybridization buffer (100 mg mL^{-1} dextran sulfate, 2 mM vanadyl ribonucleoside complex and 10% formamide in 2 X SSC) was added 5 μL of the decoding probe stock solution. Then the mixture was vortexed and centrifuged to obtain the decoding hybridization solution.

Cells labeled with pre-decoding probes were directly incubated with 100 μL of decoding hybridization solution at 37 ℃ for 30 min, and washed once with wash buffer at 37 ℃ for 30 min. Nuclear staining was subsequently processed incubating the cells with 4',6-diamidino-2-phenylindole (DAPI) solution (5 ng mL^{-1} in was buffer) at 37 ℃ for 30 min. After incubation with GLOX buffer (0.4% glucose and 10 mM Tris HCl in 2 X SSC) for 1-2 min at room temperature, the stained cells were imaged in GLOX solution (0.37 mg mL^{-1} glucose oxidase and 1% catalase in GLOX buffer). After imaging, each cell was photobleached in photobleaching buffer (2 mM vanadyl ribonucleoside complex in 2 X SSC) individually with Quasar 570 filter for 20 s and Cy5 filter for 5 s respectively at each z step, followed by the next round of decoding hybridization. Photobleaching buffer was changed every 3 min during photobleaching to remove the radicals.

3.5.8 Imaging and data analysis

Stained cells were imaged under a Nikon Ti-E epofluorescence microscope equipped with a 100X objective, using a 5 μm range and 0.3 μm z spacing. Images were captured using a CoolSNAP HQ2 camera and NIS-Elements Imaging software. Chroma filters 49004 and 49009 were used for Quasar 579 and Cy5, respectively.

Raw images of the same cell in different rounds of hybridization were aligned to the same coordination system established by the images collected in the first round of hybridization based on the DAPI channel of each image.

Fluorescent spots in each image were then identified and localized by using SpotDetector developed by Fabrice de Chaumont[115] with appropriate threshold. Spots in the first hybridization round with the distance less than 2 pixels (320 nm) to those in the second hybridization round were extracted as the barcodes which corresponded to a potential mRNA molecule. Spots in the following hybridization rounds that shared the distance less than 2 pixels (320 nm) with the barcodes were identified as the reappearance of the barcodes. And the barcode reappearance percentage in each hybridization round was then calculated.

CHAPTER 4

SINGLE-CELL IN SITU RNA ANALYSIS WITH SWITCHABLE FLUORESCENT OLIGONUCLEOTIDES

4.1 Abstract

Comprehensive RNA analyses in individual cells in their native spatial contexts promise to transform our understanding of normal physiology and disease pathogenesis. Here we report a single-cell *in situ* RNA analysis approach using switchable fluorescent oligonucleotides (SFO). In this method, transcripts are first hybridized by pre-decoding oligonucleotides. These oligonucleotides subsequently recruit SFO to stain their corresponding RNA target. After fluorescence imaging, all the SFO in the whole specimen are simultaneously removed by DNA strand displacement reactions. Through continuous cycles of target staining, fluorescence imaging, and SFO removal, a large number of different transcripts can be identified by unique fluorophore sequences and visualized at the optical resolution. To demonstrate the feasibility of this approach, we show that the hybridized SFO can be efficiently stripped by strand displacement reactions within 30 min. We also demonstrate that this SFO removal process maintains the integrity of the RNA targets and the pre-decoding oligonucleotides, and keeps them hybridized. Applying this approach, we show that transcripts can be restained in at least eight hybridization cycles with high analysis accuracy, which theoretically would enable the whole transcriptome to be quantified at the single molecule sensitivity in individual cells. This in situ RNA analysis technology will have wide application in systems biology, molecular diagnosis, and targeted therapies.

4.2 Introduction

The ability to profile a large number of distinct transcripts in single cells in situ is crucial for our understanding of cancer, neurobiology and stem cell biology [94]. The differences between individual cells in complex biological systems may have significant consequences in the function and health of the entire systems. Thus, single cell analysis is required to explore such cell heterogeneity. Due to the inherent complexity of gene expression regulatory networks, comprehensive molecular profiling is required to systematically infer the functions and interactions of different RNA species. The precise location of cells in a tissue and transcripts in a cell is critical for effective cell-cell interactions and gene expression regulation, which can determine cell fates and functions. Therefore, to fully understand the organization, regulation and function of a heterogeneous biological system, highly multiplexed single-cell in situ RNA analysis is critically needed.

Next-generation sequencing [96,97] and microarray technologies [95] have been widely used to study gene expression regulation in health and disease by profiling RNA on a genome-wide scale. However, as transcripts are extracted, purified and then analyzed in these approaches, the RNA location information is lost. Imaging-based methods, such as molecular beacons [100,116] and fluorescence in situ hybridization (FISH) [98], allow transcripts to be quantified in their native spatial contexts in single cells. Nonetheless, due to the spectral overlap of commonly available fluorophores, these methods can only detect a handful of different RNA species in one sample.

To enable comprehensive single-cell in situ RNA analysis, several approaches have been investigated. For instance, in situ sequencing [108,109] has been explored to enable

transcriptome profiling in individual cells. However, this method has limited detection efficiency and may miss low-expression transcripts. Combinatorial labeling [105–107] and reiterative hybridization [102–104] offer single-molecule detection sensitivity, but these approaches suffer from limited multiplexing capacities. Recently, sequential hybridization [110,117] and multiplexed error-robust fluorescence in situ hybridization (MER-FISH) [111,118,119] have been developed for highly multiplexed single-molecule RNA detection. In these methods, to stain the same RNA molecules in different analysis cycles, several approaches have been explored to remove the fluorescence signals at the end of each cycle. Such approaches include probe degradation by DNase, photobleaching, and disulfide based chemical cleavage. Nevertheless, probe degradation by DNase is limited by its low signal removal efficiency. In addition, DNase removes all the probes, including the large oligonucleotides library hybridized to their RNA targets. Consequently, this expensive oligonucleotides library has to be re-hybridized in every analysis cycle, which will increase the assay time and cost. Photobleaching erases fluorescence signals in different imaging areas sequentially. As a result, it is less time-effective and has low sample throughput. The disulfide based probes can cross-react with the endogenous thiol groups and the thiol groups generated by fluorophore cleavage in previous cycles, which will lead to high backgcycle and false positive signals.

Here, we report a highly multiplexed single-cell in situ RNA analysis approach using switchable fluorescent oligonucleotides (SFO). In this method, RNA molecules are first hybridized by pre-decoding oligonucleotides, which subsequently recruit SFO to stain their RNA targets. After imaging, SFO are removed by strand displacement reactions. Upon

continuous cycles of target staining, fluorescence imaging, and SFO removal, varied RNA species are identified by unique fluorophore sequences at the optical resolution. To demonstrate the feasibility of this approach, we show that the hybridized SFO can be efficiently removed by strand displacement reactions within the cellular environment in 30 minutes. We also demonstrate that this probe removal process maintains the RNA integrity and keeps the pre-decoding oligonucleotides hybridized to their RNA targets. Additionally, we show that RNA can be quantified with high accuracy in at least eight continuous hybridization cycles, which theoretically would allow the whole transcriptome to be profiled in individual cells in situ.

4.3 Results and discussion

4.3.1 Platform design

In this SFO-based RNA profiling approach (Figure 4.5.1), individual RNA target is first hybridized by a set of non-fluorescent pre-decoding oligonucleotides with varied target binding sequences. These oligonucleotides also have one or multiple decoding oligonucleotides binding sequences, which can recruit SFO as decoding probes. Each of the subsequent analysis cycles consists of three steps. First, SFO are hybridized to pre-decoding probes to stain the RNA targets. In the second step, fluorescence images are acquired with each RNA molecule visualized as a single spot. Finally, oligonucleotide erasers, which are perfectly complementary to SFO, are applied to remove SFO by strand displacement reactions [120]. These oligonucleotide erasers hybridize to the toehold on SFO, branch migrate and release SFO from the pre-decoding probes. Through reiterative cycles of target staining, fluorescence imaging and SFO release, each transcript is identified by a

fluorescence sequence barcode. With M fluorophores applied in each cycle and N sequential cycles, a total of M^N RNA species can be quantified in single cells in situ.

4.3.2 SFO removal efficiency

One requirement for the success of this SFO-based RNA profiling technology is that fluorescent decoding probes need to be removed very efficiently at the end of each analysis cycle. In this way, the minimized fluorescence signal leftover will not lead to false positive signals in the subsequent cycles. Additionally, the efficient removal of SFO will regenerate the single-stranded SFO-binding sequences on pre-decoding probes, so that SFO can be recruited in the following cycle to stain the target RNA again. To assess the SFO stripping efficiency, we stained mRNA GAPDH with Cy3 labeled decoding probes (Figure 4.5.2A). After incubating the stained cells with the oligonucleotide eraser for 30 minutes at 37°C, almost all the original FISH spots become undetectable (Figure 4.5.2B, C). We also performed control experiments by incubating the stained cells with an SFO-orthogonal oligonucleotide (Figure 4.5.2D). The fluorescence intensities of the Cy3 stained GAPDH remained largely the same before and after the oligonucleotide incubation (Figure 4.5.2E, F). These results indicate that SFO can be efficiently removed by strand displacement reactions.

4.3.3 Effects of the strand displacement reaction

Another requirement for the success of this SFO-based approach is that the strand displacement reactions should maintain the RNA integrity, so that the same transcripts can be restained in the subsequent cycles. Additionally, it is preferred to keep the pre-decoding probes hybridized to their RNA targets throughout the assay, rather than to apply them in

every analysis cycle. This is essential for the following reasons. First, due to the theoretical hybridization efficiency of ~75% [106], a small percentage of transcripts are not hybridized with enough pre-decoding probes to make them detectable. And these undetectable RNA can be different transcripts in different analysis cycles, if the pre-decoding probes are removed and rehybridized in each cycle. Consequently, many missing spots in the aligned fluorophore sequences will be generated, leading to the increased error rate. Furthermore, as the hybridization of the pre-decoding probes takes overnight to 36 hours, it is time-consuming to apply this step in each cycle. Finally, for highly multiplexed RNA profiling, the pre-decoding probes library is usually composed of thousands of oligonucleotides. Thus, it will make the assay less cost-effective if the expensive pre-decoding library is removed and re-hybridized in every cycle.

To assess the effects of the strand displacement reactions on the RNA targets and the hybridized pre-decoding probes, we stained mRNA GAPDH in three continuous hybridization cycles (Figure 4.5.3). In each cycle, Cy3 or Cy5 labeled SFO were applied to stain the transcripts, and were subsequently removed very efficiently using the same oligonucleotide eraser. We counted 1032 and 1045 spots in the first and second cycle, respectively. Among these spots, 800 spots were colocalized. These results are consistent with the ones obtained using two sets of different colored FISH probes to stain the same transcripts [98]. The small fraction of spots that did not colocalize may correspond to the non-specifically bound probes. To exclude these off-target signals, we define only the spots colocalized in the first two cycles as true mRNA signals. With our approach, 99% of the true signals reappeared in the third cycle. In comparison, when both pre-decoding and

decoding probes are degraded using DNase, only 78% of spots reoccur in the third cycle [121]. These results suggest that the DNA displacement reactions do not damage the RNA integrity, and the pre-decoding probes remain hybridized to their RNA targets throughout the assay. In this way, the analysis accuracy is improved and the assay time and cost are reduced.

4.3.4 Eight-cycle RNA restaining

To demonstrate the multi-cycle potential of our approach, we stained mRNA GAPDH in eight consecutive hybridization cycles using SFO (Figure 4.5.4). To evaluate the target staining specificity, we incubated the cells with Cy3 conjugated SFO together with a Cy5 labeled orthogonal oligonucleotide in the odd hybridization cycles, and with Cy5 conjugated SFO and a Cy3 labeled orthogonal oligonucleotide in the even cycles. In the first cycle, the FISH spots were only observed in the Cy3 channel, suggesting that mRNA GAPDH is specifically stained by the corresponding SFO. After signal detection and strand displacement reactions, we imaged the cells again to confirm the efficient stripping of SFO. This process of staining, imaging and stripping was repeated eight times to obtain the 8-bit fluorophore sequence barcode for the target mRNA. For the spots co-localized in the first two cycles (n = 1470), more than 97% of these spots reappeared in each of the following cycles (Figure 4.5.5). And over 95% of the spots were successfully identified in all the hybridization cycles (Figure 4.5.6). A plot of the signal intensities of the FISH spots in both the Cy3 and Cy5 channels vs. the hybridization cycles is shown in Figure 4.5.7. Due to the high staining specificity, all the FISH spots were unambiguously detected in the correct fluorescence channels. We also performed control experiments to stain mRNA

GAPDH using the conventional RNA FISH method. The copy numbers per cell obtained by our method and the conventional RNA FISH (Figure 4.5.8), together with those reported previously using RNA-Seq [122], are consistent with each other. These results suggest that transcripts can be quantitatively profiled in single cells in situ by multi-cycle staining using the SFO-based approach.

In each cycle of MER-FISH, only certain transcripts are stained and other RNA targets remain unlabeled. Thus, to determine which transcripts are stained in a specific cycle, a detection threshold has to be manually selected by comparing the signal intensities of different FISH spots. However, due to the imperfect probe hybridization efficiency, RNA secondary structures, proteins bound to transcripts and other factors, even individual transcripts from the same RNA species can have significantly different staining intensities (Figure 4.5.7). As a result, the artificial detection threshold can lead to false negative signals, if the stained transcripts have low signal intensities. This threshold will also result in false positive signals, if the un-stained transcripts have high fluorescence intensities, which are generated as the signal leftovers from the previous cycles. In contrast, all the RNA targets are stained simultaneously in every cycle in the SFO-based approach. Rather than using a threshold to identify the stained transcripts, we compare the signal intensities of the same spot in different fluorescence channels to determine which SFO is hybridized to the specific RNA target. In this way, the correct fluorescence sequence can be unambiguously identified for both the weak spots (Figure 4.5.9A) and the strong spots (Figure 4.5.9B) in each analysis cycle. These results suggest that the SFO-based approach

avoids the false positive and negative signals generated by the artificial threshold, and have enhanced detection sensitivity and analysis accuracy.

4.3.5 Discussion

We have developed an SFO-based technology for highly multiplexed in situ RNA profiling. Compared with the existing methods, our approach has the following advantages. (i) By detecting transcripts directly without target sequence amplification, our technology enables RNA analysis at the single-molecule sensitivity. (ii) In this method, different RNA species are distinguished by the varied color sequences, whose number increases exponentially with the number of hybridization cycles. Thus, our approach has high multiplexing capacity. (iii) All the distinct SFO in the whole specimen can be simultaneously removed by their corresponding eraser oligonucleotides. Therefore, our approach has high sample throughput, and allows a large number of cells to be quantified in a short time. (iv) As SFO can be very efficiently removed and have minimized cross-reactions with endogenous biomolecules and other probes, our approach has enhanced signal to noise ratio. (v) By keeping the pre-decoding oligonucleotides hybridized to their targets throughout the assay, our method has increased analysis accuracy and decreased assay time and cost. (vi) With each transcript stained in every cycle, this SFO-based approach avoids the false positive and false negative signals generated by the manually selected detection thresholds.

The number of RNA species that can be quantified using this SFO-based approach depends on two factors: the number of hybridization cycles and the number of different fluorophores used in each cycle. As we have demonstrated, at least eight hybridization cycles with high analysis accuracy can be carried out in the same set of cells. And it is well established that

hundreds of thousands of oligonucleotides can be prepared cost-effectively by massively parallel synthesis on a microarray slide [123]. Thus, further implementation of the SFO-based approach with four classical fluorophores applied in each cycle will enable the whole transcriptome to be profiled using the 65, 536 (4^8) distinct fluorophore sequences. Additionally, multispectral fluorophores [124–126] coupled with the hyperspectral imaging [127] can be applied to allow more fluorophores to be distinguished and applied in each hybridization cycle. In this way, the cycle number together with the assay time can be further reduced. Furthermore, the combination of this SFO-based approach with multiplexed in situ protein analysis technologies [128,129] will enable the comprehensive and integrated RNA and protein profiling in single cells in situ. This highly multiplexed molecular imaging platform will bring new insights into systems biology, signaling network regulation, molecular diagnosis and cellular targeted therapy.

4.4 Figures

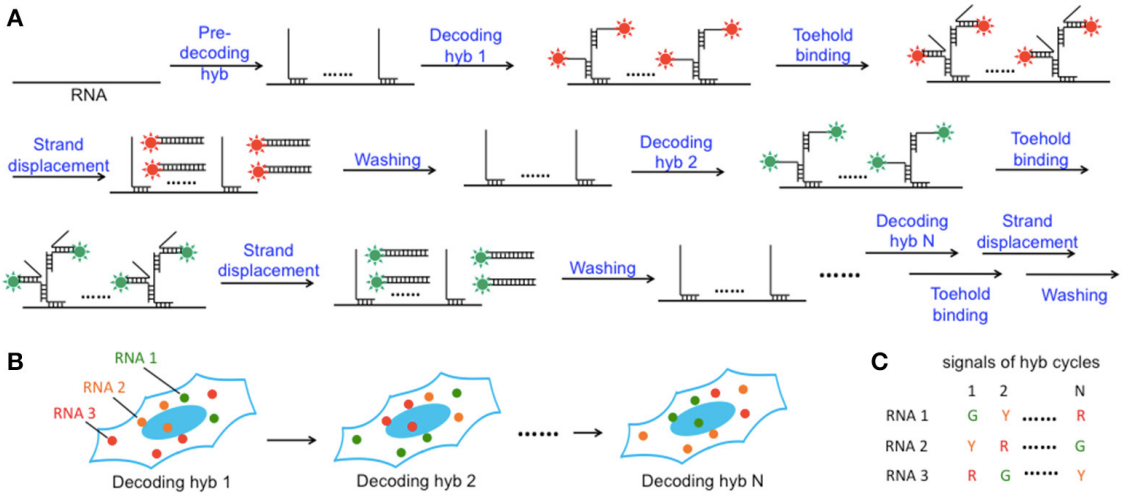

Figure 4.4.1. Highly multiplexed single-cell in situ RNA analysis with SFO. (A) Each transcript is first hybridized with a set of pre-decoding probes, which have varied target-binding sequences to hybridize to the different regions on the target RNA and the shared decoding sequence to recruit SFO as decoding probes. After imaging, the hybridized

SFO is removed by strand displacement reactions. Through reiterative cycles of SFO hybridization, fluorescence imaging and strand displacement, the target RNA is sequentially stained by a set of SFO labeled with varied fluorophores. (B) Schematic diagram of the N cycles of hybridization images. In each cycle, individual transcript is visualized as a single spot with a specific color. (C) As RNA molecules remain in place during different hybridization cycles, different RNA species can be identified by the unique color sequences.

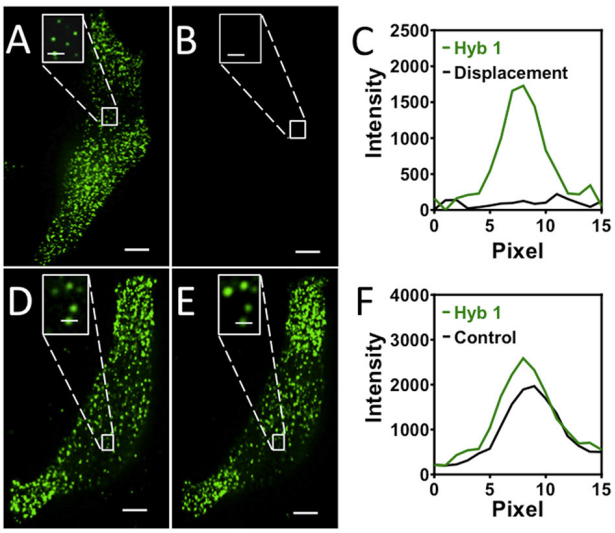

Figure 4.4.2. (A) GAPDH transcripts are stained by Cy3 labeled SFO. (B) SFO is removed by the eraser oligonucleotide. (C) Signal intensity profiles corresponding to the marked FISH spot in (A) and (B). (D) GAPDH transcripts are stained by Cy3 labeled SFO. (E) The stained cells are incubated with an orthogonal oligonucleotide. (F) Signal intensity profiles corresponding to the marked FISH spot in (D) and (E). Scale bars, 5 μm.

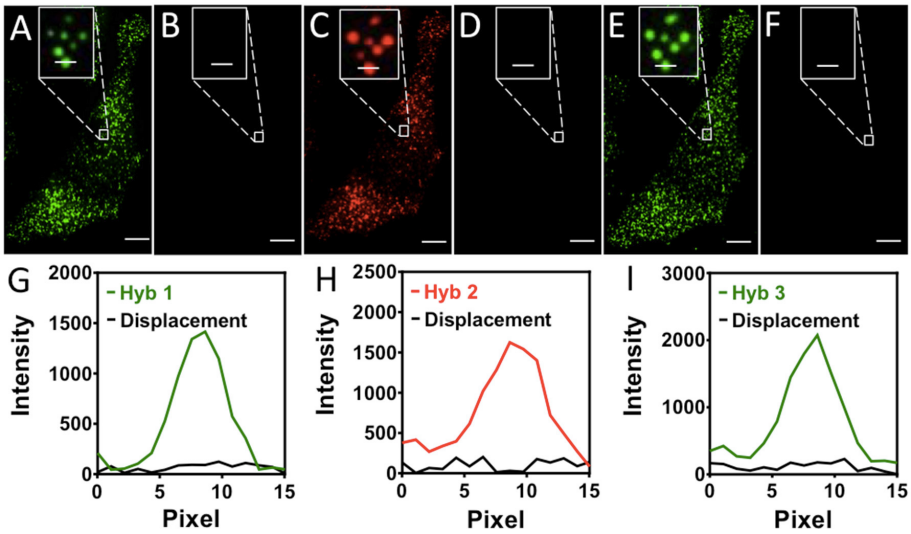

Figure 4.4.3. (A) In the first hybridization cycle, GAPDH transcripts are stained by Cy3 labeled SFO. (B) SFO is removed by the eraser oligonucleotide. (C) In the second hybridization cycle, GAPDH transcripts are stained by Cy5 labeled SFO. (D) SFO is removed by the eraser oligonucleotide. (E) In the third hybridization cycle, GAPDH transcripts are stained by Cy3 labeled SFO. (F) SFO is removed by the eraser oligonucleotide. (G) Signal intensity profiles corresponding to the marked FISH spot in (A) and (B). (H) Signal intensity profiles corresponding to the marked FISH spot in (C) and (D). (I) Signal intensity profiles corresponding to the marked FISH spot in (E) and (F). Scale bars, 5 μm.

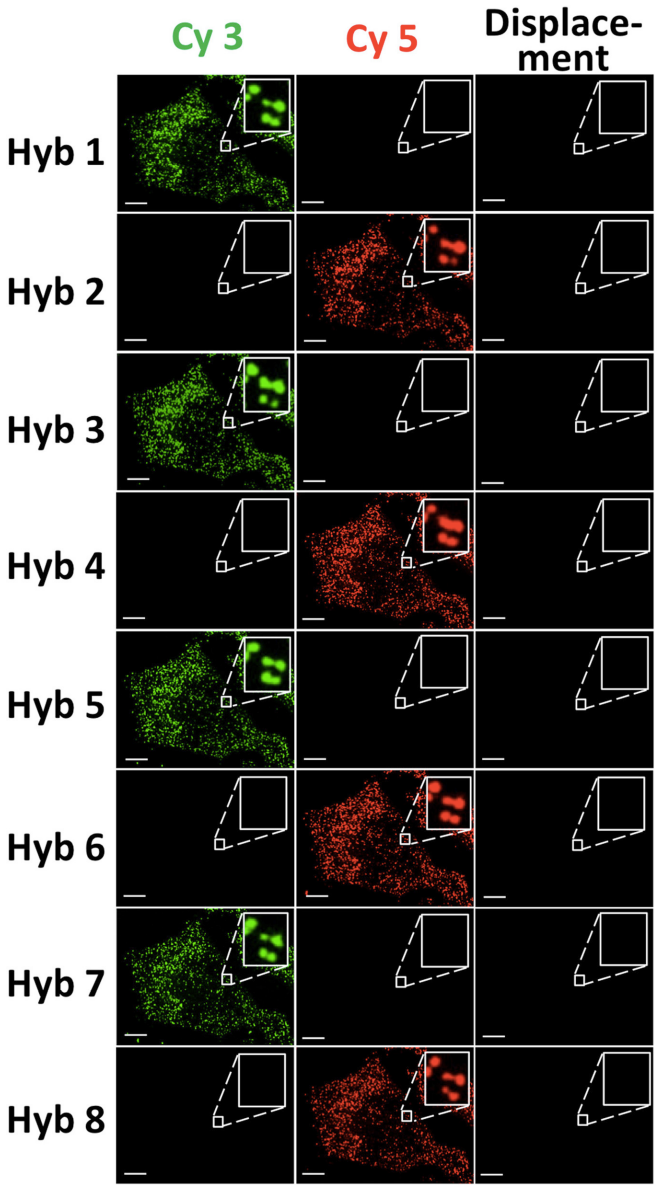

Figure 4.4.4. GAPDH transcripts are stained by SFO in eight consecutive hybridization cycles. In the odd cycles, cells are incubated with Cy3 conjugated SFO and a Cy5 labeled orthogonal oligonucleotide. In the even cycles, cells are incubated with Cy5 conjugated SFO and a Cy3 labeled orthogonal oligonucleotide. After target staining, images are captured in the Cy3 and Cy5 fluorescence channels. Following strand displacement reactions, images are captured in the Cy3 channel in the odd cycles and in the Cy5 channel in the even cycles. Scale bars, 5 μm.

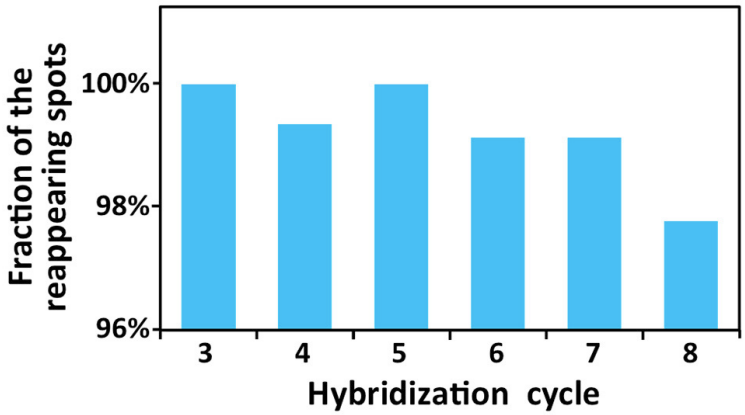

Figure 4.4.5. Fractions of the spots colocalized in the first two hybridization cycles that reappear in the following analysis cycles.

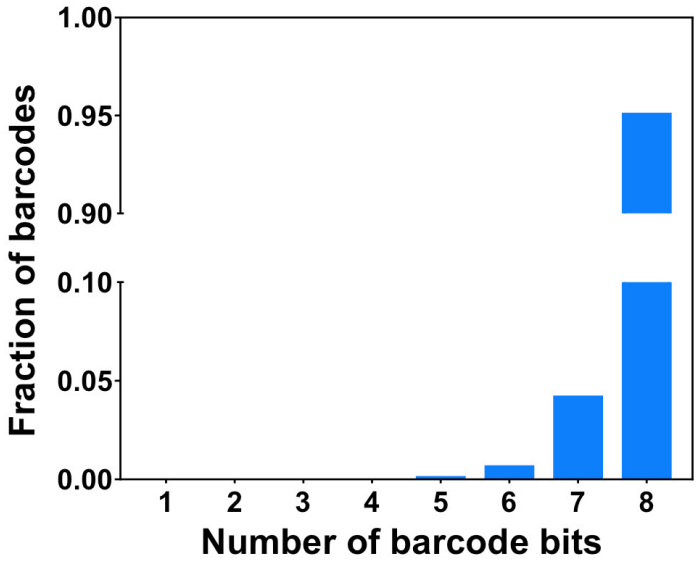

Figure 4.4.6. Fractions of the identified barcodes with different numbers of bits.

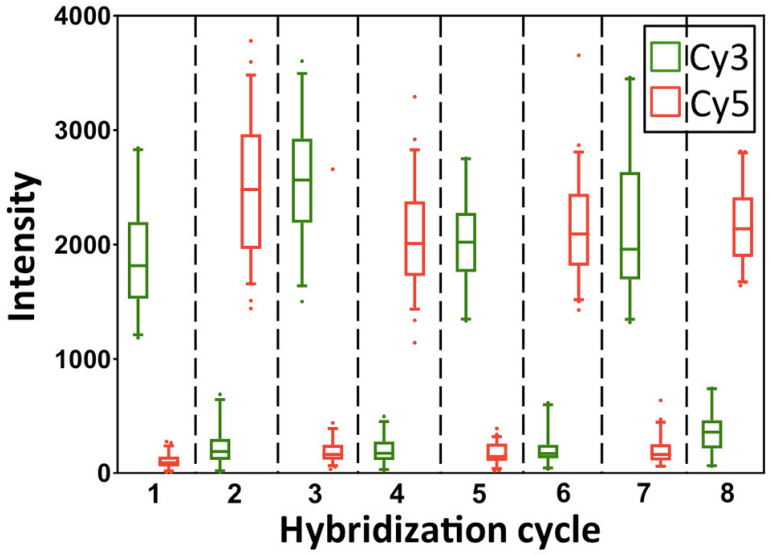

Figure 4.4.7. Intensity distributions of GAPDH FISH spots (n = 60 spots) in Cy3 and Cy5 channels over the eight hybridization cycles.

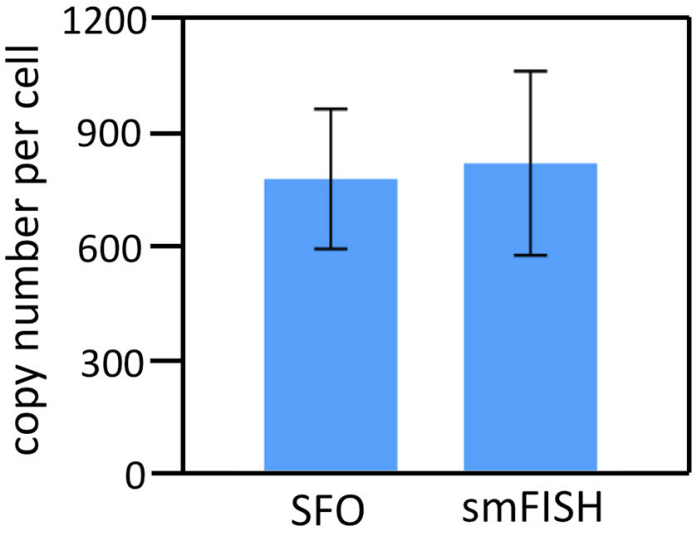

Figure 4.4.8. The GAPDH mean copy numbers per cell (n = 45 cells) obtained using the SFO-based approach and the conventional smFISH ($p > 0.65$).

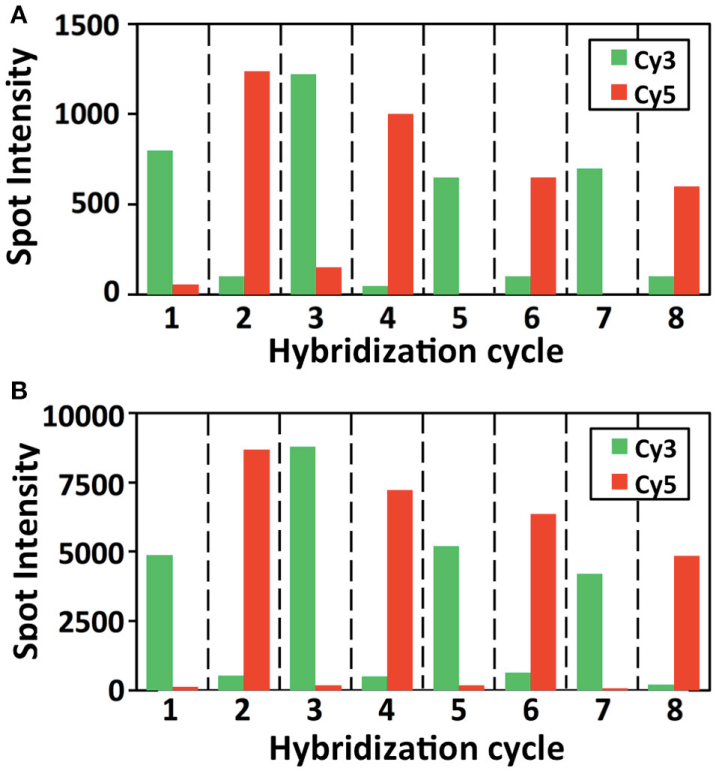

Figure 4.4.9. Signal intensities of (A) a weak and (B) a strong GAPDH FISH spot in Cy3 and Cy5 channels over the eight hybridization cycles.

4.5 Methods

4.5.1 General information

Chemicals and solvents were purchased from Sigma-Aldrich or Ambion and were used without further purification, unless otherwise noted. Biogreagents were purchased from Invitrogen, unless otherwise indicated.

4.5.2 Cell culture

HeLa CCL-2 cells (ATCC) were maintained in Dulbecco's modified Eagle's Medium supplemented with 10% fetal bovine serum, 10 U mL^{-1} penicillin and 100 g mL^{-1} streptomycin in a humidified atmosphere at 37 ℃ with 5% CO_2. Cells were plated on

chambered coverglass (Thermo Scientific) and allowed to reach 60% confluency in 1-2 days.

4.5.3 Cell fixation

Cultured HeLa CCL-2 cells were first washed with 1 X PBS at room temperature for 5 min, fixed with fixation solution (4% formaldehyde (Polusciences) in 1 X PBS) at room temperature for 10 min, and subsequently washed another 2 times with 1 X PBS at room temperature, each for 5 min. The fixed cells were then permeabilized with 70% (v/v) EtOH at 4 ℃ at least overnight.

4.5.4 Probe design

The pre-decoding probes with a length of 70 nt contain three 20 nt sequences: (i) a target-binding sequence for in situ hybridization to the target RNA, and (ii) two repeated readout sequences for decoding hybridization. The three sequences are separated from each other by a flanking 5T spacer. The target-binding sequence was designed by the online Stellaris Probe Designer provided by Biosearch Technology. The readout sequences on the pre-decoding probe are complimentary to the binding sequences of the decoding probes.

The decoding probe (SFO) with a length of 40 nt contains two 20 nt sequences: (i) a binding sequence complimentary to the readout sequence of the pre-decoding probes, and (ii) a toehold sequence for strand displacement reactions. The decoding probe is conjugated to fluorophores with the 5'-amino modification.

The eraser oligonucleotide with a length of 40 nt is complimentary to the decoding probe.

The SFO-orthogonal oligonucleotide with a length of 40 nt is conjugated to fluorophores with the 5'-amino modification.

To further ensure the specificity, all the sequences above were screened against the human transcriptome by using Basic Local A lignment Search Tool (BLAST)[130] to ensure there were no more than 10 nt of homology. Sequence alignment test were also performed by BLAST within these sequences to ensure there were no more than 8 nt of homology.

4.5.5 Probe preparation

Pre-decoding oligonucleotides belonging to one library (IDT) were mixed and then stored as pre-decoding probe stock solution (10 mM in 0.01X Tris EDTA, pH 8.0) at 4 ℃.

The decoding oligonucleotide or the SFO-orthogonal oligonucleotide, at a scale of 1 nmol, was dissolved in 3 μL of nuclease-free water. To this solution was added sodium bicarbonate aqueous solution (1M, 3 μL) and Cy3 (AAT Bioquest) or Cy5 (AAT Bioquest) in DMF (20 mM, 5 μL). The mixture was incubated at room temperature for 2 h and then purified by using a nucleotide removal kit (Qiagen). The fluorophore conjugated oligonucleotides were subsequently purified via an HPLC (Agilent) equipped with a C18 column (Aligent) and a dual wavelength detector set to detect DNA absorption (260 nm) and the fluorophore absorbtion (555 nm for Cy3, 650 nm for Cy5). For the gradient, triethyl ammonium acetate (Buffer A) (0.1 M, pH 6.5) and acetonitrile (Buffer B) (pH 6.5) were used, ranging from 7% to 30% Buffer B over the course of 30 in, the at 70% Buffer B for 10 min followed by 7% Buffer B for another 10 min, all at a flow rate of 1 mL min^{-1}. The collected fraction was then dried in a Savant SpeedVac Concentrator and stored as decoding probe stock solution or SFO-orthogonal oligonucleotide stock solution at 4 ℃ in 100 μL 0.01X Tris EDTA (pH 8.0).

The eraser oligonucleotide was dissolved and stored as displacement stock solution (10 mM in 0.01X Tris EDTA, pH 8.0) at 4 ℃.

4.5.6 Pre-decoding hybridization

To 100 μL of pre-decoding hybridization buffer (100 mg mL^{-1} dextran sulfate, 1 mg mL^{-1} Escherichia coli tRNA, 2 mM vanadyl ribonucleoside complex, 20 μg mL^{-1} bovine serum albumin and 10% formamide in 2 X SSC) was added 1 μL of pre-decoding probe stock solution. Then the mixture was vortexed and centrifuged to obtain pre-decoding hybridization solution.

HeLa CCL-2 cells after fixation and permeabilization were first incubated with wash buffer (2 mM vanadyl ribonucleoside complex and 10% formamide in 2 X SSC) for 5 min at room temperature, then incubated with 100 μL of pre-decoding hybridization solution at 37 ℃ overnight. Cells were then washed 3 times with wash buffer, each for 30 min, at 37 ℃.

Cells were then post-fixed with post-fixation solution (4% formaldehyde (Polusciences) in 2X SSC) at room temperature for 10 min, and subsequently washed another 3 times with 2X SSC at room temperature, each for 5 min.

4.5.7 Decoding hybridization

To 100 μL of decoding hybridization buffer (100 mg mL^{-1} dextran sulfate, 2 mM vanadyl ribonucleoside complex and 10% formamide in 2 X SSC) was added 5 μL of decoding probe stock solution with or without 5 μL of SFO-orthogonal oligonucleotide stock

solution. Then the mixture was vortexed and centrifuged to obtain decoding hybridization solution.

Cells labeled with pre-decoding probes were directly incubated with 100 μL of decoding hybridization solution at 37 ℃ for 30 min, and washed once with wash buffer at 37 ℃ for 30 min. After incubation with GLOX buffer (0.4% glucose and 10 mM Tris HCl in 2 X SSC) for 1-2 min at room temperature, the stained cells were imaged in GLOX solution (0.37 mg mL^{-1} glucose oxidase and 1% catalase in GLOX buffer).

To 100 μL of displacement buffer (100 mg mL^{-1} dextran sulfate, 2 mM vanadyl ribonucleoside complex and 10% formamide in 2 X SSC) was added 5 μL of displacement stock solution. Then the mixture was vortexed and centrifuged to obtain displacement solution.

Cells after imaging were incubated with 100 μL of displacement solution at 37 ℃ for 30 min, and washed 3 times with 1X PBS at 37 ℃, each for 15 min, then followed by the next cycle of decoding hybridization.

4.5.8 Imaging and data analysis

Cells were imaged under a Nikon Ti-E epofluorescence microscope equipped with a 100X objective, using a 5 μm range and 0.3 μm z spacing. Images were captured using a CoolSNAP HQ2 camera and NIS-Elements Imaging software. Chroma filters 49004 and 49009 were used for Quasar 579 and Cy5, respectively.

Fluorescent spots in each hybridization cycle were identified and localized by SpotDetector[32]. The intensities of the detected spots in the Cy3 and Cy5 channels were compared to determine the color of the spots. Raw images of the same cells in different

cycles of hybridization were aligned to the same coordination system established by the images collected in the first cycle of hybridization. Spots in the first hybridization cycle with the distance less than 2 pixels (320 nm) to those in the second hybridization cycle were extracted as the barcodes, which corresponded to a potential mRNA molecule. Spots in the following hybridization cycles that shared the distance less than 2 pixels (320 nm) with the barcodes were identified as the reappearance of the barcodes. And the barcode reappearance percentage in each hybridization cycle was then calculated.

CHAPTER 5

HIGHLY SENSITIVE AND MULTIPLEXED IN SITU RNA PROFILING WITH CLEAVABLE FLUORESCENT TYRAMIDE

5.1 Abstract

Comprehensive profiling of a wide variety of different transcripts in intact tissues in situ will provide us with a deeper understanding of health and disease. Here we report a strategy to use cleavable fluorescent tyramide (CFT) to achieve highly sensitive and multiplexed in situ RNA analysis. In this method, RNAscope® Multiplex Fluorescent v2 Assay with CFT signal development are applied to recognize their target transcripts. After fluorescence imaging, fluorophore cleavage and probe stripping, reiterative hybridization cycles could be achieved for the sensitive detection of >50 different transcripts in intact tissues at the optical resolution. The application of this comprehensive in situ RNA profiling technology will provide us with a powerful tool for the study of systems biology and development molecular diagnosis and cellular targeted therapies.

5.2 Introduction

The ability to comprehensively profile a large variety of transcripts in situ in individual cells of intact tissues plays an important role in our exploration of neuroscience, cancer and stem cell biology.[94] By revealing the spatial organization, gene expression regulation and interactions of individual cells in complex biological systems, the comprehensive RNA profiling has the potential to transform our understanding of normal physiology and disease pathogenesis. Conventional imaging-based RNA profiling technologies, such as molecular beacons [100,116] and fluorescent in situ hybridization (smFISH)[27], have enabled the

quantification of transcripts in their native spatial contexts in single cells. However, these methods could only detect a handful of transcripts in one tissue sample due to the spectral overlap of organic fluorophores[124,132,133].

Recently, different methods have been developed to enable multiplexed in situ RNA analysis[45,48,49,79,134,135]. However, due to high autofluorescence in tissues, such as formalin-fixed paraffin-embedded (FFPE) tissues[136], without proper signal amplification, these methods suffer from low detection sensitivity, which dramatically limit their applications in the study of transcripts with low expression level.

Here, we report a method to use cleavable fluorescent tyramide (CFT) for the achievement of highly sensitive and multiplexed in situ RNA analysis, which has the potential to quantify >50 different transcripts in single cells of intact tissues at the optical resolution. In this method (Figure 5.4.1A), RNAscope® Multiplex Fluorescent v2 Assay are first applied to the sample to stain target RNA with horseradish peroxidase (HRP) conjugated oligonucleotides. Signal amplification is then achieved by applying CFT to the sample and, with the catalysis of HRP, coupling CFTs with the tyrosine residues on the endogenous proteins in close proximity. After the fluorescence images are captured to generate quantitative RNA expression profiles, the fluorophores attached to tyramide are chemically cleaved and the oligonucleotide probes are stripped off. This allows the initiation of the next analysis cycle. Therefore, a wide variety of different transcripts with different expression levels could be quantified in situ via reiterative cycles of target staining, fluorescence imaging, fluorophore cleavage and probe stripping.

5.3 Results and discussion

In order to demonstrate the feasibility of this RNA profiling method, CFT (Tyramide-N3-Cy5) (Figure 5.4.1B) was designed and synthesized by conjugating Cy5 to tyramide via an azide-based cleavable linker.[129]

One critical requirement for the success of this multiplexed RNA profiling technology is that the fluorophores need to be removed very efficiently. To assess the fluorophore removal efficiency by cleavage, we stained mRNA Peptidylprolyl Isomerase B (PPIB) with RNAscope® Multiplex Fluorescent v2 Assay and tyramide-N3-Cy5 in mouse FFPE lung tissue (Figure 5.4.2A). After 30 min TCEP treatment at 40 °C, almost all the original FISH spots become undetectable (Figure 5.4.2B, E). This result suggests the TCEP treatment can efficiently remove the fluorescent signal.

Another requirement for the success of this RNA profiling technology is the efficient probe stripping at the end of each analysis cycle. In this way, there will not be any leftover target probes leading to the crosstalk in the subsequent cycles. To assess the probe stripping efficiency, the sample treated with TCEP above was further incubated with DNase I at room temperature for 1 hour and 70% formamide at 40 °C for 30 min. After DNase and formamide treatment, RNAscope® Fluorescent v2 Assay was applied to the sample in the absence of target probes. No signal development was observed with the subsequent tyramide-N3-Cy5 incubation (Figure 5.4.2C, E). This result suggests that the efficient probe stripping can be achieved by the DNase and formamide treatment.

It is important that the RNA integrity is preserved during fluorophore cleavage and probe stripping. To assess the effects of fluorophore cleavage and probe stripping on subsequent

cycles, the sample above was further treated with TCEP for 12 h at 40 °C, with DNase I for 24 h at room temperature and with 70% formamide for 12 h at 40 °C. After that, mRNA PPIB was stained again with RNAscope® Multiplex Fluorescent v2 Assay and tyramide-N3-Cy5 (Figure 5.4.2D). By comparing the fluorescence intensity of PPIB spots in this cycle with the initial PPIB staining cycle, we found they are largely comparable (Figure 5.4.2E). We also observed more than 80% of the spots appeared in the initial cycle reappeared in this cycle (Figure 5.4.2 F). This corresponded with the theoretical hybridization efficiency of ~75%[106]. These results suggests that RNA integrity was preserved during fluorophore cleavage and probe stripping.

In order to demonstrate the feasibility of applying CFT for multiplexed RNA analysis in tissues, we stained mRNA Peptidylprolyl Isomerase B (PPIB), mRNA RNA Polymerase II Subunit A (POLR2A) and mRNA Ubiquitin C (UBC) with RNAscope® Multiplex Fluorescent v2 Assay and tyramide-N3-Cy5 in mouse FFPE lung tissue through three consecutive staining cycles, and repeated this process 3 times (Figure 5.4.3). The results showed there was no crosstalk between different mRNA target staining. And by comparing the first three consecutive staining cycles with the other two, we noticed more than 80% of the spots appeared in the first three consecutive staining cycles reappeared in the second and third three consecutive staining cycles (Figure 5.4.4). These results indicate that our approach has the ability to quantitatively profile transcripts in individual cells of intact tissue.

To further demonstrate the RNA profiling potential of our approach in intact tissues, we stained 8 mRNAs sequentially in mouse fixed frozen spinal cord tissue using RNAscope®

Multiplex Fluorescent v2 Assay and tyramide-N3-Cy5. With 8 reiterative staining cycles, mRNA Natriuretic Peptide Receptor A (NPR1), mRNA Gastrin Releasing Peptide (GRP), mRNA Solute Carrier Family 32 Member 1 (SLC32A1), mRNA Phosphodiesterase 11A (PDE11A), mRNA Solute Carrier Family 17 Member 6 (SLC17A6), mRNA Carbonic Anhydrase 12 (CAR12), mRNA Parvalbumin (PVALB), and mRNA Somatostatin (SST) were successfully detected in the spinal cord tissue (Figure 5.4.5). With these multiplexed single-cell in situ RNA profiling results, heterogeneity of spinal cord cells and their spatial organization were explored. In the examined tissue, the expression levels of those 8 transcripts in >6000 individual cells were generated. By applying dimension reduction algorithm called tSNE[137] and clustering algorithm called PhenoGraph[138], the high dimensional data was then reduced to two dimensions and partitioned into 8 clusters (Figure 5.4.6A).

By analyzing the RNA expression level patterns of different clusters (Figure 5.4.6B), new biomarkers toward specific cluster could be discovered. For example, SLC32A1 could be a marker for cluster 5 cells, since it is highly expressed only in cluster 5. Additionally, high expression levels of SLC17A6 and PVALB could distinguish cluster 8 from all other clusters. Cluster 1 had extreme low expression level of all the 8 transcripts. Without prior knowledge of RNA expression information in the spinal cord, these results could facilitate the discoveries of different cell clusters and new biomarkers. By mapping these 8 clusters of cells back to their anatomic location in tissue (Figure 5.4.6C), we also noticed that different subregions of the spinal cord consisted of cells from distinct clusters.

In summary, we have developed a method for highly sensitive and multiplexed in situ RNA profiling using cleavable fluorescent tyramide. We have demonstrated the feasibility of this method in the application into FFPE tissues. By using this method, we have successfully profile eight different transcripts in mouse fixed frozen spinal cord tissues. The results have shown different subregions of the spinal cord consist of varied cell clusters. By applying CFT for signal amplification, our method has dramatically increase the detection sensitivity comparing with conventional RNA profiling technologies. Subsequent fluorophore cleavage and probe stripping could efficiently remove any remaining signal while also preserve the integrity of RNA molecules. Therefore, we envision that this CFT-based RNA profiling method has the potential to detect >50 transcripts in the same tissue sample. And the multiplexed RNA profiling will provide us with a new vision in the study of systems biology and development molecular diagnosis and cellular targeted therapies.

5.4 Figures

A

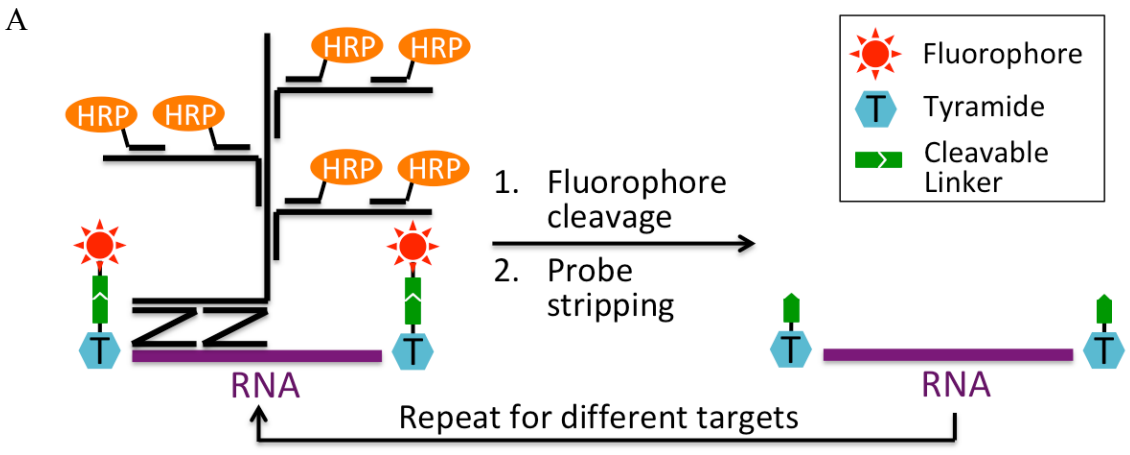

B

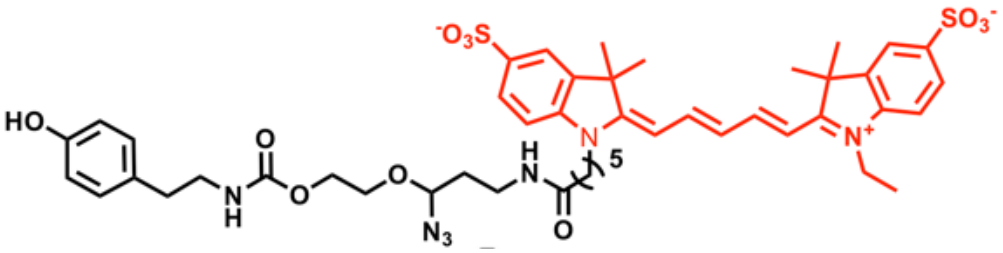

Figure 5.4.1 (A) Highly sensitive and multiplexed in situ RNA profiling with cleavable fluorescent tyramide. RNA targets are stained with HRP conjugated oligonucleotides and cleavable fluorescent tyramide. After imaging, the fluorophores are chemically cleaved and the oligonucleotide probes are stripped off. Through cycles of target staining, fluorescence imaging, fluorophore cleavage and probe stripping, comprehensive RNA profiling can be achieved in single cells in situ. (B) Structure of cleavable fluorescent tyramide, tyramide-N3-Cy5.

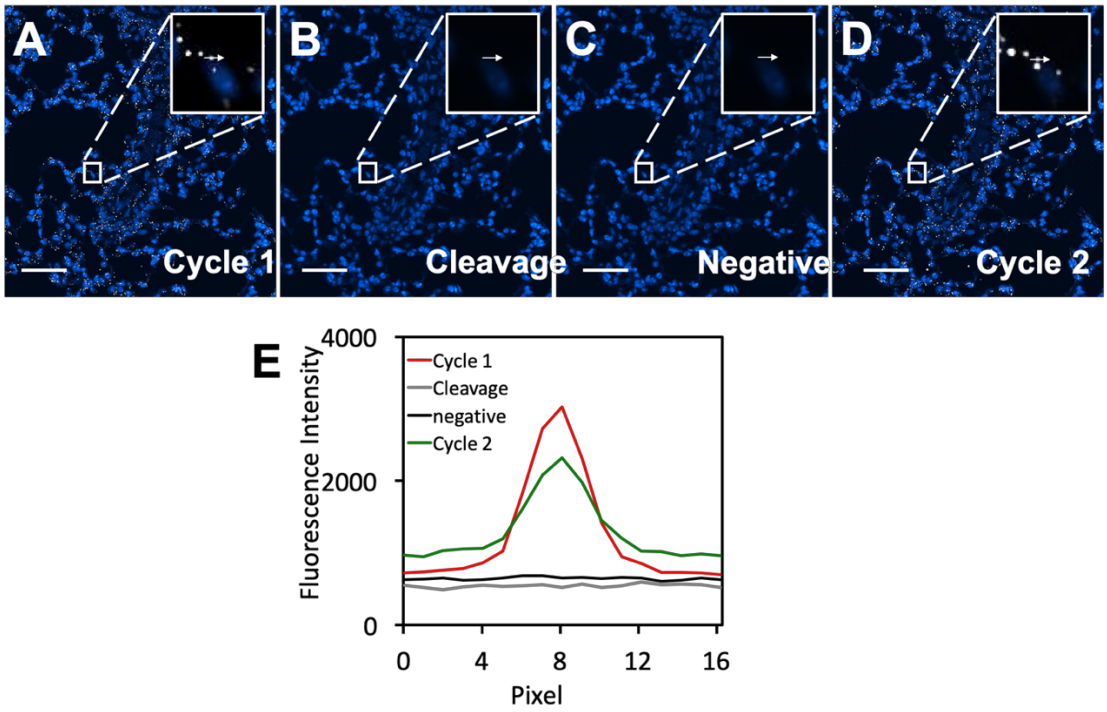

Figure 5.4.2 (A) Staining of PPIB with RNAscope® Multiplex Fluorescent v2 Assay and tyramide-N3-Cy5 in mouse FFPE lung tissue. (B) Cleavage of fluorescent signal with 30 min TCEP treatment at 40 °C. (C) Application of RNAscope® Fluorescent v2 Assay in the absence of target probes after 1 h DNase treatment at room temperature and 30 min 70% formamide treatment at 40 °C. (D) Restaining of PPIB with RNAscope® Multiplex Fluorescent v2 Assay and tyramide-N3-Cy5 after 12 h TCEP treatment at 40 °C, 24 h DNase treatment at room temperature and 12 h 70 % formamide treatment at 40 °C. (E) Fluorescent signal intensity of the sample position in four cycles. Scale bar, 50 μm.

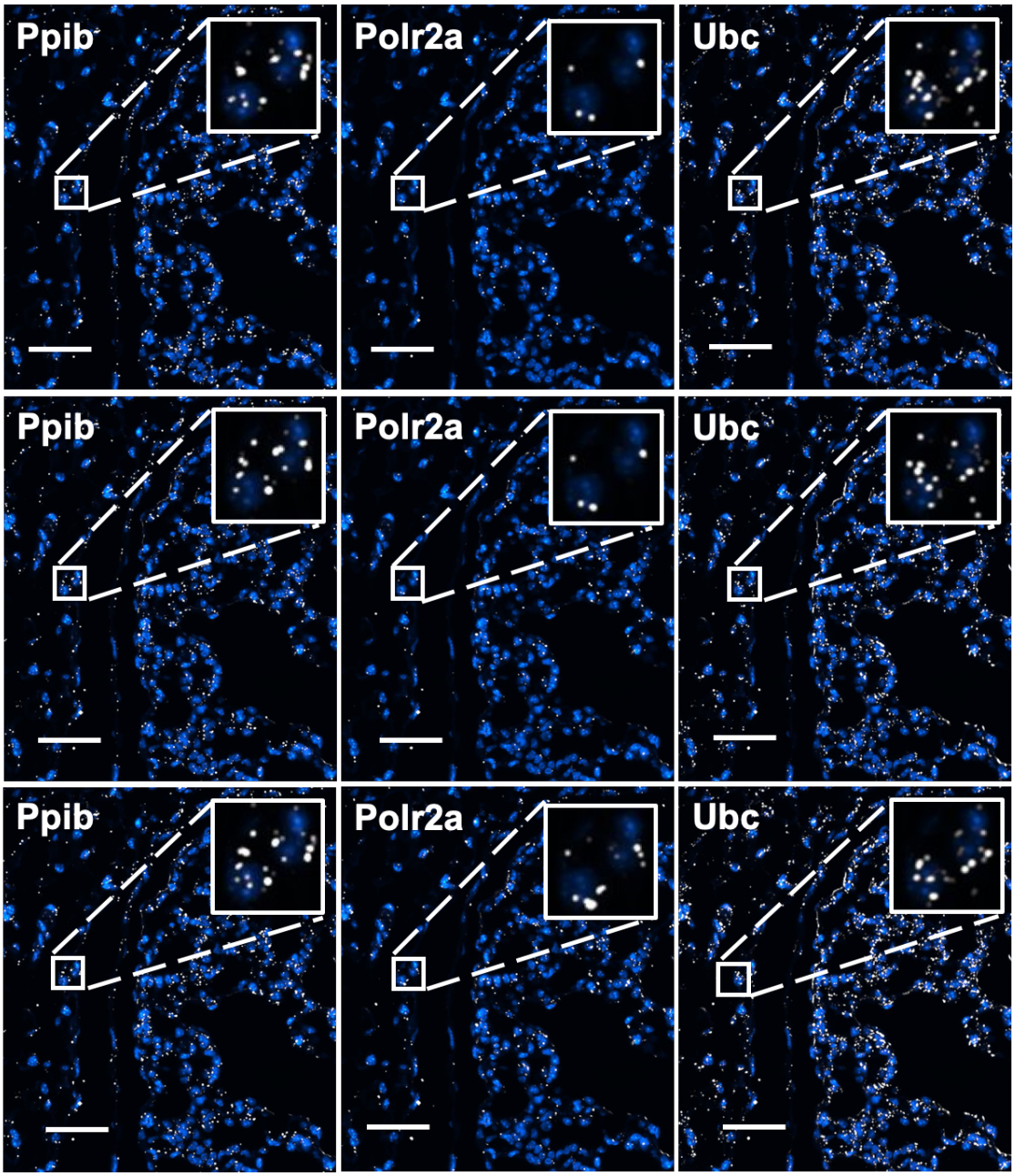

Figure 5.4.3 Three repeated rounds of consecutive staining of 3 transcripts with RNAscope® Multiplex Fluorescent v2 Assay and tyramide-N3-Cy5 in mouse FFPE lung tissue: PPIB, POLR2A and UBC. (left to right, the top to bottom). Scale bar, 50 μm.

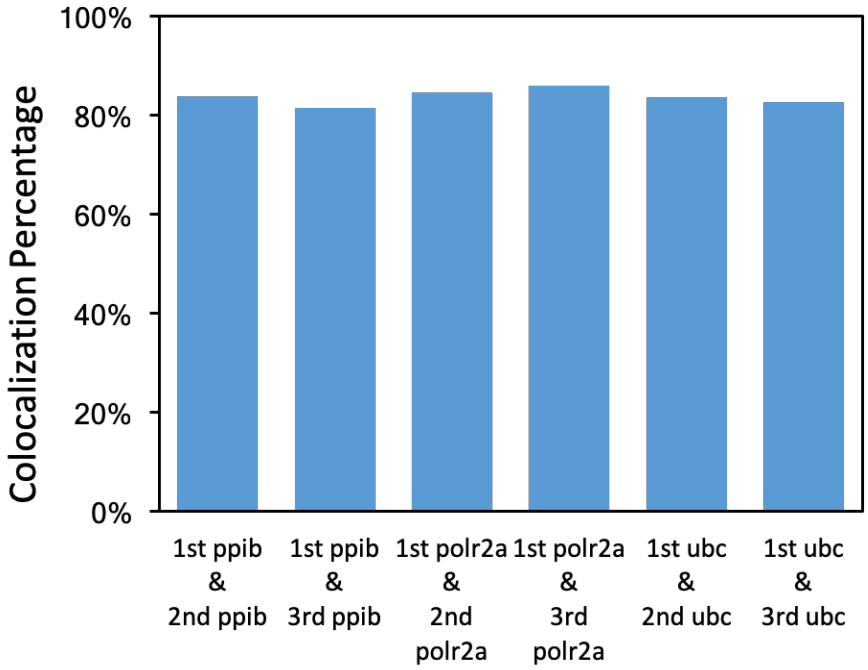

Figure 5.4.4 Fraction of spots appeared in the first three consecutive staining cycles reappeared in the second and third three consecutive staining cycles.

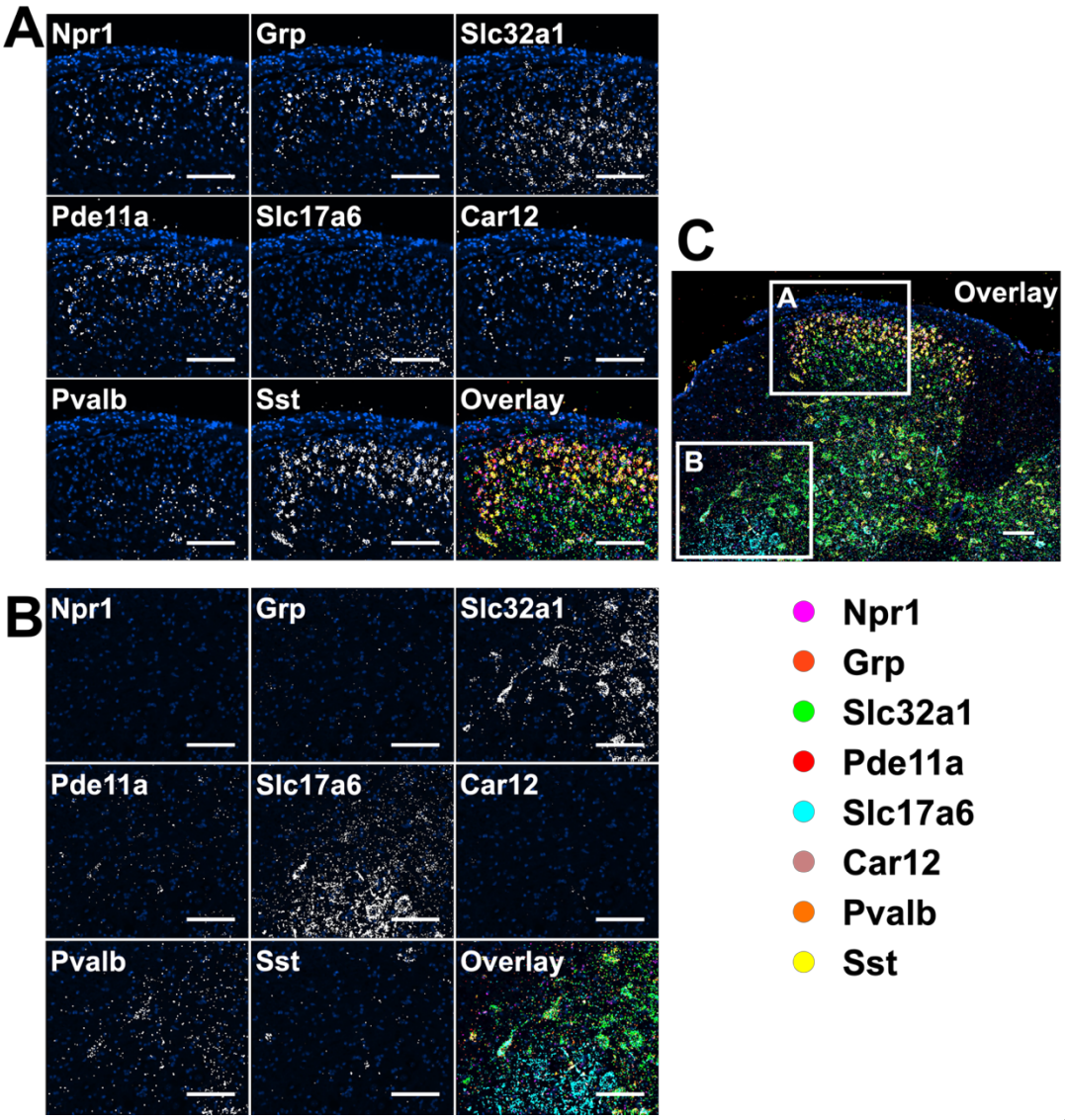

Figure 5.4.5 Eight different transcripts were detected sequentially with RNAscope® Multiplex Fluorescent v2 Assay and tyramide-N3-Cy5 in the mouse fixed frozen spinal cord tissues. (A) and (B) are the zoom-in areas corresponded to the overlay figure (C). Scale bar, 100 μm.

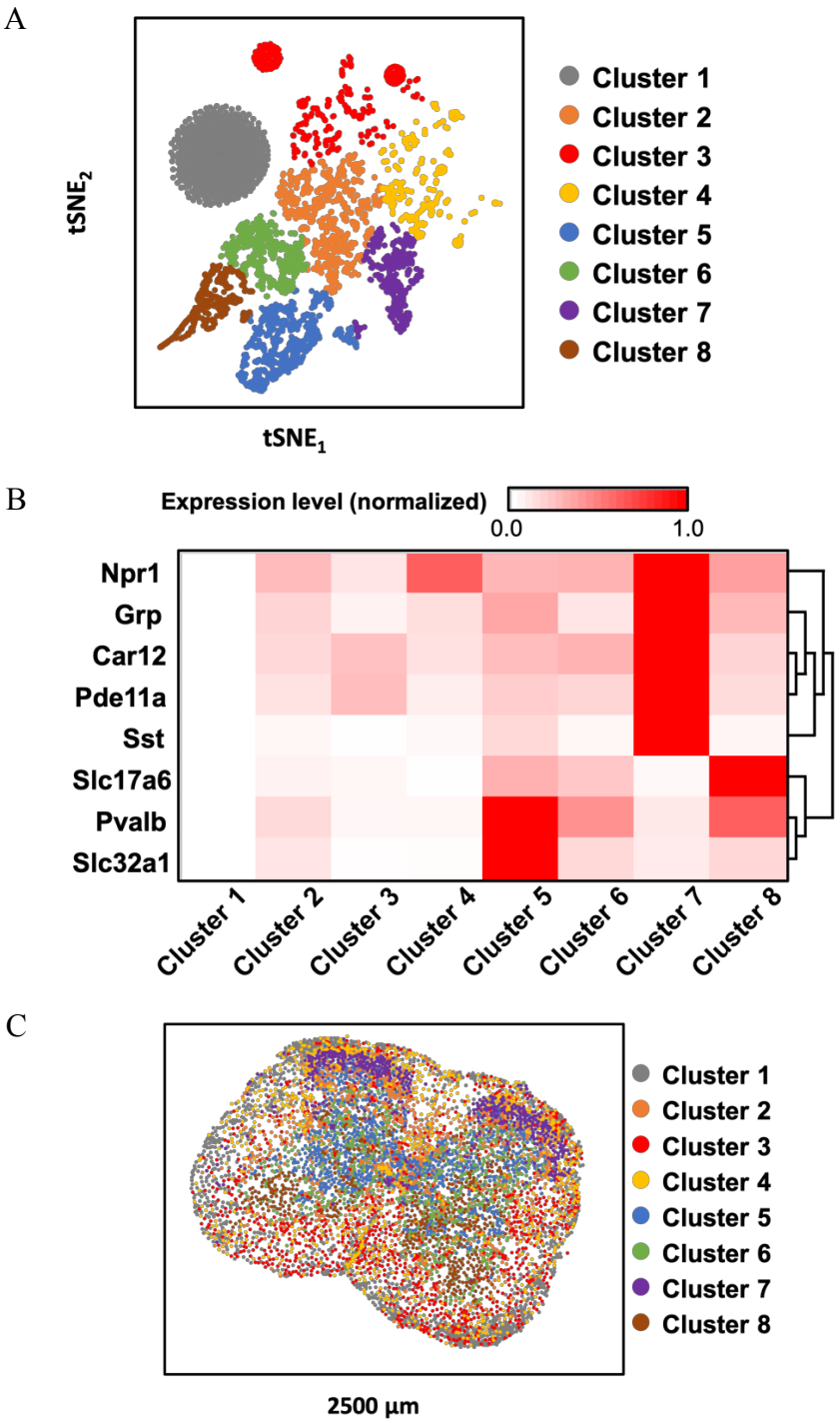

Figure 5.4.6 (A) Over 6000 cells in a mouse spinal cord were partitioned into 8 clusters. (B) The distinct RNA expression patterns in the 8 cell clusters. (C) Anatomical locations of the individual cells from the 8 clusters in the mouse spinal cord.

5.5 Method

5.5.1 Chemicals and bioreagents

Chemicals and solvents were purchased from Sigma-Aldrich or Ambion and were used without further purification, unless otherwise noted.

5.5.2 FFPE mouse lung tissue preparation and pretreatment

Mouse lung segments were dissected and post-fixed for 24 hours at room temperature. After dehydration and xylene treatment, the samples were embedded in paraffin and mounted onto Superfrost Plus (Fischer Scientific) slides in a 40 ℃ water bath.

The mouse formalin-fixed paraffin-embedded (FFPE) lung tissue slide was baked for 1 hour at 60 ℃, and deparaffinized 3 times in xylene, each for 5 min. Then the tissues were then washed 3 times with 100% ethanol at room temperature for 1 min.

The tissues were subsequently incubated with HRP blocking buffer (0.15% H_2O_2 in 1X PBT) for 10 minutes at room temperature, and subsequently washed 3 times with 1X PBS at room temperature, each for 5 minutes. After blocking, the tissues were then immersed in antigen retrieval buffer (10 M sodium citrate, 0.05% Tween 20, pH6.0) and waterbathed for 15 min at 100 ℃. After target retrieval. After that, a 30 minutes RNAscope® Protease Plus (Advanced Cell Diagnostics) treatment at room temperature was performed to the tissue, followed up with 3 times 1X PBS wash at room temperature, each for 5 minutes.

5.5.3 Fixed frozen mouse spinal cord tissue preparation and pretreatment

Lumbar spinal cord segments were dissected and post-fixed for 2 hours at 4 ℃. The spinal cords were cryo-sectioned to 14 μm, thaw-mounted onto Superfrost Plus (Fischer Scientific) slides, allowed to dry for 20 minutes at room temperature, and then stored at 80 ℃.

After post-fixation, cryo-section and thaw-mounting, spinal cord tissue was successively incubated in 50%, 70% and 100% ethanol at room temperature for 5 minutes respectively, then baked in the oven at 60 ℃ for 10 minutes.

Tissue was then incubated with HRP blocking buffer (0.15% H_2O_2 in 1X PBT) for 10 minutes at room temperature, and subsequently washed 3 times with 1X PBS at room temperature, each for 5 minutes. A 30 minutes RNAscope® Protease IV (Advanced Cell Diagnostics) treatment at room temperature was performed to the tissue after HRP blocking, followed up with 3 times 1X PBS wash at room temperature, each for 5 minutes.

5.5.4 Multi-channel *in situ* hybridization

In situ hybridization of the tissue sample was performed using the RNAscope® Multiplex Fluorescent v2 Assay (Advanced Cell Diagnostics).

The signal development of each channel was done by staining the slide with 0.25 pmol/μL cleavable Cy5 labeled tyramide in amplification buffer (0.0015% H_2O_2 and 0.1% triton X-100 in 0.1 M boric acid, pH = 8.5) at 40 ℃ for 30 minutes. After staining, the slide was washed 3 times with 1X RNAscope® Wash Buffer (Advanced Cell Diagnostics) at room temperature, each for 5 minutes. HRP blocking was subsequently performed by incubating slide with RNAscope® Multiplex FL v2 HRP blocker (Advanced Cell Diagnostics) for 15 minutes at 40 ℃, followed up with 2 times 1X RNAscope® Wash Buffer wash at room temperature, each for 2 minutes.

After incubation with GLOX buffer (0.4% glucose and 10 mM Tris HCl in 2 X SSC) for 1-2 min at room temperature, the stained slide was imaged in GLOX solution (0.37 mg mL^{-1} glucose oxidase and 1% catalase in GLOX buffer).

Fluorescent signal was removed by incubating slide with cleavage solution (100 mM TCEP in 5X SSC, pH=9.5) at 40 ℃ for 30 min, and 3 times washing with 1X RNAscope® Wash Buffer at room temperature, each for 5 minutes, then followed by the next channel signal development.

5.5.5 Probe stripping

Slide after signal development of all channels was incubated with 0.5 unit/μL DNase I (Roche Diagnostics) at room temperature for 1 hour, followed up with 6 times wash with DNase quenching buffer (0.3% lithium dodecyl sulfate and 30% formamide in TE buffer) at room temperature, each for 10 minutes.

After DNase treatment, slide was subsequently incubated with 70% formamide in 2X SSC at 40 ℃ for 30 min and washed 3 times with 1X PBS at room temperature.

Slide after probe stripping was followed up with next round of multi-channel *in situ* hybridization.

5.5.6 Imaging

Tissue was imaged under a Nikon Ti-E epofluorescence microscope equipped with a 10X objective. Images were captured using a CoolSNAP HQ2 camera and NIS-Elements Imaging software. Chroma filters 49009 was used for Cy5. Imaging processing and pseudo-color assignment were processed by ImageJ[139]. Cell segmentation and spot counting were processed by Cell Profiler[140]. tSNE maps and Phenograph clustering were genetrated from CYT (https://www.c2b2.columbia.edu/danapeerlab/html/cyt.html)[137].

CHAPTER 6

SUMMARY

In summary, we have successfully designed different approaches for the efficient and accurate detection and quantification of multiple transcripts *in situ* at sub-cellular resolution. Reiterative FISH has the ability to analyze >100 varied transcripts in single cell *in situ*. With more sophisticated consecutive FISH and switchable fluorescent oligonucleotides (SFO) based FISH, the detection throughput is dramatically increased. We have also developed cleavable fluorescent tyramide based RNA profiling approach capable of RNA detection even in intact tissues. We have demonstrated the feasibility of the approaches above and their potential to profile human transcriptome efficiently at low cost. By applying these approaches to study single-cell transcriptomics, we could have a more comprehensive understanding in system biology, molecular diagnosis and targeted therapies.

The development of technologies for spatial resolved single-cell transcriptomics analysis will provide us with broader and deeper understanding molecular mechanisms of different biological process. For example, by profiling transcriptome in situ in human brain tissue, we will have the ability to molecular examine different cell types and cell states. This will provide us with insights into human brain evolution, development and function. Additionally, single-cell transcriptomics will have huge application in the exploration of the development process of embryo at molecular level.

Furthermore, spatial resolved single-cell transcriptomics will have huge applications in personalized diagnosis and development of novel therapy precision medicine. For example,

by reconstructing gene regulatory networks at sub-cellular resolution, single-cell transcriptomic analysis will boost our understanding of molecular mechanism of diseases, which could help us find novel drug target for more effective target therapy development. The transcriptome wide profiling of tumor tissues will provide us with new tools for the discovery of new biomarkers for cancer diagnosis.

Future application of single-cell transcriptomic analysis will be also carried out together with other “omic” technologies. And the “multi-omic” approaches will provide a more precise map biomolecule regulatory networks and enable a more profound insight into biological issues.

BIBLIOGRAPHY

(1) Collins, F. S.; Green, E. D.; Guttmacher, A. E.; Guyer, M. S. A Vision for the Future of Genomics Research. *Nature* **2003**, *422* (6934), 835–847.

(2) Kalisky, T.; Oriel, S.; Bar-Lev, T. H.; Ben-Haim, N.; Trink, A.; Wineberg, Y.; Kanter, I.; Gilad, S.; Pyne, S. A Brief Review of Single-Cell Transcriptomic Technologies. *Brief. Funct. Genomics* **2018**, *17* (1), 64–76.

(3) Vera, M.; Biswas, J.; Senecal, A.; Singer, R. H.; Park, H. Y. Single-Cell and Single-Molecule Analysis of Gene Expression Regulation. *Annu. Rev. Genet.* **2016**, *50* (1), 267–291.

(4) Larson, D. R.; Singer, R. H.; Zenklusen, D. A Single Molecule View of Gene Expression. *Trends Cell Biol.* **2009**, *19* (11), 630–637.

(5) Levsky, J. M. Single-Cell Gene Expression Profiling. *Science* **2002**, *297* (5582), 836–840.

(6) Junker, J. P.; van Oudenaarden, A. Every Cell Is Special: Genome-Wide Studies Add a New Dimension to Single-Cell Biology. *Cell* **2014**, *157* (1), 8–11.

(7) Chappell, L.; Russell, A. J. C.; Voet, T. Single-Cell (Multi)Omics Technologies. *Annu. Rev. Genomics Hum. Genet.* **2018**, *19* (1), 15–41.

(8) Crosetto, N.; Bienko, M.; van Oudenaarden, A. Spatially Resolved Transcriptomics and Beyond. *Nat. Rev. Genet.* **2015**, *16* (1), 57–66.

(9) Hoheisel, J. D. Microarray Technology: Beyond Transcript Profiling and Genotype Analysis. *Nat. Rev. Genet.* **2006**, *7* (3), 200–210.

(10) Metzker, M. L. Sequencing Technologies — the next Generation. *Nat. Rev. Genet.* **2010**, *11* (1), 31–46.

(11) Navin, N.; Kendall, J.; Troge, J.; Andrews, P.; Rodgers, L.; McIndoo, J.; Cook, K.; Stepansky, A.; Levy, D.; Esposito, D.; et al. Tumour Evolution Inferred by Single-Cell Sequencing. *Nature* **2011**, *472* (7341), 90–94.

(12) Zong, C.; Lu, S.; Chapman, A. R.; Xie, X. S. Genome-Wide Detection of Single-Nucleotide and Copy-Number Variations of a Single Human Cell. *Science* **2012**, *338* (6114), 1622–1626.

(13) de Bourcy, C. F. A.; De Vlaminck, I.; Kanbar, J. N.; Wang, J.; Gawad, C.; Quake, S. R. A Quantitative Comparison of Single-Cell Whole Genome Amplification Methods. *PLoS ONE* **2014**, *9* (8), e105585.

(14) Islam, S.; Kjallquist, U.; Moliner, A.; Zajac, P.; Fan, J.-B.; Lonnerberg, P.; Linnarsson, S. Characterization of the Single-Cell Transcriptional Landscape by Highly Multiplex RNA-Seq. *Genome Res.* **2011**, *21* (7), 1160–1167.

(15) Picelli, S.; Björklund, Å. K.; Faridani, O. R.; Sagasser, S.; Winberg, G.; Sandberg, R. Smart-Seq2 for Sensitive Full-Length Transcriptome Profiling in Single Cells. *Nat. Methods* **2013**, *10* (11), 1096–1098.

(16) Hashimshony, T.; Wagner, F.; Sher, N.; Yanai, I. CEL-Seq: Single-Cell RNA-Seq by Multiplexed Linear Amplification. *Cell Rep.* **2012**, *2* (3), 666–673.

(17) Dalerba, P.; Kalisky, T.; Sahoo, D.; Rajendran, P. S.; Rothenberg, M. E.; Leyrat, A. A.; Sim, S.; Okamoto, J.; Johnston, D. M.; Qian, D.; et al. Single-Cell Dissection of Transcriptional Heterogeneity in Human Colon Tumors. *Nat. Biotechnol.* **2011**, *29* (12), 1120–1127.

(18) Brunskill, E. W.; Park, J.-S.; Chung, E.; Chen, F.; Magella, B.; Potter, S. S. Single Cell Dissection of Early Kidney Development: Multilineage Priming. *Development* **2014**, *141* (15), 3093–3101.

(19) Guo, G.; Huss, M.; Tong, G. Q.; Wang, C.; Li Sun, L.; Clarke, N. D.; Robson, P. Resolution of Cell Fate Decisions Revealed by Single-Cell Gene Expression Analysis from Zygote to Blastocyst. *Dev. Cell* **2010**, *18* (4), 675–685.

(20) Treutlein, B.; Brownfield, D. G.; Wu, A. R.; Neff, N. F.; Mantalas, G. L.; Espinoza, F. H.; Desai, T. J.; Krasnow, M. A.; Quake, S. R. Reconstructing Lineage Hierarchies of the Distal Lung Epithelium Using Single-Cell RNA-Seq. *Nature* **2014**, *509* (7500), 371–375.

(21) Bengtsson, M. Gene Expression Profiling in Single Cells from the Pancreatic Islets of Langerhans Reveals Lognormal Distribution of MRNA Levels. *Genome Res.* **2005**, *15* (10), 1388–1392.

(22) Islam, S.; Kjällquist, U.; Moliner, A.; Zajac, P.; Fan, J.-B.; Lönnerberg, P.; Linnarsson, S. Highly Multiplexed and Strand-Specific Single-Cell RNA 5′ End Sequencing. *Nat. Protoc.* **2012**, *7* (5), 813–828.

(23) Tang, F.; Barbacioru, C.; Nordman, E.; Li, B.; Xu, N.; Bashkirov, V. I.; Lao, K.; Surani, M. A. RNA-Seq Analysis to Capture the Transcriptome Landscape of a Single Cell. *Nat. Protoc.* **2010**, *5* (3), 516–535.

(24) Picelli, S.; Faridani, O. R.; Björklund, Å. K.; Winberg, G.; Sagasser, S.; Sandberg, R. Full-Length RNA-Seq from Single Cells Using Smart-Seq2. *Nat. Protoc.* **2014**, *9* (1), 171–181.

(25) Yuan, G.-C.; Cai, L.; Elowitz, M.; Enver, T.; Fan, G.; Guo, G.; Irizarry, R.; Kharchenko, P.; Kim, J.; Orkin, S.; et al. Challenges and Emerging Directions in Single-Cell Analysis. *Genome Biol.* **2017**, *18* (1), 84.

(26) Femino, A. M.; Fay, F. S.; Fogarty, K.; Singer, R. H. Visualization of Single RNA Transcripts in Situ. **1998**, *280*, 7.

(27) Raj, A.; van den Bogaard, P.; Rifkin, S. A.; van Oudenaarden, A.; Tyagi, S. Imaging Individual MRNA Molecules Using Multiple Singly Labeled Probes. *Nat. Methods* **2008**, *5* (10), 877–879.

(28) Wang, F.; Flanagan, J.; Su, N.; Wang, L.-C.; Bui, S.; Nielson, A.; Wu, X.; Vo, H.-T.; Ma, X.-J.; Luo, Y. A Novel in Situ RNA Analysis Platform for Formalin-Fixed, Paraffin-Embedded Tissues. *J. Mol. Diagn.* **2012**, *14* (1), 22–29.

(29) Guo, J.; Xu, N.; Li, Z.; Zhang, S.; Wu, J.; Kim, D. H.; Sano Marma, M.; Meng, Q.; Cao, H.; Li, X.; et al. Four-Color DNA Sequencing with 3'-O-Modified Nucleotide Reversible Terminators and Chemically Cleavable Fluorescent Dideoxynucleotides. *Proc. Natl. Acad. Sci.* **2008**, *105* (27), 9145–9150.

(30) Satija, R.; Farrell, J. A.; Gennert, D.; Schier, A. F.; Regev, A. Spatial Reconstruction of Single-Cell Gene Expression Data. *Nat. Biotechnol.* **2015**, *33* (5), 495–502.

(31) Ståhl, P. L.; Salmén, F.; Vickovic, S.; Lundmark, A.; Navarro, J. F.; Magnusson, J.; Giacomello, S.; Asp, M.; Westholm, J. O.; Huss, M.; et al. Visualization and Analysis of Gene Expression in Tissue Sections by Spatial Transcriptomics. *Science* **2016**, *353* (6294), 78–82.

(32) Luzzi, V.; Holtschlag, V.; Watson, M. A. Expression Profiling of Ductal Carcinoma in Situ by Laser Capture Microdissection and High-Density Oligonucleotide Arrays. *Am. J. Pathol.* **2001**, *158* (6), 2005–2010.

(33) Schutze, K.; Lahr, G. Identification of Expressed Genes by Laser- Tnediated Inanipulation of Single Cells. **1998**, *16*, 6.

(34) Morton, M. L.; Bai, X.; Merry, C. R.; Linden, P. A.; Khalil, A. M.; Leidner, R. S.; Thompson, C. L. Identification of MRNAs and LincRNAs Associated with Lung Cancer Progression Using Next-Generation RNA Sequencing from Laser Micro-Dissected Archival FFPE Tissue Specimens. *Lung Cancer* **2014**, *85* (1), 31–39.

(35) Lovatt, D.; Ruble, B. K.; Lee, J.; Dueck, H.; Kim, T. K.; Fisher, S.; Francis, C.; Spaethling, J. M.; Wolf, J. A.; Grady, M. S.; et al. Transcriptome in Vivo Analysis (TIVA) of Spatially Defined Single Cells in Live Tissue. *Nat. Methods* **2014**, *11* (2), 190–196.

(36) Liu, S.; Trapnell, C. Single-Cell Transcriptome Sequencing: Recent Advances and Remaining Challenges. *F1000Research* **2016**, *5*, 182.

(37) He, L.; Hannon, G. J. MicroRNAs: Small RNAs with a Big Role in Gene Regulation. *Nat. Rev. Genet.* **2004**, *5* (7), 522–531.

(38) Cai, Y.; Yu, X.; Hu, S.; Yu, J. A Brief Review on the Mechanisms of MiRNA Regulation. *Genomics Proteomics Bioinformatics* **2009**, *7* (4), 147–154.

(39) Memczak, S.; Jens, M.; Elefsinioti, A.; Torti, F.; Krueger, J.; Rybak, A.; Maier, L.; Mackowiak, S. D.; Gregersen, L. H.; Munschauer, M.; et al. Circular RNAs Are a Large Class of Animal RNAs with Regulatory Potency. *Nature* **2013**, *495* (7441), 333–338.

(40) Jeck, W. R.; Sharpless, N. E. Detecting and Characterizing Circular RNAs. *Nat. Biotechnol.* **2014**, *32* (5), 453–461.

(41) Islam, S.; Zeisel, A.; Joost, S.; La Manno, G.; Zajac, P.; Kasper, M.; Lönnerberg, P.; Linnarsson, S. Quantitative Single-Cell RNA-Seq with Unique Molecular Identifiers. *Nat. Methods* **2014**, *11* (2), 163–166.

(42) Deng, Q.; Ramskold, D.; Reinius, B.; Sandberg, R. Single-Cell RNA-Seq Reveals Dynamic, Random Monoallelic Gene Expression in Mammalian Cells. *Science* **2014**, *343* (6167), 193–196.

(43) Saliba, A.-E.; Westermann, A. J.; Gorski, S. A.; Vogel, J. Single-Cell RNA-Seq: Advances and Future Challenges. *Nucleic Acids Res.* **2014**, *42* (14), 8845–8860.

(44) Martin, K. C.; Ephrussi, A. MRNA Localization: Gene Expression in the Spatial Dimension. *Cell* **2009**, *136* (4), 719–730.

(45) Lubeck, E.; Coskun, A. F.; Zhiyentayev, T.; Ahmad, M.; Cai, L. Single-Cell in Situ RNA Profiling by Sequential Hybridization. *Nat. Methods* **2014**, *11* (4), 360–361.

(46) Choi, H. M. T.; Schwarzkopf, M.; Fornace, M. E.; Acharya, A.; Artavanis, G.; Stegmaier, J.; Cunha, A.; Pierce, N. A. *Third-Generation in Situ Hybridization Chain Reaction: Multiplexed, Quantitative, Sensitive, Versatile, Robust*; preprint; Developmental Biology, 2018.

(47) Shah, S.; Lubeck, E.; Zhou, W.; Cai, L. In Situ Transcription Profiling of Single Cells Reveals Spatial Organization of Cells in the Mouse Hippocampus. *Neuron* **2016**, *92* (2), 342–357.

(48) Chen, K. H.; Boettiger, A. N.; Moffitt, J. R.; Wang, S.; Zhuang, X. Spatially Resolved, Highly Multiplexed RNA Profiling in Single Cells. *Science* **2015**, *348* (6233), aaa6090–aaa6090.

(49) Ke, R.; Mignardi, M.; Pacureanu, A.; Svedlund, J.; Botling, J.; Wählby, C.; Nilsson, M. In Situ Sequencing for RNA Analysis in Preserved Tissue and Cells. *Nat. Methods* **2013**, *10* (9), 857–860.

(50) Lee, J. H.; Daugharthy, E. R.; Scheiman, J.; Kalhor, R.; Yang, J. L.; Ferrante, T. C.; Terry, R.; Jeanty, S. S. F.; Li, C.; Amamoto, R.; et al. Highly Multiplexed Subcellular RNA Sequencing in Situ. *Science* **2014**, *343* (6177), 1360–1363.

(51) Jaitin, D. A.; Kenigsberg, E.; Keren-Shaul, H.; Elefant, N.; Paul, F.; Zaretsky, I.; Mildner, A.; Cohen, N.; Jung, S.; Tanay, A.; et al. Massively Parallel Single-Cell RNA-Seq for Marker-Free Decomposition of Tissues into Cell Types. *Science* **2014**, *343* (6172), 776–779.

(52) Shalek, A. K.; Satija, R.; Adiconis, X.; Gertner, R. S.; Gaublomme, J. T.; Raychowdhury, R.; Schwartz, S.; Yosef, N.; Malboeuf, C.; Lu, D.; et al. Single-Cell Transcriptomics Reveals Bimodality in Expression and Splicing in Immune Cells. *Nature* **2013**, *498* (7453), 236–240.

(53) Grün, D.; Lyubimova, A.; Kester, L.; Wiebrands, K.; Basak, O.; Sasaki, N.; Clevers, H.; van Oudenaarden, A. Single-Cell Messenger RNA Sequencing Reveals Rare Intestinal Cell Types. *Nature* **2015**, *525* (7568), 251–255.

(54) Amir, E. D.; Davis, K. L.; Tadmor, M. D.; Simonds, E. F.; Levine, J. H.; Bendall, S. C.; Shenfeld, D. K.; Krishnaswamy, S.; Nolan, G. P.; Pe'er, D. ViSNE Enables Visualization of High Dimensional Single-Cell Data and Reveals Phenotypic Heterogeneity of Leukemia. *Nat. Biotechnol.* **2013**, *31* (6), 545–552.

(55) Shalek, A. K.; Satija, R.; Shuga, J.; Trombetta, J. J.; Gennert, D.; Lu, D.; Chen, P.; Gertner, R. S.; Gaublomme, J. T.; Yosef, N.; et al. Single-Cell RNA-Seq Reveals Dynamic Paracrine Control of Cellular Variation. *Nature* **2014**, *510* (7505), 363–369.

(56) Pollen, A. A.; Nowakowski, T. J.; Shuga, J.; Wang, X.; Leyrat, A. A.; Lui, J. H.; Li, N.; Szpankowski, L.; Fowler, B.; Chen, P.; et al. Low-Coverage Single-Cell MRNA Sequencing Reveals Cellular Heterogeneity and Activated Signaling Pathways in Developing Cerebral Cortex. *Nat. Biotechnol.* **2014**, *32* (10), 1053–1058.

(57) Luo, Y.; Coskun, V.; Liang, A.; Yu, J.; Cheng, L.; Ge, W.; Shi, Z.; Zhang, K.; Li, C.; Cui, Y.; et al. Single-Cell Transcriptome Analyses Reveal Signals to Activate Dormant Neural Stem Cells. *Cell* **2015**, *161* (5), 1175–1186.

(58) Usoskin, D.; Furlan, A.; Islam, S.; Abdo, H.; Lönnerberg, P.; Lou, D.; Hjerling-Leffler, J.; Haeggström, J.; Kharchenko, O.; Kharchenko, P. V.; et al. Unbiased Classification of Sensory Neuron Types by Large-Scale Single-Cell RNA Sequencing. *Nat. Neurosci.* **2015**, *18* (1), 145–153.

(59) Mahata, B.; Zhang, X.; Kolodziejczyk, A. A.; Proserpio, V.; Haim-Vilmovsky, L.; Taylor, A. E.; Hebenstreit, D.; Dingler, F. A.; Moignard, V.; Göttgens, B.; et al. Single-Cell RNA Sequencing Reveals T Helper Cells Synthesizing Steroids De Novo to Contribute to Immune Homeostasis. *Cell Rep.* **2014**, *7* (4), 1130–1142.

(60) Spaethling, J. M.; Sanchez-Alavez, M.; Lee, J.; Xia, F. C.; Dueck, H.; Wang, W.; Fisher, S. A.; Sul, J.-Y.; Seale, P.; Kim, J.; et al. Single-Cell Transcriptomics and Functional Target Validation of Brown Adipocytes Show Their Complex Roles in Metabolic Homeostasis. *FASEB J.* **2016**, *30* (1), 81–92.

(61) Padovan-Merhar, O.; Raj, A. Using Variability in Gene Expression as a Tool for Studying Gene Regulation: Characterizing Gene Regulation Using Expression Variability. *Wiley Interdiscip. Rev. Syst. Biol. Med.* **2013**, *5* (6), 751–759.

(62) Hurley, D.; Araki, H.; Tamada, Y.; Dunmore, B.; Sanders, D.; Humphreys, S.; Affara, M.; Imoto, S.; Yasuda, K.; Tomiyasu, Y.; et al. Gene Network Inference and Visualization Tools for Biologists: Application to New Human Transcriptome Datasets. *Nucleic Acids Res.* **2012**, *40* (6), 2377–2398.

(63) Bansal, M.; Belcastro, V.; Ambesi-Impiombato, A.; di Bernardo, D. How to Infer Gene Networks from Expression Profiles. *Mol. Syst. Biol.* **2007**, *3* (1), 78.

(64) Patel, A. P.; Tirosh, I.; Trombetta, J. J.; Shalek, A. K.; Gillespie, S. M.; Wakimoto, H.; Cahill, D. P.; Nahed, B. V.; Curry, W. T.; Martuza, R. L.; et al. Single-Cell RNA-Seq Highlights Intratumoral Heterogeneity in Primary Glioblastoma. *Science* **2014**, *344* (6190), 1396–1401.

(65) Min, J.-W.; Kim, W. J.; Han, J. A.; Jung, Y.-J.; Kim, K.-T.; Park, W.-Y.; Lee, H.-O.; Choi, S. S. Identification of Distinct Tumor Subpopulations in Lung Adenocarcinoma via Single-Cell RNA-Seq. *PLOS ONE* **2015**, *10* (8), e0135817.

(66) Xue, Z.; Huang, K.; Cai, C.; Cai, L.; Jiang, C.; Feng, Y.; Liu, Z.; Zeng, Q.; Cheng, L.; Sun, Y. E.; et al. Genetic Programs in Human and Mouse Early Embryos Revealed by Single-Cell RNA Sequencing. *Nature* **2013**, *500* (7464), 593–597.

(67) Gille, C.; Bölling, C.; Hoppe, A.; Bulik, S.; Hoffmann, S.; Hübner, K.; Karlstädt, A.; Ganeshan, R.; König, M.; Rother, K.; et al. HepatoNet1: A Comprehensive Metabolic Reconstruction of the Human Hepatocyte for the Analysis of Liver Physiology. *Mol. Syst. Biol.* **2010**, *6* (1), 411.

(68) Shah, S.; Lubeck, E.; Schwarzkopf, M.; He, T.-F.; Greenbaum, A.; Sohn, C. H.; Lignell, A.; Choi, H. M. T.; Gradinaru, V.; Pierce, N. A.; et al. Single-Molecule RNA Detection at Depth by Hybridization Chain Reaction and Tissue Hydrogel Embedding and Clearing. *Development* **2016**, *143* (15), 2862–2867.

(69) Chen, F.; Wassie, A. T.; Cote, A. J.; Sinha, A.; Alon, S.; Asano, S.; Daugharthy, E. R.; Chang, J.-B.; Marblestone, A.; Church, G. M.; et al. Nanoscale Imaging of RNA with Expansion Microscopy. *Nat. Methods* **2016**, *13* (8), 679–684.

(70) Jain, M.; Koren, S.; Miga, K. H.; Quick, J.; Rand, A. C.; Sasani, T. A.; Tyson, J. R.; Beggs, A. D.; Dilthey, A. T.; Fiddes, I. T.; et al. Nanopore Sequencing and Assembly of a Human Genome with Ultra-Long Reads. *Nat. Biotechnol.* **2018**, *36* (4), 338–345.

(71) Skylaki, S.; Hilsenbeck, O.; Schroeder, T. Challenges in Long-Term Imaging and Quantification of Single-Cell Dynamics. *Nat. Biotechnol.* **2016**, *34* (11), 1137–1144.

(72) Böiers, C.; Richardson, S. E.; Laycock, E.; Zriwil, A.; Turati, V. A.; Brown, J.; Wray, J. P.; Wang, D.; James, C.; Herrero, J.; et al. A Human IPS Model Implicates Embryonic B-Myeloid Fate Restriction as Developmental Susceptibility to B Acute Lymphoblastic Leukemia-Associated ETV6-RUNX1. *Dev. Cell* **2018**, *44* (3), 362-377.e7.

(73) Taliaferro, J. M. Classical and Emerging Techniques to Identify and Quantify Localized RNAs. *Wiley Interdiscip. Rev. RNA* **2019**, e1542.

(74) Guo, J.; Yu, L.; Turro, N. J.; Ju, J. An Integrated System for DNA Sequencing by Synthesis Using Novel Nucleotide Analogues. *Acc. Chem. Res.* **2010**, *43* (4), 551–563.

(75) Sims, P. A.; Greenleaf, W. J.; Duan, H.; Xie, X. S. Fluorogenic DNA Sequencing in PDMS Microreactors. *Nat. Methods* **2011**, *8* (7), 575–580.

(76) Huang, K.; Martí, A. A. Recent Trends in Molecular Beacon Design and Applications. *Anal. Bioanal. Chem.* **2012**, *402* (10), 3091–3102.

(77) Guo, J.; Ju, J.; Turro, N. J. Fluorescent Hybridization Probes for Nucleic Acid Detection. *Anal. Bioanal. Chem.* **2012**, *402* (10), 3115–3125.

(78) Levesque, M. J.; Raj, A. Single-Chromosome Transcriptional Profiling Reveals Chromosomal Gene Expression Regulation. *Nat. Methods* **2013**, *10* (3), 246–248.

(79) Lubeck, E.; Cai, L. Single-Cell Systems Biology by Super-Resolution Imaging and Combinatorial Labeling. *Nat. Methods* **2012**, *9* (7), 743–748.

(80) Lee, J. H.; Daugharthy, E. R.; Scheiman, J.; Kalhor, R.; Yang, J. L.; Ferrante, T. C.; Terry, R.; Jeanty, S. S. F.; Li, C.; Amamoto, R.; et al. Highly Multiplexed Subcellular RNA Sequencing in Situ. *Science* **2014**, *343* (6177), 1360–1363.

(81) Schubert, W.; Bonnekoh, B.; Pommer, A. J.; Philipsen, L.; Böckelmann, R.; Malykh, Y.; Gollnick, H.; Friedenberger, M.; Bode, M.; Dress, A. W. M. Analyzing Proteome

Topology and Function by Automated Multidimensional Fluorescence Microscopy. *Nat. Biotechnol.* **2006**, *24* (10), 1270–1278.

(82) Uhlen, M.; Fagerberg, L.; Hallstrom, B. M.; Lindskog, C.; Oksvold, P.; Mardinoglu, A.; Sivertsson, A.; Kampf, C.; Sjostedt, E.; Asplund, A.; et al. Tissue-Based Map of the Human Proteome. *Science* **2015**, *347* (6220), 1260419–1260419.

(83) Becskei, A.; Kaufmann, B. B.; van Oudenaarden, A. Contributions of Low Molecule Number and Chromosomal Positioning to Stochastic Gene Expression. *Nat. Genet.* **2005**, *37* (9), 937–944.

(84) Blake, W. J.; KÆrn, M.; Cantor, C. R.; Collins, J. J. Noise in Eukaryotic Gene Expression. *Nature* **2003**, *422* (6932), 633–637.

(85) Elowitz, M. B. Stochastic Gene Expression in a Single Cell. *Science* **2002**, *297* (5584), 1183–1186.

(86) Golding, I.; Paulsson, J.; Zawilski, S. M.; Cox, E. C. Real-Time Kinetics of Gene Activity in Individual Bacteria. *Cell* **2005**, *123* (6), 1025–1036.

(87) Ozbudak, E. M.; Thattai, M.; Kurtser, I.; Grossman, A. D.; van Oudenaarden, A. Regulation of Noise in the Expression of a Single Gene. *Nat. Genet.* **2002**, *31* (1), 69–73.

(88) Raj, A.; Peskin, C. S.; Tranchina, D.; Vargas, D. Y.; Tyagi, S. Stochastic MRNA Synthesis in Mammalian Cells. *PLoS Biol.* **2006**, *4* (10), e309.

(89) Raser, J. M. Control of Stochasticity in Eukaryotic Gene Expression. *Science* **2004**, *304* (5678), 1811–1814.

(90) Rosenfeld, N. Gene Regulation at the Single-Cell Level. *Science* **2005**, *307* (5717), 1962–1965.

(91) Guo, J.; Wang, S.; Dai, N.; Teo, Y. N.; Kool, E. T. Multispectral Labeling of Antibodies with Polyfluorophores on a DNA Backbone and Application in Cellular Imaging. *Proc. Natl. Acad. Sci.* **2011**, *108* (9), 3493–3498.

(92) Wang, S.; Guo, J.; Ono, T.; Kool, E. T. DNA Polyfluorophores for Real-Time Multicolor Tracking of Dynamic Biological Systems. *Angew. Chem. Int. Ed.* **2012**, *51* (29), 7176–7180.

(93) Dai, N.; Guo, J.; Teo, Y. N.; Kool, E. T. Protease Probes Built from DNA: Multispectral Fluorescent DNA-Peptide Conjugates as Caspase Chemosensors. *Angew. Chem. Int. Ed.* **2011**, *50* (22), 5105–5109.

(94) Crosetto, N.; Bienko, M.; Oudenaarden, A. Van. Spatially Resolved Transcriptomics and Beyond. *Nat. Rev. Genet.* **2014**, *16* (January), 57–66.

(95) Hoheisel, J. D. Microarray Technology: Beyond Transcript Profiling and Genotype Analysis. *Nat. Rev. Genet.* **2006**, *7* (3), 200–210.

(96) Metzker, M. L. Sequencing Technologies - the next Generation. *Nat. Rev. Genet.* **2010**, *11* (1), 31–46.

(97) Guo, J.; Yu, L.; Turro, N. J.; Ju, J. An Integrated System for DNA Sequencing by Synthesis Using Novel Nucleotide Analogues. *Acc. Chem. Res.* **2010**, *43* (4), 551–563.

(98) Raj, A.; Bogaard, P. Van Den; Rifkin, S. A.; Oudenaarden, A. Van; Tyagi, S. Imaging Individual MRNA Molecules Using Multiple Singly Labeled Probes. *Nat. Methods* **2008**, *5* (10), 877–879.

(99) Beliveau, B. J.; Joyce, E. F.; Apostolopoulos, N.; Yilmaz, F.; Fonseka, C. Y.; McCole, R. B.; Chang, Y.; Li, J. B.; Senaratne, T. N.; Williams, B. R.; et al. Versatile Design and Synthesis Platform for Visualizing Genomes with Oligopaint FISH Probes. *Proc. Natl. Acad. Sci. U. S. A.* **2012**, *109* (52), 21301–21306.

(100) Huang, K.; Martí, A. a. Recent Trends in Molecular Beacon Design and Applications. *Anal. Bioanal. Chem.* **2012**, *402* (10), 3091–3102.

(101) Franzini, R. M.; Kool, E. T. Efficient Nucleic Acid Detection by Templated Reductive Quencher Release. *J. Am. Chem. Soc.* **2009**, *131* (44), 16021–16023.

(102) Xiao, L.; Guo, J. Multiplexed Single-Cell in Situ RNA Analysis by Reiterative Hybridization. *Anal Methods* **2015**, *7* (17), 7290–7295.

(103) Guo, J. US Patent Application 20160054308A1. 2016.

(104) Shaffer, S. M.; Dunagin, M. C.; Torborg, S. R.; Torre, E. A.; Emert, B.; Krepler, C.; Beqiri, M.; Sproesser, K.; Brafford, P. A.; Xiao, M.; et al. Rare Cell Variability and Drug-Induced Reprogramming as a Mode of Cancer Drug Resistance. *Nature* **2017**, *546* (7658), 431–435.

(105) Levsky, J. M.; Shenoy, S. M.; Pezo, R. C.; Singer, R. H. Single-Cell Gene Expression Profiling. *Science* **2002**, *297* (5582), 836–840.

(106) Lubeck, E.; Cai, L. Single-Cell Systems Biology by Super-Resolution Imaging and Combinatorial Labeling. *Nat. Methods* **2012**, *9* (7), 743–748.

(107) Levesque, M. J.; Raj, A. Single-Chromosome Transcriptional Profiling Reveals Chromosomal Gene Expression Regulation. *Nat. Methods* **2013**, *10* (JaNuaRy), 246–248.

(108) Lee, J. H.; Daugharthy, E. R.; Scheiman, J.; Kalhor, R.; Yang, J. L.; Ferrante, T. C.; Terry, R.; Jeanty, S. S. F.; Li, C.; Amamoto, R.; et al. Highly Multiplexed Subcellular RNA Sequencing in Situ. *Science* **2014**, *343* (6177), 1360–1363.

(109) Ke, R.; Mignardi, M.; Pacureanu, A.; Svedlund, J.; Botling, J.; Wählby, C.; Nilsson, M. In Situ Sequencing for RNA Analysis in Preserved Tissue and Cells. *Nat. Methods* **2013**, *10* (9), 857–860.

(110) Lubeck, E.; Coskun, A. F.; Zhiyentayev, T.; Ahmad, M.; Cai, L. Single-Cell in Situ RNA Profiling by Sequential Hybridization. *Nat. Methods* **2014**, *11* (4), 360–361.

(111) Chen, K. H.; Boettiger, a. N.; Moffitt, J. R.; Wang, S.; Zhuang, X. Spatially Resolved, Highly Multiplexed RNA Profiling in Single Cells. *Science* **2015**, *1363* (2014), 1360–1363.

(112) Murgha, Y. E.; Rouillard, J.-M.; Gulari, E. Methods for the Preparation of Large Quantities of Complex Single-Stranded Oligonucleotide Libraries. *PLoS ONE* **2014**, *9* (4), e94752.

(113) Xu, Q.; Schlabach, M. R.; Hannon, G. J.; Elledge, S. J. Design of 240,000 Orthogonal 25mer DNA Barcode Probes. *Proc. Natl. Acad. Sci.* **2009**, *106* (7), 2289–2294.

(114) Camacho, C.; Coulouris, G.; Avagyan, V.; Ma, N.; Papadopoulos, J.; Bealer, K.; Madden, T. L. BLAST+: Architecture and Applications. *BMC Bioinformatics* **2009**, *10* (1), 421.

(115) Olivo-Marin, J.-C. Extraction of Spots in Biological Images Using Multiscale Products. *Pattern Recognit.* **2002**, *35* (9), 1989–1996.

(116) Guo, J.; Ju, J.; Turro, N. J. Fluorescent Hybridization Probes for Nucleic Acid Detection. *Anal. Bioanal. Chem.* **2012**, *402* (10), 3115–3125.

(117) Shah, S.; Lubeck, E.; Zhou, W.; Cai, L. In Situ Transcription Profiling of Single Cells Reveals Spatial Organization of Cells in the Mouse Hippocampus. *Neuron* **2016**, *92* (2), 342–357.

(118) Moffitt, J. R.; Hao, J.; Bambah-Mukku, D.; Lu, T.; Dulac, C.; Zhuang, X. High-Performance Multiplexed Fluorescence in Situ Hybridization in Culture and Tissue with Matrix Imprinting and Clearing. *Proc. Natl. Acad. Sci.* **2016**, *113*, 14456–14461.

(119) Moffitt, J. R.; Hao, J.; Wang, G.; Chen, K. H.; Babcock, H. P.; Zhuang, X. High-Throughput Single-Cell Gene-Expression Profiling with Multiplexed Error-Robust Fluorescence in Situ Hybridization. *Proc. Natl. Acad. Sci.* **2016**, *113*, 11046–11051.

(120) Zhang, D. Y.; Seelig, G. Dynamic DNA Nanotechnology Using Strand-Displacement Reactions. *Nat. Chem.* **2011**, *3* (2), 103–113.

(121) Lubeck, E.; Coskun, A. F.; Zhiyentayev, T.; Ahmad, M.; Cai, L. Single-Cell in Situ RNA Profiling by Sequential Hybridization. *Nat. Methods* **2014**, *11* (4), 360–361.

(122) Uhlén, M.; Fagerberg, L.; Hallström, B. M.; Lindskog, C.; Oksvold, P.; Mardinoglu, A.; Sivertsson, Å.; Kampf, C.; Sjöstedt, E.; Asplund, A.; et al. Tissue-Based Map of the Human Proteome. *Science* **2015**, *347* (6220), 1260419.

(123) Murgha, Y. E.; Rouillard, J. M.; Gulari, E. Methods for the Preparation of Large Quantities of Complex Single-Stranded Oligonucleotide Libraries. *PLoS ONE* **2014**, *9* (4), 1–10.

(124) Guo, J.; Wang, S.; Dai, N.; Teo, Y. N.; Kool, E. T. Multispectral Labeling of Antibodies with Polyfluorophores on a DNA Backbone and Application in Cellular Imaging. *Proc. Natl. Acad. Sci. U. S. A.* **2011**, *108* (9), 3493–3498.

(125) Dai, N.; Guo, J.; Teo, Y. N.; Kool, E. T. Protease Probes Built from DNA: Multispectral Fluorescent DNA-Peptide Conjugates as Caspase Chemosensors. *Angew. Chem. Int. Ed Engl.* **2011**, *50* (22), 5105–5109.

(126) Wang, S.; Guo, J.; Ono, T.; Kool, E. T. DNA Polyfluorophores for Real-Time Multicolor Tracking of Dynamic Biological Systems. *Angew. Chem. Int. Ed.* **2012**, *51*, 7176–7180.

(127) Garini, Y.; Young, I. T.; McNamara, G. Spectral Imaging: Principles and Applications. *Cytom. Part J. Int. Soc. Anal. Cytol.* **2006**, *69* (8), 735–747.

(128) Bodenmiller, B. Multiplexed Epitope-Based Tissue Imaging for Discovery and Healthcare Applications. *Cell Syst.* **2016**, *2* (4), 225–238.

(129) Mondal, M.; Liao, R.; Xiao, L.; Eno, T.; Guo, J. Highly Multiplexed Single-Cell In Situ Protein Analysis with Cleavable Fluorescent Antibodies. *Angew. Chem. Int. Ed.* **2017**, *56*, 2636–2639.

(130) Camacho, C.; Coulouris, G.; Avagyan, V.; Ma, N.; Papadopoulos, J.; Bealer, K.; Madden, T. L. BLAST+: Architecture and Applications. *BMC Bioinformatics* **2009**, *10* (1), 421.

(131) Olivo-Marin, J.-C. Extraction of Spots in Biological Images Using Multiscale Products. *Pattern Recognit.* **2002**, *35* (9), 1989–1996.

(132) Cook, N. P.; Kilpatrick, K.; Segatori, L.; Martí, A. A. Detection of α-Synuclein Amyloidogenic Aggregates in Vitro and in Cells Using Light-Switching Dipyridophenazine Ruthenium(II) Complexes. *J. Am. Chem. Soc.* **2012**, *134* (51), 20776–20782.

(133) Martí, A. A.; Jockusch, S.; Stevens, N.; Ju, J.; Turro, N. J. Fluorescent Hybridization Probes for Sensitive and Selective DNA and RNA Detection. *Acc. Chem. Res.* **2007**, *40* (6), 402–409.

(134) Xiao, L.; Guo, J. Multiplexed Single-Cell in Situ RNA Analysis by Reiterative Hybridization. *Anal. Methods* **2015**, *7* (17), 7290–7295.

(135) Xiao, L.; Guo, J. Single-Cell in Situ RNA Analysis With Switchable Fluorescent Oligonucleotides. *Front. Cell Dev. Biol.* **2018**, *6*, 42.

(136) Robertson, D.; Savage, K.; Reis-Filho, J. S.; Isacke, C. M. Multiple Immunofluorescence Labelling of Formalin-Fixed Paraffin-Embedded (FFPE) Tissue. *BMC Cell Biol.* **2008**, *9*, 13.

(137) Amir, E. D.; Davis, K. L.; Tadmor, M. D.; Simonds, E. F.; Levine, J. H.; Bendall, S. C.; Shenfeld, D. K.; Krishnaswamy, S.; Nolan, G. P.; Pe'er, D. ViSNE Enables Visualization of High Dimensional Single-Cell Data and Reveals Phenotypic Heterogeneity of Leukemia. *Nat. Biotechnol.* **2013**, *31* (6), 545–552.

(138) Levine, J. H.; Simonds, E. F.; Bendall, S. C.; Davis, K. L.; Amir, E. D.; Tadmor, M. D.; Litvin, O.; Fienberg, H. G.; Jager, A.; Zunder, E. R.; et al. Data-Driven Phenotypic Dissection of AML Reveals Progenitor-like Cells That Correlate with Prognosis. *Cell* **2015**, *162* (1), 184–197.

(139) Rueden, C. T.; Schindelin, J.; Hiner, M. C.; DeZonia, B. E.; Walter, A. E.; Arena, E. T.; Eliceiri, K. W. ImageJ2: ImageJ for the next Generation of Scientific Image Data. *BMC Bioinformatics* **2017**, *18* (1), 529.

(140) McQuin, C.; Goodman, A.; Chernyshev, V.; Kamentsky, L.; Cimini, B. A.; Karhohs, K. W.; Doan, M.; Ding, L.; Rafelski, S. M.; Thirstrup, D.; et al. CellProfiler 3.0: Next-Generation Image Processing for Biology. *PLOS Biol.* **2018**, *16* (7), e2005970.

APPENDIX A

COPYRIGHT AND PERMISSIONS

Figure 1.5.1 is taken from “Ståhl, P. L.; Salmén, F.; Vickovic, S.; Lundmark, A.; Navarro, J. F.; Magnusson, J.;Giacomello, S.; Asp, M.; Westholm, J. O.; Huss, M.; et al. Science 2016, 353(6294), 78–82.”

Reproduced with permission from The American Association for the Advancement of Science.

This Agreement between Arizona State University -- Lu Xiao ("You") and The American Association for the Advancement of Science ("The American Association for the Advancement of Science") consists of your license details and the terms and conditions provided by The American Association for the Advancement of Science and Copyright Clearance Center.

License Number	4704321192387
License date	Nov 08, 2019
Licensed Content Publisher	The American Association for the Advancement of Science
Licensed Content Publication	Science
Licensed Content Title	Visualization and analysis of gene expression in tissue sections by spatial transcriptomics
Licensed Content Author	Patrik L. Ståhl,Fredrik Salmén,Sanja Vickovic,Anna Lundmark,José Fernández Navarro,Jens Magnusson,Stefania Giacomello,Michaela Asp,Jakub O. Westholm,Mikael Huss,Annelie Mollbrink,Sten Linnarsson,Simone Codeluppi,Åke Borg,Fredrik Pontén,Paul Igor Costea,Pelin Sahlén,Jan Mulder,Olaf Bergmann,Joakim Lundeberg,Jonas Frisén
Licensed Content Date	Jul 1, 2016
Licensed Content Volume	353
Licensed Content Issue	6294
Type of Use	Thesis/Dissertation
Requestor type	Scientist/individual at a research institution
Format	electronic
Portion	Text Excerpt
Number of pages requested	1
Title of thesis/dissertation	Highly Multiplexed Single Cell in situ Transcriptomic Analysis
Expected completion data	Dec 2019
Estimated size(pages)	120

Figure 1.5.2 is taken from “Lovatt, D.; Ruble, B. K.; Lee, J.; Dueck, H.; Kim, T. K.; Fisher, S.; Francis, C.; Spaethling, J. M.; Wolf, J. A.; Grady, M. S.; et al. Nat. Methods 2014, 11 (2), 190–196.”

Reproduced with permission from Springer Nature.

This Agreement between Arizona State University -- Lu Xiao ("You") and Springer Nature ("Springer Nature") consists of your license details and the terms and conditions provided by Springer Nature and Copyright Clearance Center.

License Number	4704391344925
License date	Nov 08, 2019
Licensed Content Publisher	Springer Nature
Licensed Content Publication	Nature Methods
Licensed Content Title	Transcriptome in vivo analysis (TIVA) of spatially defined single cells in live tissue
Licensed Content Author	Ditte Lovatt, Brittani K Ruble, Jaehee Lee, Hannah Dueck, Tae Kyung Kim et al.
Licensed Content Date	Jan 12, 2014
Licensed Content Volume	11
Licensed Content Issue	2
Type of Use	Thesis/Dissertation
Requestor type	Academic/university or research institute
Format	electronic
Portion	Figures/tables/illustrations
Number of figures/tables/illustrations	1
High-res required	No
Circulation/distribution	200-499
Title of thesis/dissertation	Highly Multiplexed Single Cell in situ Transcriptomic Analysis
Expected completion data	Dec 2019

Figure 1.5.3 is taken from “Taliaferro, J. M. Wiley Interdiscip. Rev. RNA 2019, e1542.”

Reproduced with permission from John Wiley Sons.

This Agreement between Arizona State University -- Lu Xiao ("You") and John Wiley and Sons ("John Wiley and Sons") consists of your license details and the terms and conditions provided by John Wiley and Sons and Copyright Clearance Center.

License Number	4704410857114
License date	Nov 08, 2019
Licensed Content Publisher	John Wiley and Sons
Licensed Content Publication	WILEY INTERDISCIPLINARY REVIEWS: RNA
Licensed Content Title	Classical and emerging techniques to identify and quantify localized RNAs
Licensed Content Author	J. Matthew Taliaferro
Licensed Content Date	May 1, 2019
Licensed Content Volume	10
Licensed Content Issue	5
Licensed Content Pages	14
Type of Use	Thesis/Dissertation
Requestor type	University/Academic
Format	electronic
Portion	Figures/tables/illustrations
Number of figures/tables/illustrations	1
Will you be translating?	No
Title of thesis/dissertation	Highly Multiplexed Single Cell in situ Transcriptomic Analysis
Expected completion data	Dec 2019
Expected size (number of pages)	120